THE MECHANISM AND FUNCTION OF AUTOPHAGY INDUCTION

BY CYTOSOLIC DNA

APPROVED BY SUPERVISORY COMMITTEE

Zhijian J. Chen, Ph.D.

Eric N. Olson, Ph.D. (Chair)

Lora V. Hooper, Ph.D.

Zhigao Wang, Ph.D.

DEDICATION

I sincerely thank my mentor, Dr. Zhijian J. Chen for his mentoring and support, both personally and professionally during my Ph.D. life. He has been my role model in scientific research. I would also like to thank my thesis committee, Dr. Eric N. Olson, Dr. Lora V. Hooper and Dr. Zhigao Wang for their broad guidance. I am indebted to all the present and past Chen lab members, my second family, whose care and inspiration make my life full of joy. I am also grateful to every one of my friends who I met during my PhD journey at UT Southwestern Medical Center.

I dedicate this work to my parents, Huchun Gui and Qiaoyan Gui, who raise me up and support me with their endless and unconditional love, and my wife, Cheng Chen, whose continuous love, understanding and encouragement support me during my study abroad. Moreover, I am particularly grateful to her for bringing our daughter Abigail into my life. Without them, I would be nowhere close to today's achievement.

THE MECHANISM AND FUNCTION OF AUTOPHAGY INDUCTION BY CYTOSOLIC DNA

by

XIANG GUI

DISSERTATION

Presented to the Faculty of the Graduate School of Biomedical Sciences

The University of Texas Southwestern Medical Center at Dallas

In Partial Fulfillment of the Requirements

For the Degree of

DOCTOR OF PHILOSOPHY

The University of Texas Southwestern Medical Center at Dallas

Dallas, Texas

August, 2018

THE MECHANISM AND FUNCTION OF AUTOPHAGY INDUCTION

BY CYTOSOLIC DNA

XIANG GUI, Ph.D.

The University of Texas Southwestern Medical Center at Dallas, 2018

Supervising Professor: Zhijian J. Chen, Ph.D.

Cyclic GMP-AMP (cGAMP) synthase (cGAS) detects pathogen infections or tissue damage by binding to microbial or self-DNA in the cytoplasm. Upon binding to DNA, cGAS produces cGAMP that binds and activates the adaptor protein stimulator of interferon genes (STING), which activates the kinases IKK and TBK1 to induce interferons and other inflammatory cytokines. Here, we report that STING also activates autophagy and induces cell death through a mechanism independent of TBK1 and IRF3 activation, which canonically triggers innate immunity signaling.

Upon binding to cGAMP, STING translocates to the ER-Golgi intermediate compartments (ERGIC) and the Golgi in a process that depends on the COP-II complex and ARF GTPases. The STING-containing ERGIC serves as a membrane source for LC3 lipidation, a key step in autophagosome biogenesis. Interestingly, STING lacking its C tail for interferon signaling is still capable of membrane trafficking and autophagy induction. Through endosomes or autophagosomes, STING is further degraded in the lysosome to shut down its activation. Interestingly, we determined that cGAMP-induced autophagy is important for the clearance of DNA and viruses in the cytosol. Furthermore, sea anemone STING induces autophagy but not interferons in response to stimulation by cGAMP, suggesting that induction of autophagy is a primordial function of the cGAS-STING pathway.

TABLE OF CONTENTS

LIST OF FIGURES

LIST OF TABLES

LIST OF DEFINITIONS

cGAS – cyclic GMP-AMP synthase

cGAMP – cyclic GMP-AMP

STING – Stimulator of interferon genes protein

IFN – Interferon

TBK1 – TANK-Binding Kinase 1

IRF3/7 – Interferon Regulatory Factor 3/7

IKK – IκB kinase

NF-κB – Nuclear Factor kappa B

TLR – Toll-like receptor

HSV – Herpes simplex virus

HIV – Human Immunodeficiency Virus

RIG-I – Retinoic acid-inducible gene 1

MDA5 – Melanoma Differentiation-Associated protein 5

MAVS – mitochondrial antiviral signaling protein

MyD88 – Myeloid differentiation primary response gene 88

TRIF – TIR-domain-containing adaptor-inducing interferon-β

TNF – Tumor necrosis factors

TRAF – TNF receptor associated factor

ISG – IFN stimulated gene

CXCL10 – C-X-C motif chemokine 10

IFIT3 – Interferon-induced protein with tetratricopeptide repeats 3

BECN1 – Coiled-coil myosin-like BCL2-interacting protein

PI3KC3 (VPS34) – Phosphatidylinositol 3-kinase VPS34

WIPI2 – WD repeat domain phosphoinositide-interacting protein 2

ARFs – ADP-ribosylation factor

GBF1 – Golgi-specific brefeldin A-resistance guanine nucleotide exchange factor 1

ARFGEF1 – Brefeldin A-inhibited guanine nucleotide-exchange protein 1

ARFGEF2 – Brefeldin A-inhibited guanine nucleotide-exchange protein 1

SEC24C – Protein transport SEC24-related protein C

SAR1 – Secretion-associated RAS-related protein 1

MAP1LC3 – Microtubule-associated proteins 1A/1B light chain 3

ERGIC – ER-Golgi intermediate compartment

mTOR – The mechanistic target of rapamycin

4E-BP1 – Eukaryotic translation initiation factor 4E-binding protein 1

ATF6 – Activating transcription factor 6

PI3P – Phosphatidylinositol 3-phosphate

MVB – multivesicular bodies

GGA3 – Golgi-localized, gamma ear-containing, ARF-binding protein 3

CHAPTER ONE

INTRODUCTION

The cGAS-STING pathway of cytosolic DNA sensing

With the exception of RNA viruses, all microorganisms contain and require DNA in their life cycle. As the blueprint of life which carries genetic information for almost all living organisms, DNA is also a key pathogen-associated molecular pattern (PAMP) that is recognized by innate immune receptors in the cytosol and endosomal compartments (Paludan, 2015), for detecting a large variety of microbial pathogens that contains DNA (Chen et al., 2016b). Moreover, DNA is also a danger-associated molecular pattern (DAMP) when self-DNA, which is normally confined to the nucleus and mitochondria in a eukaryotic cell, is inadvertently present in the cytosol (Ablasser and Gulen, 2016). cGMP-AMP (cGAMP) synthase (cGAS) is a cytosolic DNA sensor that is activated by binding to double-stranded DNA (Fig. 1.1), including both microbial and self-DNA (Sun et al., 2013; Wu et al., 2013). cGAS contains a nucleotidyltransferase domain and two major DNA-binding domains (Sun et al., 2013) which binds to DNA to form a 2:2 complex (Civril et al., 2013; Kranzusch et al., 2013; Li et al., 2013a; Zhang et al., 2014a). Binding to DNA then catalyzes the synthesis of cyclic GMP-AMP (cGAMP) from ATP and GTP (Li et al., 2013a; Sun et al., 2013; Wu et al., 2013; Zhang et al., 2013; Zhang et al., 2014a). cGAMP contains a mixture of phosphodiester bonds with one between the 2'-OH of GMP and 5'-phosphate of AMP, and the other between the 2'3'-OH of AMP and 5'-phosphate of GMP (Ablasser et al., 2013a; Diner et al., 2013; Gao

et al., 2013b; Zhang et al., 2013). This cGAMP isomer, called 2'3'-cGAMP, is unique when compared to other cyclic dinucleotides from bacteria such as di-AMP, di-GMP and 3'3'-cGAMP that all contain the 3'-5' linkage, as 2'3'-cGAMP functions more potently as a second messenger that binds to the Stimulator of Interferon Genes (STING, also known as MITA, MPYS, ERIS, and TMEM173) (Ishikawa and Barber, 2008; Wu et al., 2013; Zhang et al., 2013; Zhong et al., 2008). The endoplasmic-reticulum (ER)-membrane adaptor, STING contains four trans-membrane helices (TM1–TM4), a cytosolic cyclic dinucleotide binding domain and a carboxyl terminal activation domain for downstream kinase activation. Upon cGAMP binding, STING traffics from the ER to an ER-Golgi intermediate compartment and the Golgi apparatus (Dobbs et al., 2015; Ishikawa et al., 2009; Saitoh et al., 2009). During this process, the carboxyl terminus of STING recruits and activates the kinase TBK1, and the serine 366 site in this domain is subsequently phosphorylated by TBK1, which also licenses the phosphorylation of transcription factor IRF3 by TBK1 (Fitzgerald et al., 2003; Liu et al., 2015a; Sharma et al., 2003; Tanaka and Chen, 2012). STING also activates the kinase IKK, which phosphorylates the IkB family of inhibitors of the transcription factor NF-kB (Ishikawa et al., 2009). Phosphorylated IkB proteins are degraded by the ubiquitin-proteasome pathway to release NF-kB. Dimerized IRF3 and NF-kB then enter the nucleus where they function together with other transcription factors to trigger the expression of interferons and inflammatory cytokines such as TNF, IL-1b and IL-6.

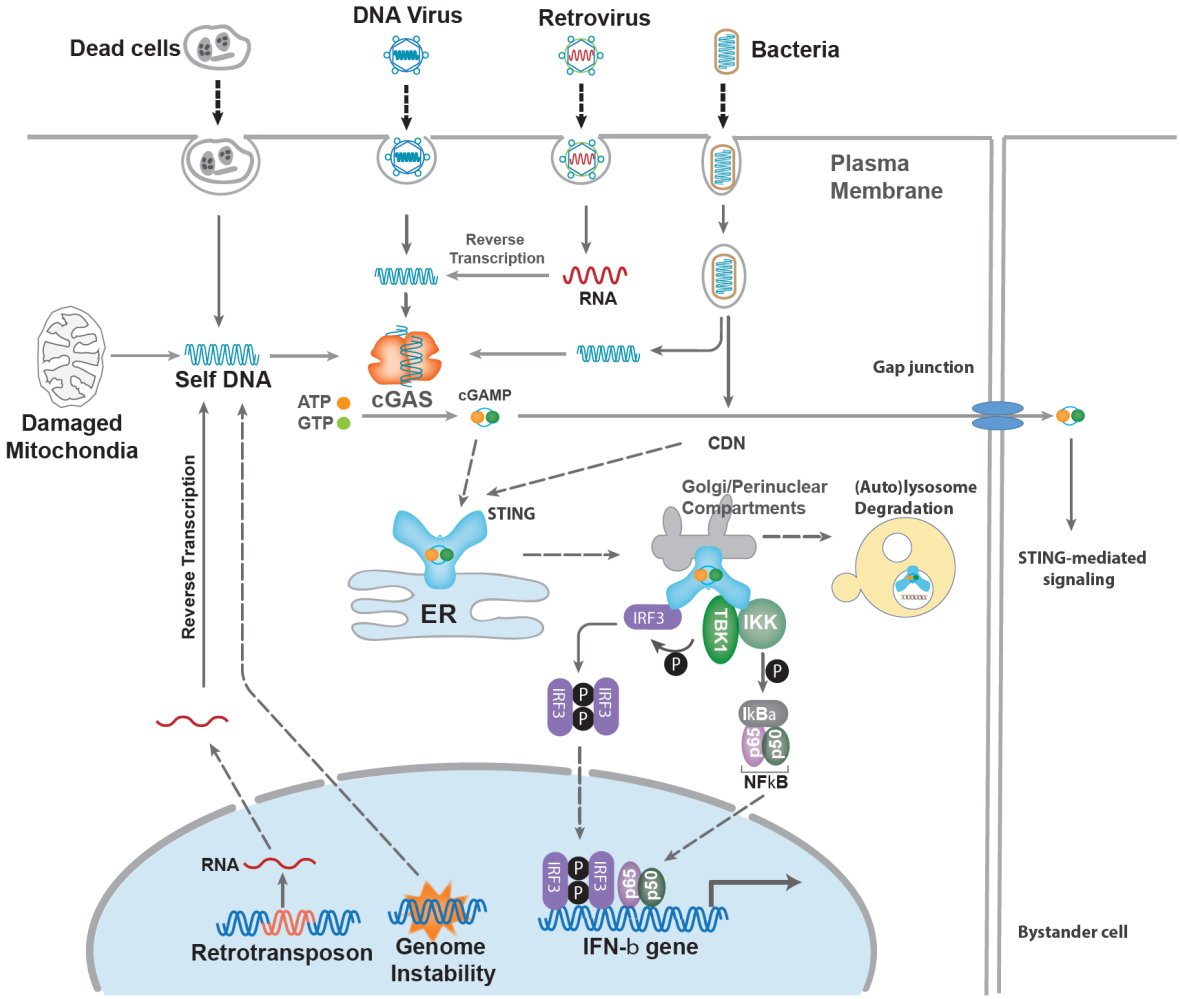

Figure 1.1. The cGAS–STING pathway of cytosolic DNA sensing. DNA is a pathogen-associated molecular pattern (PAMP) when it is delivered to the host cytoplasm by microbial infection and is also a danger-associated molecular pattern (DAMP) when it enters the cytoplasm from the nucleus (e.g., through DNA damage and reverse transcription of retroelements), mitochondria or dead cells. Cytosolic DNA binds to and activates cGAS, which catalyzes the synthesis of 2′3′-cGAMP from ATP and GTP. 2′3′-cGAMP binds to the ER adaptor STING, which traffics to the Golgi apparatus and is degraded in the lysosome. STING then activates IKK and TBK1. TBK1 phosphorylates STING, which in turn recruits IRF3 for phosphorylation by TBK1. Phosphorylated IRF3 dimerizes and then enters the nucleus, where it functions with NF-kB to turn on the expression of type I interferons and other immunomodulatory cytokines. cGAMP can be also transferred through gap junctions to bystander cells to activate STING-mediated signaling. Adjusted from Chen et al., Nat Immunol. 2016 Sep 20;17(10):1142-9.

Regulation of cGAS activation

The crystal structure of the cGAS–DNA complex shows that cGAS prefers to bind to the sugar-phosphate backbone of B-form double-stranded DNA, resulting in rearrangement of the active site for activation (Civril et al., 2013; Kranzusch et al., 2013; Li et al., 2013a; Wu et al., 2013). This explains why cGAS is activated by dsDNA independently of its sequence and is not activated by dsRNA. Some stem-loop structures of single-stranded DNA (ssDNA) derived from human immunodeficiency virus type 1 (HIV-1), are highly stimulatory and specifically activate cGAS in a sequence-dependent manner. They form a Y-shaped structure that includes a duplex with single-stranded overhangs containing a stretch of guanine residues that may stabilize the binding with cGAS; nevertheless, the structural basis of this activation remains to be determined (Herzner et al., 2015). Although the main mechanism for cGAS activation is through direct binding to DNA, several studies have suggested the importance of post-translational modifications of cGAS in regulating its enzymatic activity. Akt kinase phosphorylates human cGAS at Ser305 (mouse cGAS at Ser291) to inhibit cGAS activity (Seo et al., 2015). cGAS is glutamylated by the enzymes TTLL4 and TTLL6 that respectively block cGAS synthase's activity and DNA-binding ability. Reversal of this modification by the carboxylpeptidases CCP5 and CCP6 activates cGAS activity (Xia et al., 2016a). However, only a small fraction of cGAS proteins are modified in both cases with either inhibitory phosphorylation or glutamylation, which raises the question of how such modifications influence the overall activity of cGAS enzyme. Recent studies also suggest that cGAS binds to chromosomes and relocates to the nucleus during the cell cycle (Yang et al., 2017). The loss

of enzymatic activity of cGAS in the nucleus implies the potential existence of inhibitory factors that regulate cGAS during mitosis.

The gene encoding cGAS is also induced by interferon which provides a positive feedback mechanism for amplification of cGAS activity (Ma et al., 2015a; Schoggins et al., 2011). The expression of cGAS is recurrently suppressed in many tumor cell lines due to loss-of-function mutation or epigenetic silencing of the cGAS promoter regions (Konno et al., 2018). Similar to cGAS, STING signaling is also deregulated in some cancer cell lines that constrains the DNA-damage response and correlates with tumorigenesis (Xia et al., 2016b). The frequent disabling of the cGAS-STING pathway in cancer cells suggests that activation of this pathway might be an impediment to cellular immortalization as recent studies also link this pathway to cellular senescence (Yang et al., 2017). Moreover, the production of cytokines in response to DNA damage is an important host defense response that prevents the escape of pre-cancerous cells. Thus, inactivation of this pathway might assist the evasion of cancer cells from surveillance by the host immune system. Microbes have also evolved ways to evade attack from the host immune system by inhibiting cGAS activity. Kaposi's sarcoma-associated herpesvirus (KSHV) encodes ORF52, a tegument protein, which inhibits cGAS enzymatic activity through a mechanism involving binding to cGAS as well as binding to DNA (Wu et al., 2015). A cytoplasmic isoform of the latency-associated nuclear antigen (LANA) from KSHV also antagonizes the cGAS-mediated restriction of KSHV lytic replication by directly binding to and inhibiting cGAS (Zhang et al., 2016).

Regulation of STING activation, trafficking and degradation

The identification of 2′3′-cGAMP as the first metazoan cyclic dinucleotide messenger and the structural studies of STING in its free and 2′3′-cGAMP-bound states provided insights into the mechanism of STING activation. However, the current structural studies do not fully explain how STING is activated because both the N-terminal transmembrane domains and C-terminal tail (CTT) are not visible in any of the STING crystal structures. STING contains four transmembrane domains at the amino terminus that anchor the protein to the ER membrane, with the large carboxy-terminal domain facing into the cytoplasm for ligand binding and kinase recruitment. STING forms a dimer on the ER membrane in the presence or absence of a ligand (Gao et al., 2013c; Ouyang et al., 2012; Shang et al., 2012; Shu et al., 2012; Yin et al., 2012; Zhang et al., 2013). The binding of cGAMP to a central crevice of the STING dimer induces an extensive conformational change that is postulated to release the CTT tail to recruit TBK1 (Tsuchiya et al., 2016). Further analyses of the 2’3’-cGAMP-STING-bound conformation have revealed that 2’3’-cGAMP, but not the other isomers, adopts an organized conformation with the lowest enthalpy and entropy costs (Shi et al., 2015). This model offers an explanation as to why 2’3’-cGAMP obtains the highest affinity for STING compared with other cGAMP isomers or bacterial CDNs. Certain flavonoid compounds, such as DMXAA and CMA, can only bind to the same cGAMP-binding site of mouse STING but not human STING (Cavlar et al., 2013; Conlon et al., 2013; Kim et al., 2013b). Thus, these observations explain in part the finding that these compounds have antitumor effects in mice but failed in human clinical trials. The phosphorylation of STING serine 366 is critical for the recruitment of IRF3 and subsequent phosphorylation of IRF3 by TBK1 (Liu et al., 2015a). Once IRF3 is

phosphorylated, it forms a homodimer which enters the nucleus to trigger interferon expression. Notably, a highly conserved motif pLxIS (p, hydrophilic residue; x, any residue; S, phosphorylation site which is serine 366 in STING) is shared by several adaptors of innate immunity such as MAVS, TRIF and STING. Phosphorylation at this motif "licenses" the downstream phosphorylation of IRF3 by TBK1 to ensure that only a few immune adaptors among all agents that activate TBK1 lead to the activation of IRF3 and interferon induction. The phosphorylation of STING at Ser366 has been also reported to lead to the degradation of STING (Konno et al., 2013). However, this model was challenged by data showing that a STING mutant at serine 366 is still degraded in response to stimulation by DNA or cGAMP (Konno et al., 2013; Liu et al., 2015a; Tanaka and Chen, 2012).

Different ubiquitination of STING has been suggested to play multiple roles in both the activation and inhibition of STING. Three distinct ubiquitin E3 ligases have been reported to positively regulate STING activity. The E3 ligases TRIM56 and TRIM32 have been found to promote Lys63 (K63) polyubiquitination of STING, which enhances its activation (Tsuchida et al., 2010; Zhang et al., 2012). The ER-localized E3 ligase complex consisting of AMFR-GP78 and INSIG1 promotes another form of polyubiquitination (K27) of STING which is important for recruitment of TBK1 (Wang et al., 2014). In contrast, the E3 ligases RNF5 and TRIM30a promote K48 polyubiquitination of STING, leading to degradation by the proteasome (Wang et al., 2015; Zhong et al., 2009). Overall, the roles of ubiquitination in STING activation or inactivation appear to be quite complex as some E3 ligases were reported to function at the same site but cause different STING outcomes. Future work is needed to

clarify the roles of different types of ubiquitination and different E3 ligases in the STING pathway in vivo. Other modifications like palmitoylation were reported to be required for STING activation at the Golgi (Mukai et al., 2016). Upon binding to cGAMP, STING rapidly traffics from the ER to perinuclear compartments and forms large punctate structures (Saitoh et al., 2009). Inhibition of the trafficking of STING by brefeldin A, an inhibitor of ARF GTPase, blocks its downstream activities (Konno et al., 2013), suggesting the importance of STING membrane trafficking in its activation. The autophagy kinase ULK1 is reported to phosphorylate STING to trigger its degradation through autophagy; however, the mechanism by which STING is targeted to the autophagy pathway remains to be elucidated (Konno et al., 2013). The Shigella effector protein IpaJ inhibits the STING-mediated interferon response by inactivating the ARF family of GTPases and blocking STING trafficking (Dobbs et al., 2015). The viral interferon-regulatory factor (vIRF1) of KSHV inhibits STING by preventing it from interacting with TBK1 (Ma et al., 2015b). Herpes simplex virus type 1 encodes the regulatory protein ICP27, which prevents the phosphorylation of IRF3 by targeting the TBK1-activated STING signalosome (Christensen et al., 2016). The adenovirus protein E1A and human papilloma virus protein E7 inhibit STING signaling by directly binding to STING, revealing a host-virus conflict that may shape the evolution of viral oncogenes (Lau et al., 2015).

Regulation of cGAMP transport and stability

Intercellular cGAMP can be directly transferred between cells through their gap junctions (Ablasser et al., 2013b). This mechanism allows the local immune collaboration by which virus-infected cells can alert uninfected neighboring cells to elicit a more robust interferon

response to defend against infection even if the immune response in virus-infected cells has been antagonized. cGAMP can be also incorporated into viral particles and delivered into the next infected cell (Bridgeman et al., 2015; Gentili et al., 2015); such a mechanism also allows the host cells to mount a rapid response to viral infection. The intracellular amount of cGAMP is regulated not only by the rate of synthesis and transport but probably also by the rate of degradation. Although no intracellular cGAMP phosphodiesterase has been identified so far, the extracellular enzyme ENPP1 is reported to cleave the 2'-5' phosphodiester bond of 2'3'-cGAMP with high specificity (Li et al., 2014). It would be interesting to test if cGAMP can be exported outside of the cell for clearance by ENPP1. Whether ENPP1 serves as a major enzyme for degrading 2'3'-cGAMP in vivo requires further investigation. cGAMP binds tightly to STING which triggers robust trafficking activity and degradation of STING at the lysosome. It would be interesting to test whether certain portions of cGAMP would be also degraded together with STING at the lysosome. Higher amounts of cGAMP can be observed in Trex1 and STING double deficient cells (Gao et al., 2015), indicating that STING plays an important role in facilitating the decay of intracellular cGAMP. Interestingly, RNase T2, which is majorly localized at the endoplasmic reticulum (ER) or lysosome, degrades 2'3'-cGAMP through cleavage of the 3'-5' phosphodiester bond in vitro (Ablasser et al., 2013a; Hillwig et al., 2011).

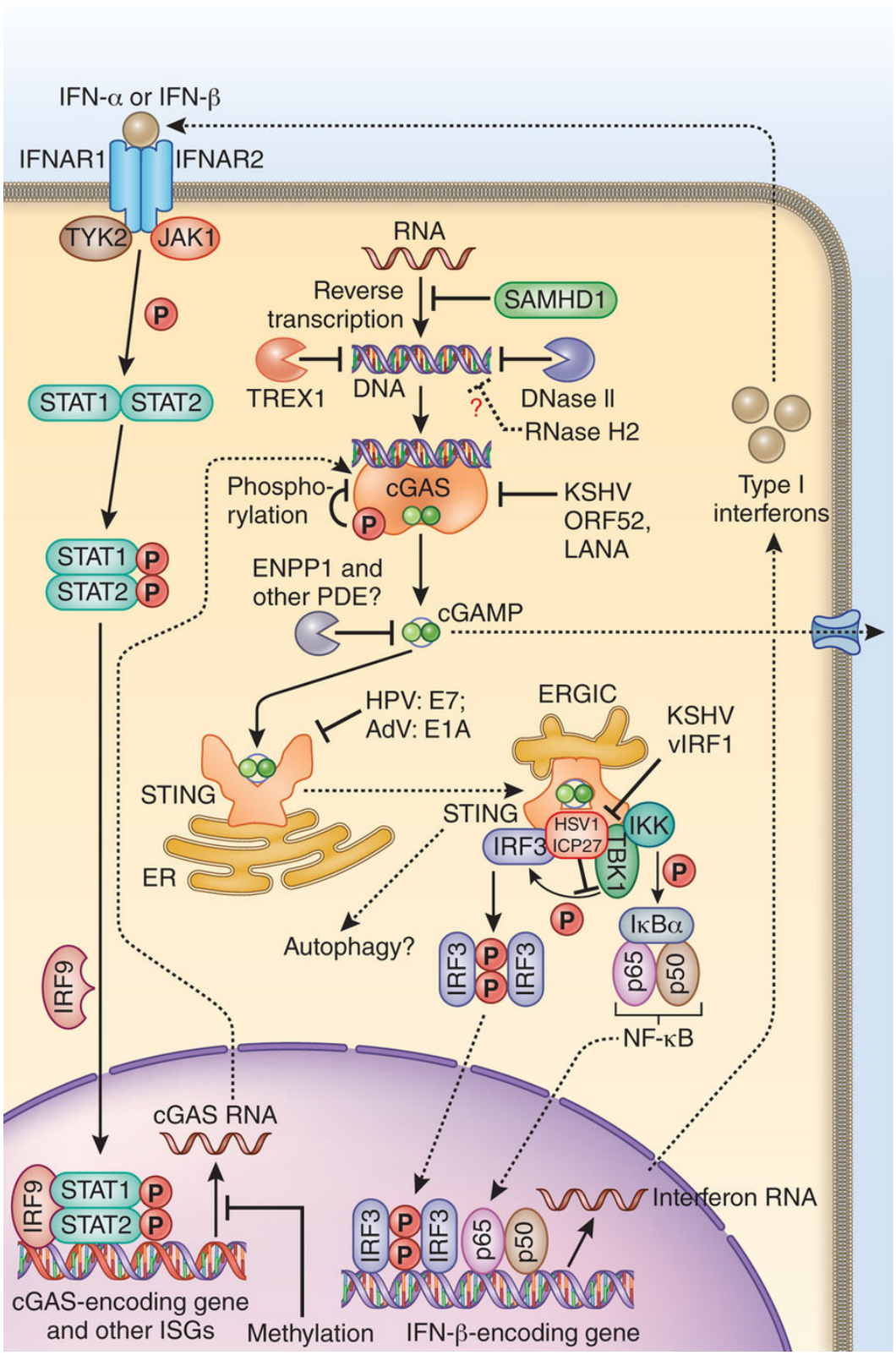
IFN-α or IFN-β
IFNAR1
IFNAR2
TYK2
JAK1
P
STAT1
STAT2
STAT1
STAT2
P
P
IRF9
RNA
Reverse transcription
SAMHD1
TREX1
DNA
?
DNase II
RNase H2
Phospho-rylation
cGAS
P
KSHV ORF52, LANA
ENPP1 and other PDE?
cGAMP
Type I interferons
HPV: E7; AdV: E1A
ERGIC
KSHV vIRF1
STING
ER
STING
HSV1 ICP27
IRF3
IKK
TBK1
P
P
Autophagy?
IRF3
P
P
IRF3
IκBα
p65
p50
NF-κB
cGAS RNA
IRF9
STAT1
STAT2
P
P
cGAS-encoding gene and other ISGs
Methylation
IRF3
P
P
IRF3
p65
p50
Interferon RNA
IFN-β-encoding gene

Figure 1.2. Regulation of the cGAS–STING pathway. The cGAS-STING pathway is regulated at multiple steps by host or viral factors. The synthesis or clearance of cytosolic DNA is tightly controlled by enzymes (including SAMHD1, TREX1, DNase II and RNase H2). cGAS expression is induced by interferon signaling and is suppressed by DNA methylation. cGAS activity is also regulated by phosphorylation or other post-translational modifications. Intracellular 2′3′-cGAMP is degraded by ENPP1 and perhaps other enzymes. cGAMP also binds to STING possibly for lysosome degradation. cGAMP can also spread to neighboring cells through gap junctions. STING is regulated by its trafficking to the ER-Golgi intermediate compartment and the Golgi apparatus and by its degradation at lysosomes. Several viral proteins (ORF52 and LANA of KHSV; E7 of human papilloma virus (HPV); E1A of adenovirus (AdV); and vIRF1 of KSHV) inhibit cGAS and STING in the pathway. TYK and SYK, kinases; STAT, signal transducer and transcription activator; PDE, phosphodiesterase; HSV-1, herpes simplex virus type 1; ISG, interferon-stimulated gene. Adapted from Chen et al., Nat Immunol. 2016 Sep 20;17(10):1142-9.

Physiological functions of the cGAS-STING pathway

The ability of cGAS to detect almost any dsDNA to elicit an immune response suggests the central role of cGAS in host immune defense against a large variety of microbial pathogens that contain DNA. This has been further validated by recent genetic studies in cGAS-deficient mice. Infectioen studies in *cGas-/-* mice demonstrate that cGAS-cGAMP signaling is essential for the interferon response against infection by DNA viruses such as herpes simplex virus 1 (HSV1), vaccinia virus (VACV), Kaposi's sarcoma-associated herpesvirus (KSHV) and murine g-herpesvirus virus 68 (MHV68) (Li et al., 2013b; Lio et al., 2016; Ma et al., 2015b; Paijo et al., 2016; Schoggins et al., 2014; Wu et al., 2015; Zhang et al., 2016). Thus, mice deficient in cGAS or STING maintains higher viral titers and become more vulnerable to those infections. Interestingly, *cGas-/-* mice are also more susceptible to lethal infections by West Nile virus, an RNA virus, despite the fact that *cGas-/-* mice still induce IFNs in response to RNA virus infections (Schoggins et al., 2014). It is possible that cGAS function importantly through its indirect role in immune protection against RNA viruses in vivo. For example,

infection with RNA viruses in vivo might cause cellular damage that results in 'leakage' of cellular DNA, which in turn activates cGAS for immune defense against infection with RNA viruses. Alternatively, cGAS may be involved in constitutive production of basal levels of type I IFNs, which protects against a large variety of microbial infections through “tonic” signaling (Gough et al., 2012). Membrane fusion between viral envelopes and target cells is also reported to activate the STING pathway and might contribute to immune defense against RNA viruses (Holm et al., 2012).

In addition to DNA viruses, retroviruses such as HIV, which require reverse-transcribed DNA to propagate their infections, also activate the host innate immune system through cGAS (Gao et al., 2013a; Lahaye et al., 2013). During retrovirus infection, the viral RNA inside the viral capsid is reversely transcribed into cDNA, which is injected directly into the nucleus for host genome integration, without triggering strong innate immune responses in normal cases. However, if the integrity of the viral capsid is compromised or if some of the host DNA nucleases such as SAMHD1and TREX1 lose their function in preventing the accumulation of cytoplasmic DNA, the reversely transcribed viral DNA will be detected by cGAS, resulting in the induction of interferons and other cytokines. The role of cGAS in detecting pathogens can be extended to bacteria that contain abundant DNA. Bacteria utilize their secretion system to deliver effector molecules into the cytoplasm. Although it is still not clear how bacterial DNA might be delivered to the cytoplasm, many intracellular bacteria such as *Mycobacteria, Legionella, Listeria, Shigella, Francisella, Chlamydia,* and *Neisseria*, trigger robust interferons through cGAS-STING signaling (Andrade et al., 2016; Collins et al., 2015; Dobbs

et al., 2015; Hansen et al., 2014; Storek et al., 2015; Wassermann et al., 2015; Watson et al., 2015; Zhang et al., 2014b). With the exception of *Listeria monocytogenes*, which directly produces cyclic di-AMP to induce interferons in a STING-dependent manner in mouse macrophages, the induction of interferon by most bacteria is largely abolished in the absence of cGAS.

The cGAS-STING pathway and autophagy

Autophagy is a highly conserved lysosomal degradation pathway that regulates cellular homeostasis under normal and stressed conditions and also contributes to host defense against infections (Deretic et al., 2013; Mizushima et al., 2011). As an important homeostatic mechanism, it involves in the formation of double-membrane vesicles called autophagosomes, which function to sequester and degrade protein aggregates, damaged organelles, and invading intracellular pathogens from the cytoplasm (Levine et al., 2011). Recent studies have revealed a crosstalk between the cGAS-STING pathway and autophagy. During macrophage infection with *Mycobacterium tuberculosis* (Mtb), bacterial DNA can elicit ubiquitin-mediated autophagy through a STING-dependent cytosolic pathway, which then delivers bacilli to autophagosomes for degradation (Watson et al., 2012). cGAS functions as a vital innate immune sensor of Mtb infection and produces cGAMP that activates STING to induce type I interferons and other cytokines (Collins et al., 2015). How the cGAS-STING pathway mediates autophagy and whether this is a major mechanism for host defense require further study. Upon DNA stimulation, STING partially colocalizes with the autophagy marker LC3 (ATG8 in yeast), which is regulated by ATG9 (Saitoh et al., 2009). The depletion of ATG9, but not

ATG7, leads to aberrant activation of the innate immune response by greatly enhancing the assembly of STING and TBK1 after dsDNA stimulation. As ATG9 is the only transmembrane autophagy-related protein, distinct from other cytosolic ATGs in the ubiquitination system, it would be interesting to investigate whether STING induces a non-canonical autophagy pathway directly via its membrane trafficking and undergoes degradation at the lysosome through the autophagosome. cGAS also binds to beclin-1, a key autophagy regulator that functions in complex with VPS34 and ATG14 (Kang et al., 2011). Binding of cGAS to beclin-1 releases RUBICON, a negative regulator of autophagy, from the beclin-1 complex and thereby leads to the lipidation of LC3, indicating autophagy induction, which may facilitate the clearance of cytosolic DNA. This interaction also suppresses cGAS catalytic activity, thereby functioning as a negative feedback mechanism to prevent prolonged immune activation (Liang et al., 2014). Although this study stated that this interaction induces autophagy through a STING-independent mechanism (Liang et al., 2014), cGAMP-induced autophagy seems to be primarily dependent on STING. How the cGAS-STING pathway interacts with autophagy appears to be complex. It was also reported that STING was phosphorylated by the autophagy-related kinase ULK1 at Ser-366 and that this phosphorylation targeted STING for degradation by autophagy (Konno et al., 2013). However, this model was challenged by the finding that mutation of Ser-366 to alanine on STING did not impair its degradation but rather abrogates its ability to activate IRF3 (Liu et al., 2015a; Tanaka and Chen, 2012). Thus, how the cGAS-STING pathway crosstalks with the autophagy pathway remains to be further explored.

The cGAS-STING pathway and programming cell death

Both cGAS and STING were originally described as key molecules to promote type I IFN and inflammatory cytokine production by DCs, macrophages, endothelial cells, fibroblasts, and many other primary cells upon infection with viruses and bacteria. These discoveries establish the central role of cGAS-STING in innate immunity. However, whether other outcomes of the cGAS-STING response exist remains largely unknown. Recent studies extended the paradigm of innate control of adaptive immunity by establishing the antiproliferative and apoptotic capacity of STING activation in T and B lymphocytes (Cerboni et al., 2017; Gaidt et al., 2017; Gulen et al., 2017; Heidegger et al., 2017; Tang et al., 2016). STING activation reduces the proliferation of T lymphocytes through a TBK1 and IRF3 independent manner of recruitment. T lymphocytes from patients carrying constitutive active mutations in the gene encoding STING showed impaired proliferation, mitotic errors and reduced memory phenotype skewing (Cerboni et al., 2017). Although activation of STING in T lymphocytes led to upregulation of antiviral genes, the most prominent effect observed was the initiation of apoptosis (Gulen et al., 2017). STING agonists also selectively trigger apoptosis in normal and malignant B cells (Tang et al., 2016). Additional evidence indicates that the mechanism of apoptosis induced by STING activation is from increased ER stress as upregulation of genes involved in the unfolded protein response (UPR) such as XBP-1 were observed in both B cells and T cells upon cGAMP or other STING agonist stimulation (Larkin et al., 2017; Tang et al., 2016). However, the cell death phenotype in human myeloid cells and STING-reconstituted HEK293T cells was reported to be associated with lysosomal cell death (Gaidt et al., 2017). It is possible that this cell type-specific apoptosis is caused by exhibition of intensified STING responses in both T

and B cells, as both of those cell lines with STING-mediated apoptosis obtain very high endogenous level of STING. The stress may come from large amounts of STING activation and trafficking upon cGAMP stimulation that would explain the unique phenotypes of ER stress and lysosome membrane permeabilization in those cells. Of note, this proapoptotic STING response is still functional in cancerous T cells and B cells, and delivery of STING agonists prevents in vivo growth of lymphocyte-derived tumors independent of its adjuvant activity (Gulen et al., 2017; Tang et al., 2016). These demonstrate the possibility that distinct effector responses including interferon induction, autophagy, and programming cell death can be shaped by the magnitude of cGAS-STING signaling, which may permit cell type-adjusted responses towards endogenous or exogenous insults.

The cGAS-STING pathway in autoimmune and inflammatory disease

While the cGAS-STING pathway functions as a major defense mechanism for DNA-derived PAMPs, activation of cGAS by self-DNA-derived DAMPs represents a threat for triggering host autoimmunity. Normally sequestered in the nucleus and mitochondria, host DNA inadvertently leaked from these compartments to the cytoplasm has been associated with autoimmune diseases in humans. For example, humans with mutations in TREX1, RNase H2, SAMHD1, the adenosine deaminase ADAR1 and the cytosolic receptor MDA5 develop Aicardi-Gourtières syndrome (AGS), an SLE-like immune-mediated disorder characterized by elevated expression of genes induced by type I interferon (Crow, 2015). Furthermore, mice lacking functional TREX1 or RNase H2 develop multi-organ inflammation through the activation of the cGAS-STING pathway (Gall et al., 2012; Gao et al., 2015; Gray et al., 2015;

Mackenzie et al., 2016; Pokatayev et al., 2016). TREX1 is an exonuclease that degrades cytosolic nicked dsDNA and single-stranded DNA (Lindahl et al., 2009). One-allele deletion of the gene encoding cGAS or STING largely rescues TREX1-deficient mice from developing myocarditis and other forms of inflammation (Gao et al., 2015). RNase H2 degrades RNA in the RNA–DNA hybrid complex and is essential for removing ribonucleotides incorporated into genomic DNA during replication. Deletion of cGAS or STING leads to the rescue of perinatal lethality as well as the elevated expression of ISG phenotypes from a knock-in mouse model with an RNase H2 AGS mutation (Pokatayev et al., 2016). DNase II is a major enzyme that digests DNA in the lysosome, deletion of which causes embryonic death in mice due to excessive production of type I interferons in embryos, which kills erythrocytes (Kawane et al., 2001). Deletion of the interferon receptor (IFNAR) rescues mice from the embryonic lethality but they still develop polyarthritis, probably due to the continued production of inflammatory cytokines such as TNF. Deletion of cGAS or STING in Dnase-II-deficient mice completely rescues them from embryonic lethality, as well as from autoimmune and inflammatory phenotypes (Gao et al., 2015).

Gain-of-function mutations in the gene encoding STING underlie a recently described type I interferonopathy called STING-associated vasculopathy with onset in infancy (SAVI) (Liu et al., 2014). This provides direct evidence that links STING to human autoinflammatory disease. Human patients with SAVI develop early-onset vasculopathy and pulmonary inflammation which affect mainly the skin, blood vessels and lungs. In addition to developing cutaneous inflammation in skin, patients with SAVI may also develop interstitial lung diseases that lead

to pulmonary fibrosis and also myositis in rare conditions. In contrast, AGS presents as an early-onset neuroinflammatory condition while SAVI is thought to begin as vasculitis. The unique tissue-specific clinical manifestations of SAVI and AGS are possibly due to the tissue specificity of gene expression. These STING gain-of-function mutations render the protein constitutively active or more sensitive to cGAMP, which results in elevated production of interferons by a variety of cells, including vascular endothelial cells (Liu et al., 2014; Melki et al., 2017). Whether these mutations cause similar conformational changes that mimic the cGAMP-bound form or disrupt the retention signal of STING in the ER needs to be further investigated. Collectively, these genetic studies provide proof-of-concept findings for targeting the cGAS-STING pathway to treat certain human autoimmune and inflammatory diseases.

Role of the cGAS-STING pathway in cancer

The mechanism of innate immune system sensing of tumor cells for the production of interferons and generation of adaptive T cell responses remain a longstanding mystery. Tumor-cell-derived DNA has been suggested to trigger the cGAS-STING pathway to induce interferons and further elicit the adaptive immune response (Fig. 1.3). Spontaneous CD8(+) T cell priming against tumors was defective in mice lacking STING but not in mice lacking TLRs, MyD88 or MAVS, suggesting the involvement of the cytosolic DNA sensing pathway as a major mechanism for innate immune sensing of cancer (Woo et al., 2014). Furthermore, the anti-tumor effect of several cancer therapies including blockade of immune-system checkpoints using anti-PD-(L)1 or anti-CD47 antibodies or radiation have all been proven to depend on cGAS or STING (Deng et al., 2014; Liu et al., 2015b; Wang et al., 2017). The recent

findings on the antiproliferative and apoptotic capacity of STING activation in T lymphocytes and B lymphocytes also suggest the potential for STING agonists to directly eradicate lymphoma malignancy (Cerboni et al., 2017; Gulen et al., 2017; Larkin et al., 2017; Tang et al., 2016). Another strong piece of evidence for cGAS-STING involvement in antitumor immunity arises from the dramatic antitumor effect of intratumor administration of cGAMP or its analogs into tumor-bearing mice which results in substantial inhibition of tumor growth and improvement of the survival of mice (Corrales et al., 2015; Demaria et al., 2015). Furthermore, the combination of cGAMP with irradiation or immune-system-checkpoint inhibitors including anti-PD-(L)1 produces synergistic antitumor effects, again suggesting the pivotal role of the cGAS-STING pathway in intrinsic antitumor immunity. However, recent observations also suggest that cGAS-STING-mediated inflammation may promote tumor initiation, growth and metastasis in certain malignancies (Ng et al., 2018). Activation of the cGAS-STING pathway can lead to tolerogenic responses through the induction of indolamine 2,3-dioxygenase (IDO) (Huang et al., 2013; Lemos et al., 2016). STING activation or deficiency were respectively associated with different carcinoma mouse models (Ahn et al., 2015) or viral oncogenesis (Lau et al., 2015; Liang et al., 2015). Brain-metastatic cancer cells produce cGAMP, which is transferred to neighboring astrocytes to activate an inflammatory response to facilitate metastasis (Chen et al., 2016a). Chromosomal instability can also promote metastasis through cGAS-mediated cytosolic DNA response to micronuclei (Bakhoum et al., 2018). Such studies indicate that cancer immunotherapies must achieve a fine balance between stimulating antitumor response through the cGAS-STING pathway and avoiding inflammation-mediated tumor growth. Ultimately, a successful clinical therapy

should be an optimal combination of different treatments, including stimulation of the innate immune system, blockade of immune-system checkpoints, and even adoptive T cell transfer.

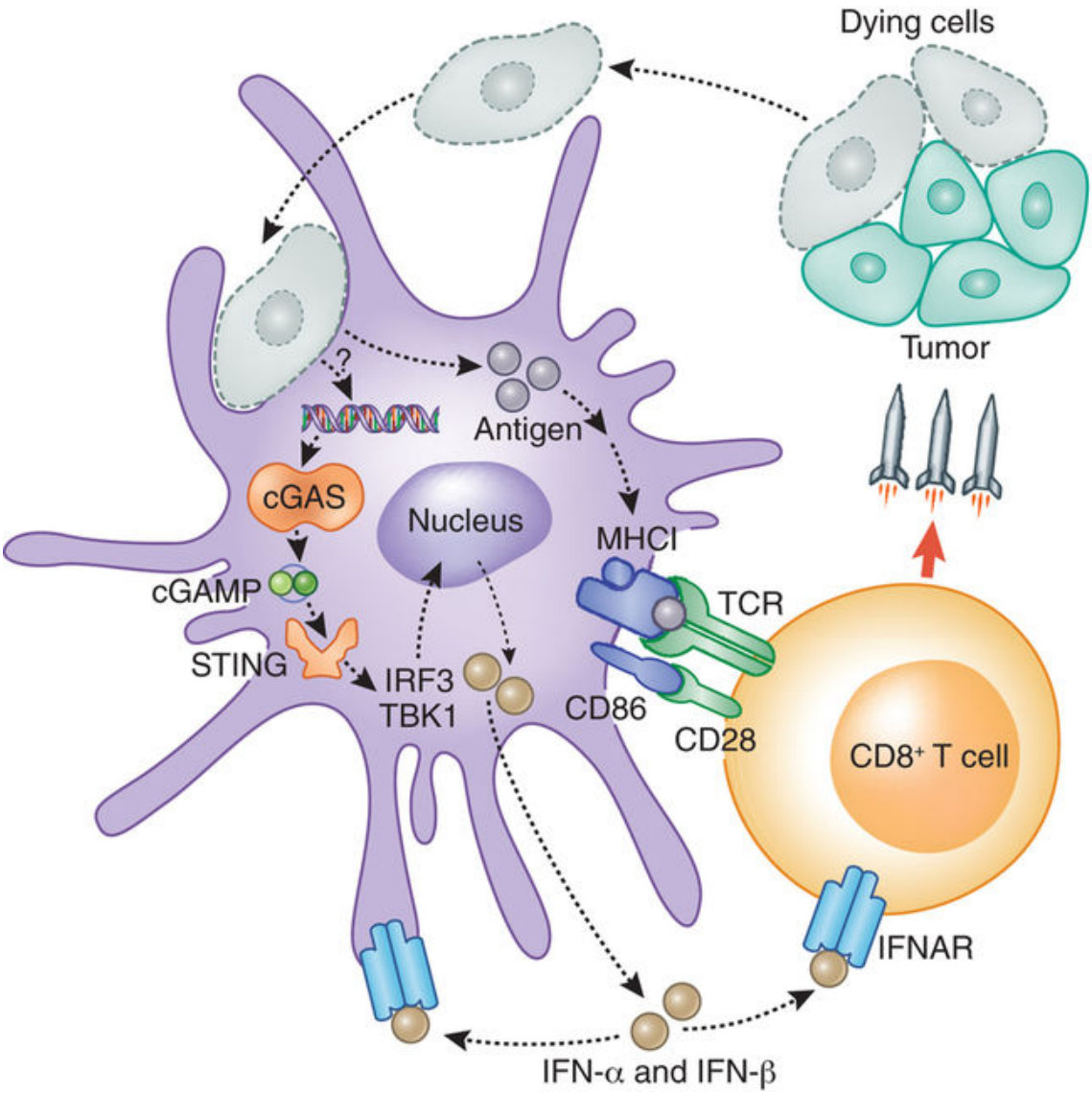

Figure 1.3. Role of the cGAS–STING pathway in antitumor immunity. Dying tumor cells are taken up by DCs, and the tumor DNA is delivered to the cytoplasm through an unknown mechanism. The DNA activates the cGAS pathway to induce the expression of interferons, major histocompatibility complex class I (MHCI) and co-stimulatory molecules such as CD86. Interferons stimulate the maturation of DCs and facilitate presentation of tumor associated

antigens on MHCI. The DCs then migrate to lymph nodes to activate CD8+ T cells, which seek and attack tumors in target tissues. TCR, T cell antigen receptor; CD28, costimulatory receptor; IFN, interferon. complex. Adapted from Chen et al., Nat Immunol. 2016 Sep 20;17(10):1142-9.

In conclusion, cGAS is a cytosolic DNA sensor that activates innate immune defense against a large variety of pathogens and malignant cells (Sun et al., 2013; Wu et al., 2013). Upon binding to DNA, cGAS is activated to catalyze cGAMP synthesis from ATP and GTP. cGAMP in turn binds and activates STING to induce type-I and type-III interferons (IFNs) and other inflammatory cytokines. After binding to cGAMP, STING traffics from ER to Golgi and other perinuclear compartments (Chen et al., 2016b; Ishikawa et al., 2009; Saitoh et al., 2009). During this process, STING recruits and activates the protein kinases IKK and TBK1, which activate the transcription factors NF-κB and IRF3, respectively, leading to induction of IFNs and other cytokines (Ishikawa et al., 2009; Liu et al., 2015a; Tanaka and Chen, 2012). However, the mechanism of STING trafficking and activation after cGAMP binding and the functional significance of STING trafficking remain poorly understood.

Recent studies have revealed a crosstalk between the cGAS-STING pathway and autophagy. Upon DNA stimulation, STING partially colocalizes with the autophagy marker LC3 (Atg8 in yeast), which is regulated by ATG9 but surprisingly not ATG7 (Saitoh et al., 2009). cGAS was also shown to interact with Beclin-1 to promote autophagy; this interaction also suppresses cGAS catalytic activity, thereby functioning as a negative feedback mechanism to prevent prolonged immune activation (Liang et al., 2014). It was also reported that STING was phosphorylated by the autophagy-related kinase ULK1 at Ser-366 and that this

phosphorylation targeted STING for degradation by autophagy (Konno et al., 2013). However, this model was challenged by the finding that mutation of Ser-366 to alanine on STING did not impair its degradation but rather abrogated its ability to activate IRF3 (Liu et al., 2015a; Tanaka and Chen, 2012). Thus, how the cGAS-STING pathway interplays with the autophagy pathway remains to be explored.

In this study, we aimed to dissect the mechanism and function of DNA-induced autophagy. Here we show that DNA induces autophagy through the cGAS-STING pathway via a mechanism that is independent of TBK1 activation or IFN induction. Upon binding to cGAMP, STING traffics to ERGIC in a process that depends on the GTPases SAR1 and ARFs and COP-II complex protein SEC24C. STING-containing ERGIC then serves as a membrane source for LC3 lipidation, an essential step in autophagosome formation. STING-induced LC3 lipidation requires WIPI2 but not conventional autophagy induction from the cytosol like mTOR inhibition. However, STING degradation does not require autophagy related genes including ATG5, WIPI2, ULK1 and BECN1, but is inhibited by lysosomal inhibitors. Deficiency in VPS34 which involves in both autophagy and the MVB pathway blocks STING degradation, suggesting that STING can traffic to lysosome through a Golgi-endosome pathway in addition to the ERGIC-autophagosome pathway. STING-mediated autophagy promotes clearance of DNA and viruses from the cytoplasm. Interestingly, Sea anemone STING, which lacks the C-terminal domain required for TBK1 activation and IFN induction (Kranzusch et al., 2015), also promotes LC3 conversion through binding to cGAMP,

suggesting that autophagy induction is an ancient and evolutionarily conserved role of STING that precedes its function in inducing the IFN pathway.

CHAPTER TWO

RESULTS

DNA induces autophagy through the cGAS-cGAMP-STING pathway

Both DNA and RNA can stimulate the cytosolic innate immune response respectively through cGAS-STING pathway or RIG-I/MDA5-MAVS pathway. The phosphorylation of immune adaptor protein STING or MAVS by TBK1 kinase licenses IRF3 activation and downstream interferon response. To study other downstream events in addition to interferon response by cytosolic DNA, we transfected interferon-stimulatory DNA (ISD) into BJ cells, which are human fibroblasts immortalized by the telomerase (hTERT). Interestingly, in addition to the phosphorylation of endogenous STING, TBK1 and IRF3, it also stimulated the conversion of LC3 into a lipidated form (LC3-II) (Fig. 2.1a). In contrast, Poly(I:C), a synthetic double-stranded RNA analogue that activates the RNA sensors retinoic acid-inducible gene I (RIG-I) and melanoma differentiation-associated protein 5 (MDA5), failed to stimulate LC3 lipidation or STING degradation despite its ability to stimulate phosphorylation of TBK1 and IRF3. Similarly, infection with herpes simplex virus-1 (HSV-1), a DNA virus, stimulated LC3 lipidation, which was not observed with Sendai virus, an RNA virus that activates the RIG-I pathway (Extended Data Fig. 2.1a). An HSV-1 mutant lacking ICP34.5, a viral protein known to inhibit the host immune response (Leib et al., 2009; Li et al., 2011; Liu et al., 2003; Orvedahl et al., 2007), also stimulated LC3 conversion. This indicates that, despite sharing the same

mechanism of interferon response with the MAVS pathway, the cGAS-STING pathway uniquely triggers autophagy activity. Furthermore, delivery of cGAMP into BJ cells was sufficient to induce robust LC3 lipidation and STING degradation, similarly to ISD (Fig. 2.1a). The cGAMP-induced LC3 conversion was more prominent when cells were treated with chloroquine, suggesting that the LC3 vesicles were targeted to the lysosome (Extended Data Fig. 2.1b). The cGAMP-stimulated autophagosome formation was also visualized by GFP-LC3 live cell imaging (Supplementary Video 1) and by electron microscopy (Extended Data Fig. 2.1c). Upon cGAMP treatment, STING translocated to perinuclear compartments where it partially colocalized with GFP-LC3 puncta, whereas starvation only induced GFP-LC3 puncta formation but not STING translocation (Extended Data Fig. 2.1d and 2.1e). To determine if LC3 lipidation depends on cGAS or STING, we tested primary MEF and BMDM cells from cGAS- or STING-deficient mice (Fig. 2.1b and Extended Data Fig. 2.1f). Knockout of cGAS blocked LC3 conversion triggered by HT-DNA but not cGAMP, whereas knockout of STING blocked LC3 conversion induced by both HT-DNA and cGAMP. We further tested BJ cells deficient in STING using CRISPR technology and HEK293T cells lacking both endogenous cGAS and STING. Reconstitution of wild type cGAS but not a catalytically inactive mutant (cGAS G198A/S199A) in STING-expressing HEK293T cells rescued LC3 lipidation (Extended Data Fig. 2.1h). Similarly, reconstitution of STING in the STING knockout BJ cells restored LC3 conversion induced by DNA and cGAMP (Extended Data Fig. 2.1g). Taken together, these results indicate that cytosolic DNA but not RNA induces autophagy, that DNA-induced autophagy depends on the catalytic activity of cGAS, and that cGAMP is sufficient to induce autophagy through STING.

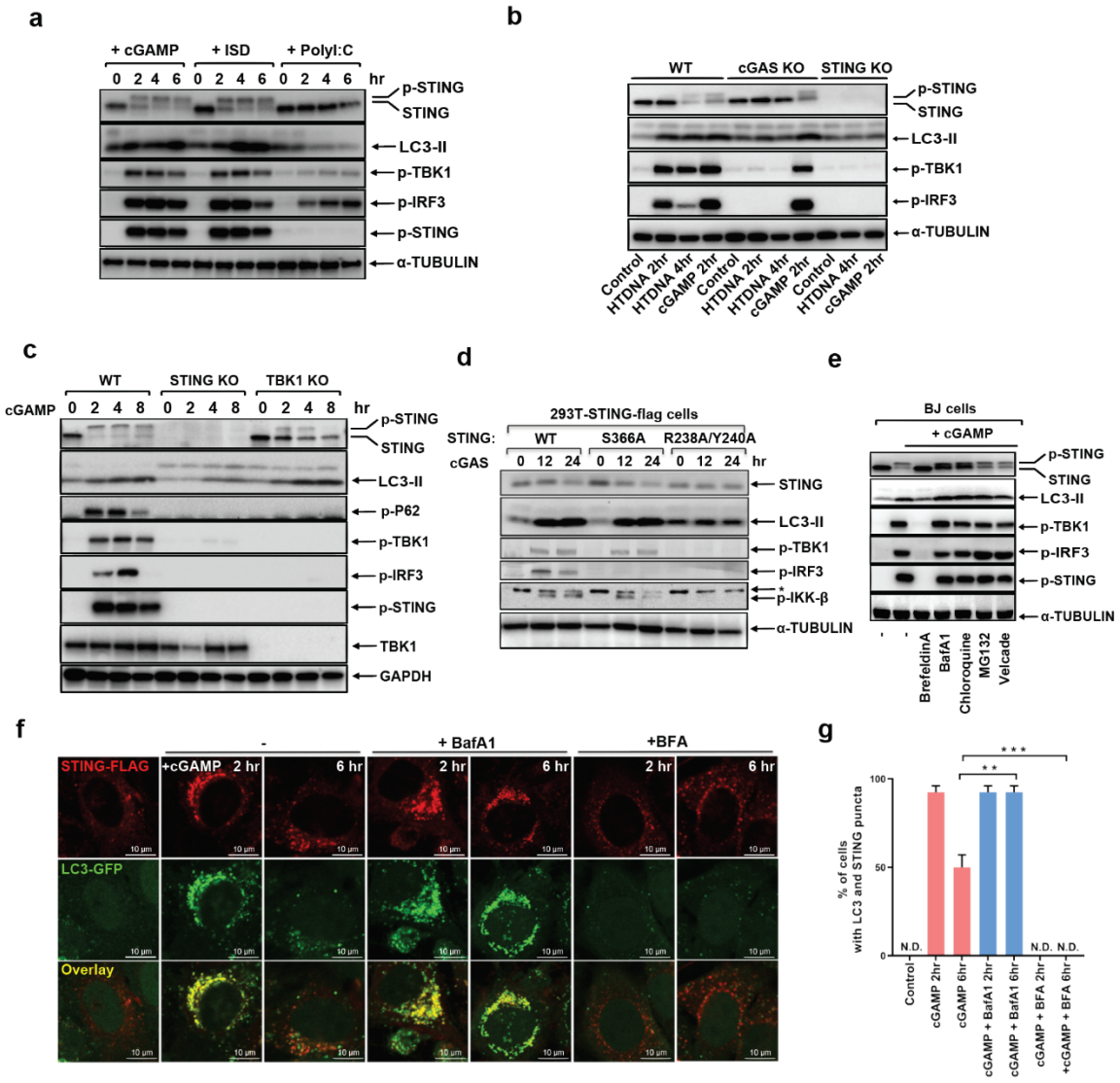

Figure 2.1. DNA-induced autophagy is dependent on cGAMP-induced STING trafficking but not TBK1 or IRF3 activation. a, DNA and cGAMP but not RNA triggers LC3 lipidation. BJ cells were stimulated with cGAMP by digitonin permeabilization or transfected with ISD or Poly(I:C). Cell lysates were analyzed by immunoblotting with the indicated antibodies. **b,** DNA-induced LC3 lipidation requires cGAS and STING. WT, *cGas*$^{-/-}$ or *Sting*$^{gt/gt}$ primary MEF cells were stimulated with cGAMP or transfected with HT-DNA for the indicated time, followed by immunoblotting. **c,** TBK1 is dispensable for LC3 conversion. WT, *Sting*$^{-/-}$ or *Tbk1*$^{-/-}$ BJ cells were stimulated with cGAMP before cell lysates were analyzed by immunoblotting. **d,** STING S366 phosphorylation by TBK1 is essential for IRF3 activation but not LC3 conversion. HEK293T cells stably expressing WT or mutant STING (S366A or R238/Y240A) were transfected with a cGAS expression plasmid followed by immunoblotting. **e&f,** cGAMP

stimulates STING trafficking and degradation in the lysosome. **e,** BJ cells were treated with Brefeldin A (BFA), lysosome inhibitors Bafilomycin A1 (BafA1) or Chloroquine or proteasome inhibitors (MG132 or Velcade) before stimulation with cGAMP. Cell lysates were analyzed by immunoblotting. **f,** BJ cells were treated with Bafilomycin A1 or Brefeldin A followed by stimulation with cGAMP and confocal immunofluorescence microscopy. **g,** Quantification of the cell percentage with colocalized LC3 and STING puncta. All results in this and other figures are representative of at least two independent experiments. N.D., not detectable.

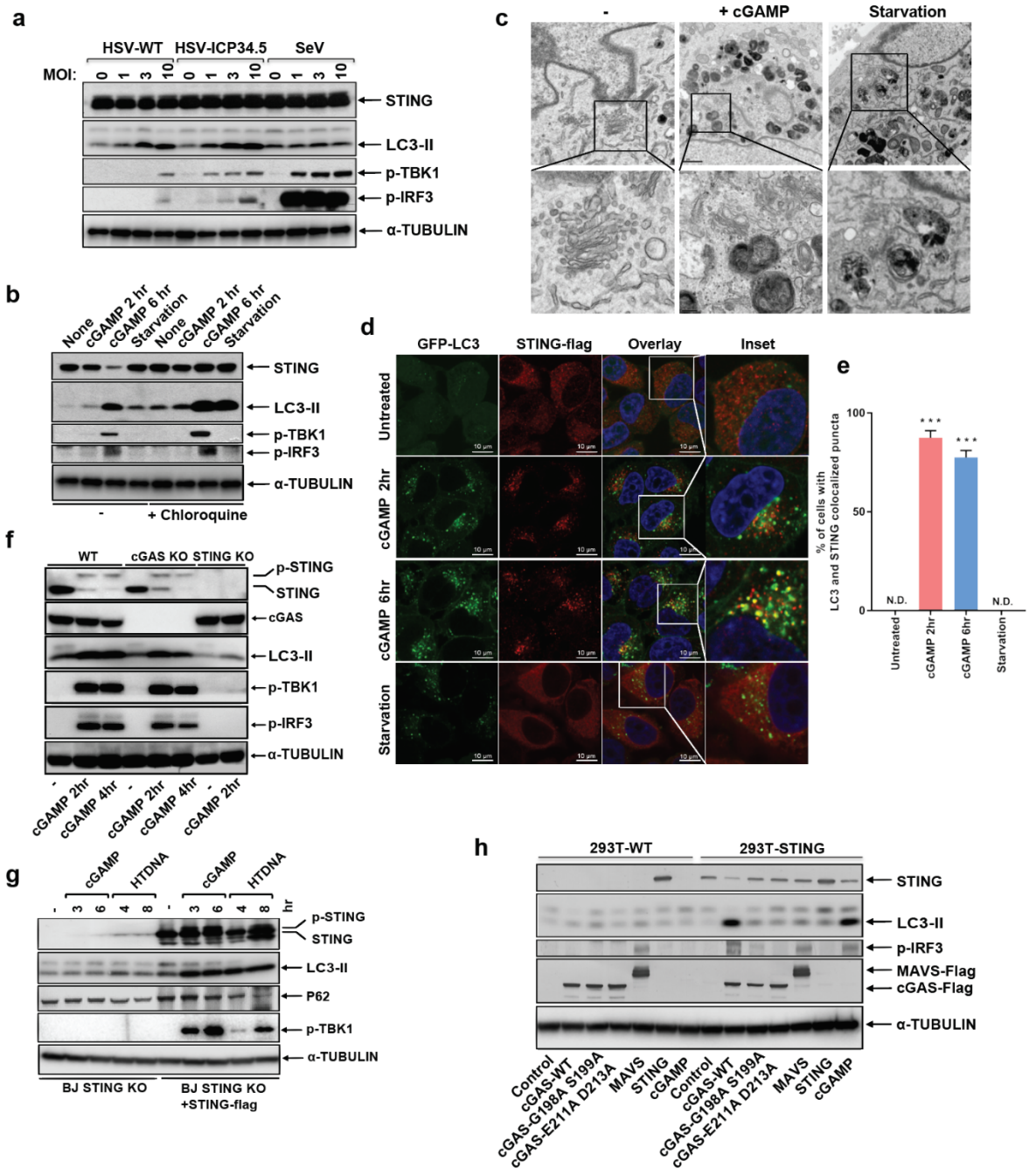

Extended Data Figure 2.1. cGAMP directly triggers autophagosome formation which requires STING. a, DNA virus but not RNA virus induces LC3 conversion. BJ cells were infected with wild type (WT) HSV1, HSV1ΔICP34.5 or Sendai virus (SeV) at indicated multiplicity of infection (MOI) followed by immunoblotting. **b,** cGAMP induces STING degradation in the lysosome. HeLa cells stably expressing STING-Flag were treated with cGAMP or starved in the presence or absence of chloroquine, followed by immunoblotting. **c,**

cGAMP induces autophagosome formation. Electron micrographs of BJ cells stimulated with cGAMP or growing in starvation media (EBSS). Boxed areas are enlarged to show high density organelles that represent autophagosomes. **d,** STING traffics to GFP-LC3 puncta. HeLa cells stably expressing STING-Flag and GFP-LC3 were treated with cGAMP or with starvation medium. Cells were immunostained with an anti-Flag antibody (to detect STING) followed by fluorescence microscopy. **e,** Quantification of the cell percentage with colocalized LC3 and STING puncta. N.D., not detectable. **f,** cGAMP induces STING-dependent LC3 lipidation in macrophages. WT, *cGas*$^{-/-}$ or *Sting*$^{gt/gt}$ BMDM cells were stimulated with cGAMP before cell lysates were analyzed by immunoblotting. **g,** STING is essential for LC3 lipidation induced by DNA and cGAMP. *Sting*$^{-/-}$ BJ cells and those reconstituted with STING-Flag were stimulated with cGAMP or HT-DNA, followed by immunoblotting. **h,** DNA induces LC3 lipidation through cGAS and STING. HEK293T cells or HEK293T STING cells were transiently transfected with WT or catalytically inactive mutant (G198A/S199A) of cGAS plasmid, MAVS or STING plasmids, or stimulated with cGAMP in the presence of digitonin. Cell lysates were analyzed by immunoblotting.

cGAMP-induced autophagy requires STING trafficking but not TBK1 activation

Since cGAMP strongly activates both TBK1 and autophagy, and previous studies have shown that TBK1 regulates autophagy (Wild et al., 2011), we tested whether TBK1 is required for cGAMP-induced autophagy. Surprisingly, BJ cells deficient in TBK1 still had normal LC3 lipidation in response to cGAMP treatment (Fig. 2.1c). Consistently, inhibitors of TBK1 (BX785 and MRT 67307) or IKKβ (TPCA1) did not impair LC3 conversion or STING degradation (Extended Data Fig. 2.2a). We have previously shown that TBK1 phosphorylates Ser-366 of human STING in response to cGAMP stimulation and that this phosphorylation is important for recruiting IRF3 to STING and TBK1, permitting TBK1 to phosphorylate IRF3 (Liu et al., 2015a). Consistent with a dispensable role of TBK1 in cGAS-induced autophagy, STING-S366A mutant still mediated normal LC3 lipidation and was degraded in response to cGAS transfection (Fig. 2.1d). In contrast, a STING mutant (R238A/Y240A) defective in cGAMP binding did not stimulate LC3 lipidation or phosphorylation of TBK1, IRF3 or IKKβ

(Fig. 2.1d). These results indicate that cGAMP binding, but not S366 phosphorylation, of STING is important for autophagy and STING trafficking.

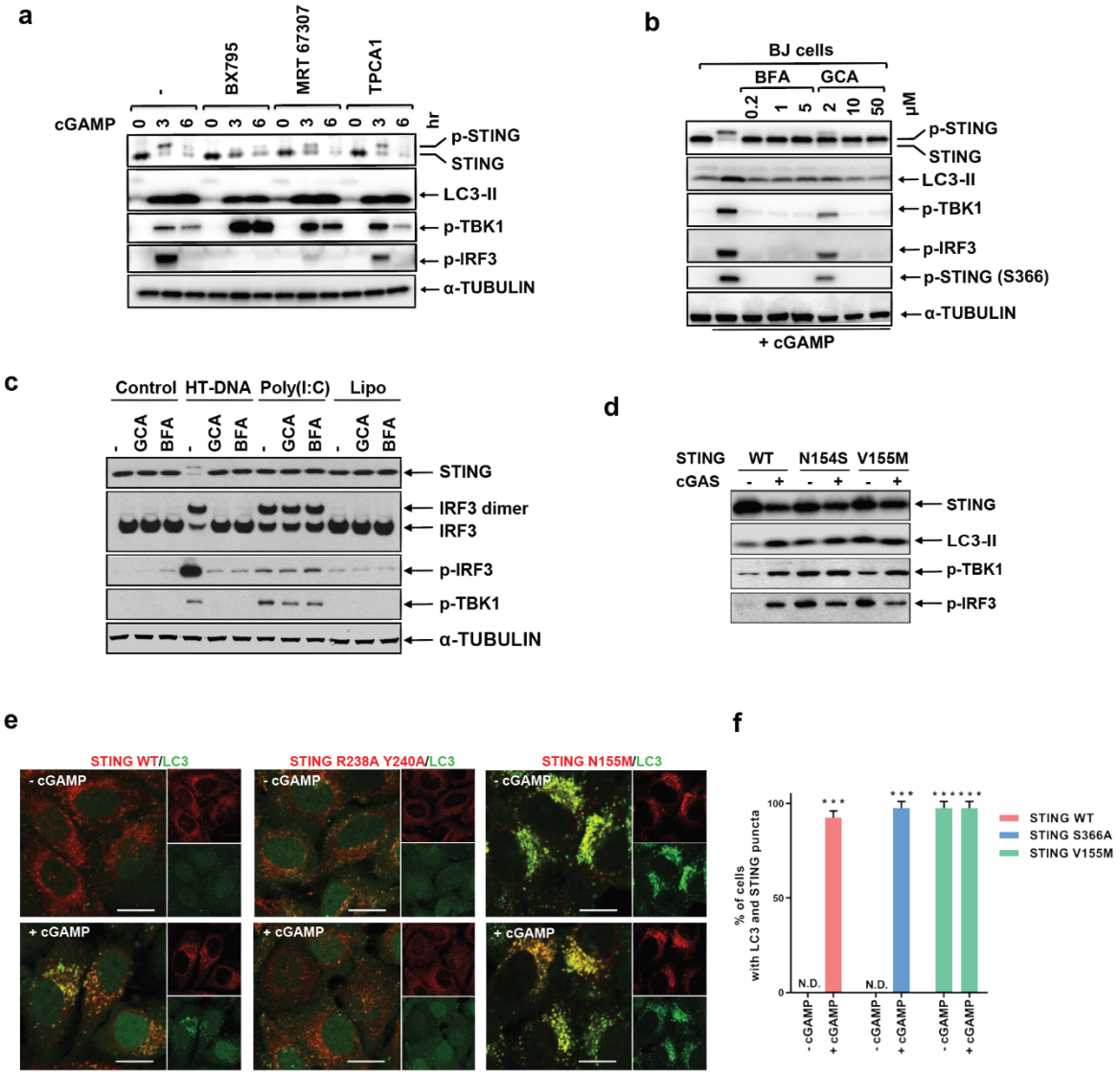

Extended Data Figure 2.2. cGAMP-induced autophagy requires STING membrane trafficking but not TBK1 or IRF3. a, Inhibition of TBK1 or IKK does not impair LC3 lipidation. Inhibitors of TBK1 (BX-795, MRT 67307) or IKK (TPCA1) were incubated with BJ cells before stimulation of the cells with cGAMP. Cell lysates were analyzed by immunoblotting. **b,** Inhibition of membrane trafficking blocks STING degradation and LC3 lipidation. BJ cells were treated with indicated concentrations of Brefeldin A (BFA) or

Golgicide A (GCA) for 60 min, followed by stimulation with cGAMP before cell lysates were analyzed by immunoblotting. **c,** Membrane trafficking is essential for cytosolic DNA but not RNA signaling. BJ cells were stimulated with Brefeldin A (BFA) or Golgicide A (GCA) before transfection with HT-DNA or Poly(I:C) or lipofectamine (Lipo) alone. Cell lysates were analyzed by native gel (for IRF3 dimerization) or SDS-PAGE followed by immunoblotting with the indicated antibodies. **d&e**, Constitutively active mutants of STING stimulate LC3 lipidation independently of cGAMP binding. **d,** HEK293T cells transiently expressing WT or mutant STING (N154S and V155M) were transfected with a cGAS expression plasmid followed by immunoblotting. **e,** Hela cells expressing GFP-LC3 and WT or mutant STING-Flag as indicated were treated with cGAMP or untreated, and examined by fluorescence microscopy. **f,** Quantification of the cell percentage with colocalized LC3 and STING puncta. N.D., not detectable.

To investigate the role of STING trafficking in LC3 lipidation, we treated BJ cells with brefeldin A (BFA) or golgicide A (GCA), which inhibits ER-to-Golgi membrane trafficking by binding to the guanine nucleotide exchange factor GBF1 (Donaldson et al., 1992; Helms and Rothman, 1992; Niu et al., 2005; Saenz et al., 2009). Both compounds inhibited LC3 lipidation and STING degradation as well as phosphorylation of TBK1 and IRF3 in response to HT-DNA transfection or cGAMP stimulation but not Poly(I:C) (Fig. 2.1e and Extended Data Fig. 2.2b, 2.2c). Treatments of BJ cells with bafilomycin A1 (BafA1) or chloroquine, which inhibit lysosomal acidification, did not impair LC3 lipidation or IRF3 phosphorylation but stabilized STING (Fig. 2.1e). The proteasome inhibitors MG132 and Velcade did not inhibit STING degradation or LC3 lipidation induced by cGAMP (Fig. 2.1e). Confocal immunofluorescence and live cell imaging also revealed that BafA1 prolonged the appearance of STING and LC3 puncta induced by cGAMP, whereas BFA blocked the formation of these puncta (Fig. 2.1f and Supplementary Videos 2 and 3). Recently, several point mutations of STING have been linked to a human autoinflammatory disease known as STING associated vasculopathy with onset in infancy (SAVI) (Liu et al., 2014). We tested two of these mutations,

N154S and V155M, and found that they caused constitutive lipidation of LC3, phosphorylation of TBK1 and IRF3, and accumulation of STING and LC3 puncta even in the absence of cGAS or cGAMP (Extended Data Fig. 2.2d, 2.2e and 2.2f). Collectively, these results indicate that cGAMP-induced LC3 lipidation and STING degradation require trafficking from ER to Golgi, that lysosomal acidification is important for STING degradation. and that SAVI-associated mutations of STING constitutively enhance autophagy and IRF3 activation.

Autophagy induction is an evolutionarily conserved, primordial function of STING

Because TBK1 and phosphorylation of S366 of STING are dispensable for cGAMP-induced autophagy, we sought to delineate the domains within STING that are important for autophagy induction. STING contains four transmembrane domains at the N-terminus, a dimerization domain and a cyclic dinucleotide (CDN) binding domain in the center and a C-terminal activation domain (residue 340-379) that includes S366 (Fig. 2.2a). Interestingly, deletion of the C-terminal activation domain (STING 1-340), which abolished phosphorylation of TBK1 and IRF3, did not impair LC3 conversion or STING degradation induced by cGAS or cGAMP (Fig. 2.2b and 2.2c). Mutation of a cGAMP-binding residue (R238A) in STING 1-340 blocked STING degradation and LC3 conversion while V155M mutation in STING 1-340 caused automatic formation of LC3 marked autophagosomes (Fig. 2.2b and 2.2c). Further truncations of STING into the N-terminus destroyed its ability to induce LC3 lipidation, and finer mapping identified a small region spanning residues 330-334 of STING as being important for autophagy induction (Extended Data Fig. 2.3a and 2.3b). Point mutations of residues within this region revealed that mutation of L333 and R334 to alanine within full-length STING

abrogated LC3 conversion, phosphorylation of TBK1 and IRF3, and the formation of STING and LC3 puncta induced by cGAMP (Fig. 2.2d and Extended Data Fig. 2.3c).

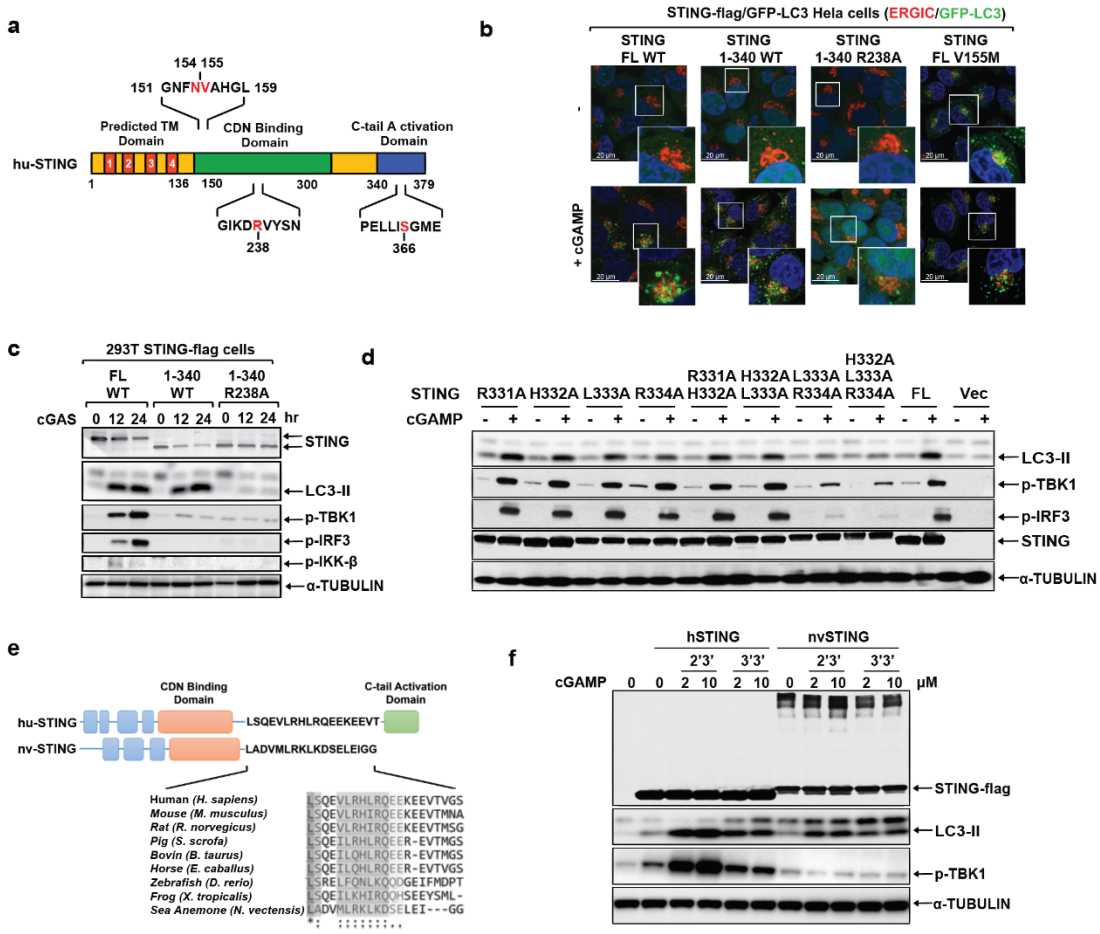

Figure 2.2. Autophagy induction by STING is evolutionarily conserved and separable from interferon induction. a, Schematic of functional domains and key residues of human STING. TM: transmembrane domain; CDN: cyclic dinucleotide; C-tail: C-terminal tail. **b&c,** The C terminal activation domain of STING is important for TBK1 and IRF3 activation but dispensable for LC3 lipidation. **b,** STING knockout Hela cells stably expressing GFP-LC3 and different STING mutants were stimulated with cGAMP using digitonin permeabilization. Immunofluorescence using ERGIC53 antibody and GF-LC3 were detected in those cell lines. **c,** HEK293T cells stably expressing the indicated STING were transfected with a cGAS expression plasmid before cell lysates were analyzed by immunoblotting. **d,** L333 and R334 of STING are important for LC3 lipidation and TBK1 activation. Expression plasmids encoding full-length STING harboring the indicated mutations were transiently transfected

into HEK293T cells, followed by stimulation with cGAMP. Cell lysates were analyzed by immunoblotting. **e,** Schematic of functional domains and residues of human and sea anemone STING (nvSTING), highlighting the evolutionary conservation of the sequence between the CDN binding domain and C-terminal activation domain. **f,** Sea anemone STING stimulates LC3 conversion but not TBK1 activation. HEK293T cells expressing human STING or nvSTING were treated with indicated concentrations of 2'3'-cGAMP or 3'3-cGAMP followed by immunoblotting.

The sequence surrounding this 'LR' motif is evolutionarily conserved (Fig. 2.2e) and is also found in STING of *Nematostella vectensis* (nvSTING), an anemone species that was recently found to possess a functional cGAS-STING pathway (Kranzusch et al., 2015). Interestingly, nvSTING does not contain the C-terminal domain found in vertebrate STING, which is required for activation of the type-I interferon pathway (Fig. 2.2e). We established HEK293T cells stably expressing human STING or nvSTING and stimulated them with 2'3'-cGAMP or 3'3-cGAMP, which have been reported to be the product of human cGAS and *Nematostella vectensis* cGAS (nvcGAS), respectively (Fig. 2.2f). 2'3'-cGAMP stimulated stronger LC3 conversion and TBK1 activation than did 3'3'-cGAMP in hSTING expressing cells, consistent with the previous report that 2'3'-cGAMP is a higher affinity ligand of STING than 3'3'-cGAMP (Zhang et al., 2013). Similarly, 2'3'-cGAMP stimulated more robust LC3 conversion than did 3'3'-cGAMP in nvSTING-expressing cells, but neither compounds stimulated TBK1 activation through nvSTING (Fig. 2.2f). Truncated huSTING (1-340) mimics nvSTING function in triggering LC3 lipidation after 2'3'-cGAMP stimulation with no evident TBK1 or IRF3 phosphorylation (Extended Data Fig. 2.4a).

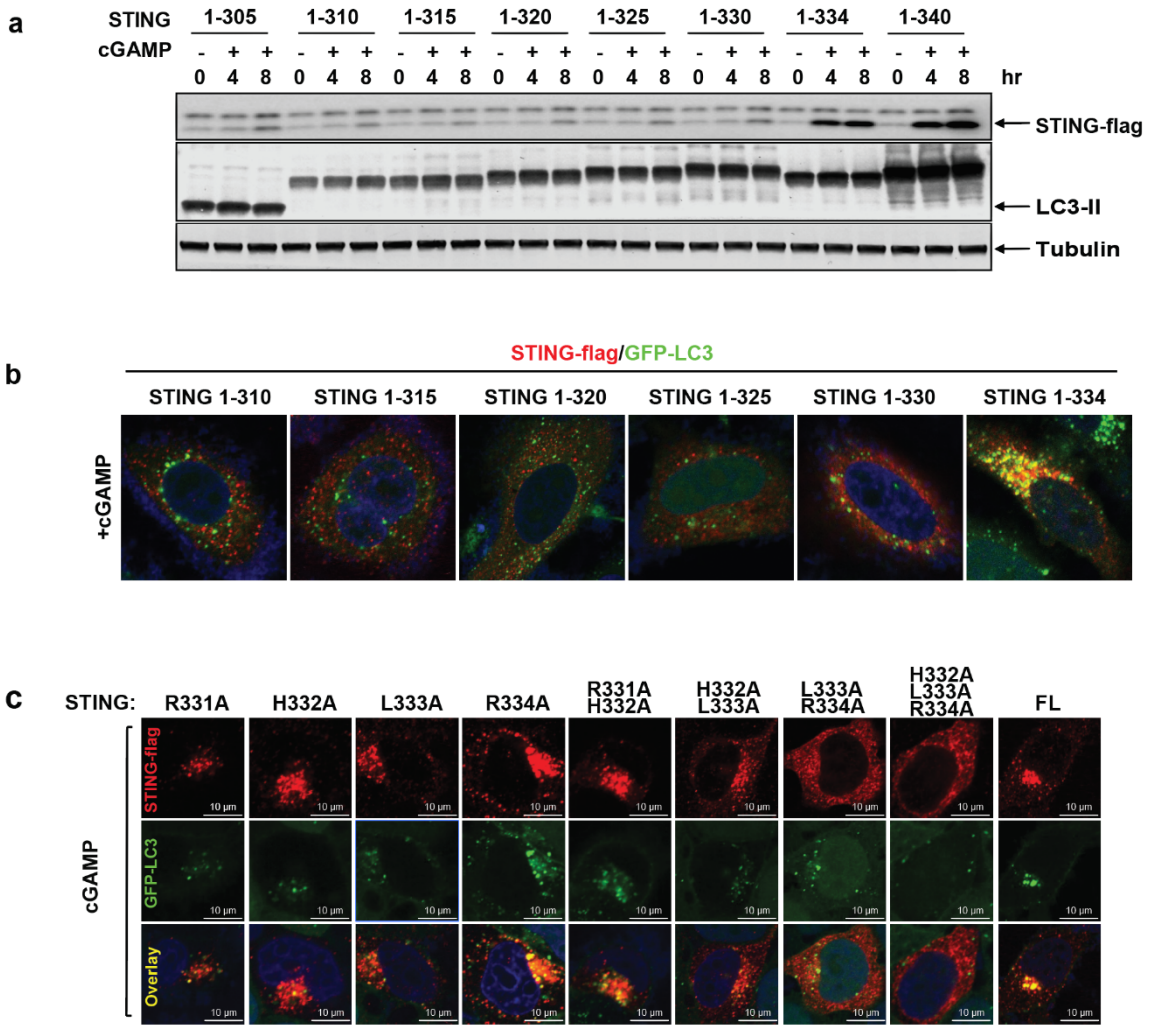

Extended Data Figure 2.3. Delineation of a STING region (residue 330-334) required for LC3 lipidation. a, Expression plasmids encoding truncated STING mutants were transiently transfected into HEK293T cells for 24 hr, followed by stimulation with cGAMP for 4 hr. Cell lysates were analyzed by immunoblotting. **b,** Expression plasmids of indicated STING truncation mutants were transfected into HeLa GFP-LC3 cells for 24 hr. The cells were stimulated with cGAMP followed by immunostaining and fluorescence microscopy. **c,** STING mutants as indicated were transfected and stimulated as described in (**b**) followed by immunostaining and fluorescence microscopy.

STING from *Xenopus tropicalis* also lacks the C-terminus required for TBK1 and IRF3 activation (Extended Data Fig. 2.4b). In response to 2'3'-cGAMP stimulation, Xenopus

STING translocated from ER and triggered LC3 conversion without activating TBK1 or IRF3 (Extended Data Fig. 2.4c, 2.4d and 2.4e). In contrast, STING from *Danio rerio*, which contains a C-terminal activation domain homologous to that of human STING, stimulated LC3 conversion as well as phosphorylation of TBK1 and IRF3 (Extended Data Fig. 2.4c, 2.4d and 2.4e). Taken together, our data show that the autophagy-inducing, but not interferon-inducing, function of vertebrate STING is conserved in Nematostella and Xenopus, suggesting that the autophagy-inducing function is a primordial function of the cGAS-STING pathway.

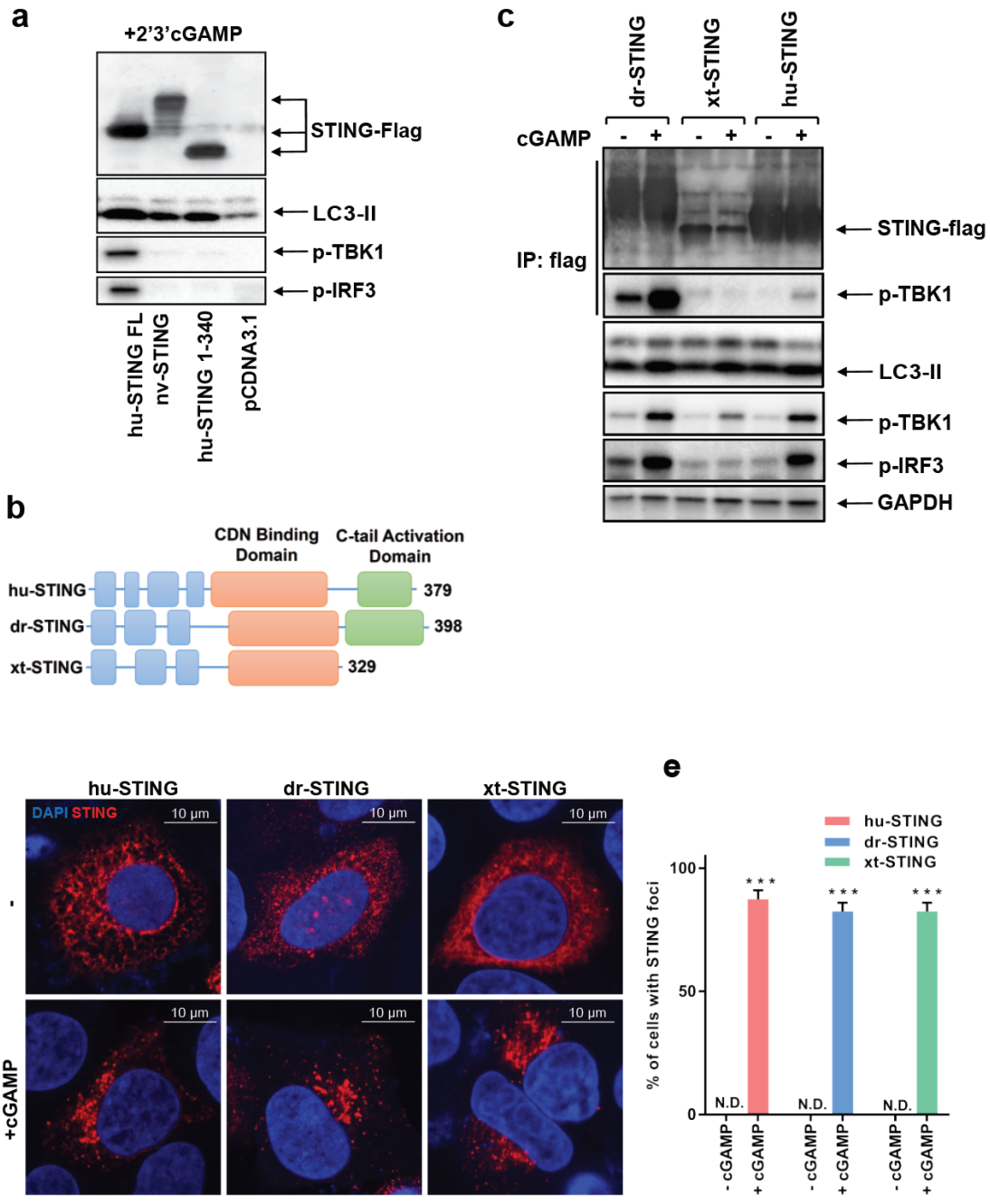

Extended Data Figure 2.4. STING-induced LC3 conversion is a primordial function of the cGAS-STING pathway. a, nvSTING induces LC3 conversion but not TBK1 activation

in response to 2'3'-cGAMP. HEK293T cells were transfected with expression plasmids encoding full-length (FL) human STING, human STING (1-340) or sea anemone STING (nvSTING) for 24 hr and then treated with 2'3'-cGAMP for 3 hr. Cell lysates were analyzed by immunoblotting. **b,** Domain organization of STING from human, danio rerio (dr) and xenopus tropicalis (xt). **c,** Xenopus STING stimulates LC3 lipidation but not IRF3 phosphorylation. HEK293T cells were transfected with expression plasmids for STING-Flag from human, danio or xenopus for 24 hr, then stimulated with cGAMP for 1 hr. A Flag antibody was used to immunoprecipitate STING from cell lysates, followed by immunoblotting with the indicated antibodies. **d,** Xenopus STING stimulates formation of perinuclear puncta of STING. Hela cells transiently expressing STING-Flag from human, danio or xenopus were stimulated with cGAMP for 3 hr. Cells were immunostained with a Flag antibody followed by fluorescence microscopy. **e,** Quantification of the percentage of cells with STING peri-nuclear foci formation. All results in this are representative of at least two independent experiments. N.D., not detectable.

STING translocates to ERGIC to trigger autophagosome formation upon cGAMP stimulation

To investigate the mechanism by which STING activates autophagy, we examined STING trafficking by confocal microscopy. Upon cGAMP stimulation, STING first colocalized at the perinuclear region with ERGIC-53, a marker of ER Golgi intermediate compartment (ERGIC), followed by colocalization with GFP-LC3-positive autophagosomes (Fig. 2.3a and Supplementary Video 4). The trafficking of STING to ERGIC was blocked by golgicide A (Fig. 2.3b). These results are intriguing because recent studies have suggested that ERGIC is a major source of membranes for starvation-induced LC3 lipidation (Ge et al., 2013). To test if ERGIC serves as a membrane source for cGAMP-induced LC3 lipidation, we performed in vitro reconstitution assay using membrane (P25) fractions from *Atg5*$^{-/-}$ HEK293T-STING cells stimulated by cGAS transfection which should contain multiple organelle membranes and cytosol (S100) from WT HEK293T cells (Fig. 2.3c). Consistent with a previous report (Ge et

al., 2013), when membranes from *Atg5*$^{-/-}$ cells were incubated with cytosol of starved WT cells, LC3 conversion was detected 1 hour after incubation (Extended Data Fig. 2.5a). Importantly, LC3 conversion was detected when membranes from cGAS-stimulated *Atg5*$^{-/-}$ cells were incubated with cytosol of unstimulated WT cells (Fig. 2.3c and Extended Data Fig. 2.5a). Membranes from unstimulated cells or cytosol from *Atg5*$^{-/-}$ cells did not stimulate LC3 conversion. Membranes from cGAS-stimulated cells that were treated with Brefeldin A lost the ability to stimulate LC3 conversion (Fig. 2.3d). These results suggest that vesicles budded from ER and/or Golgi in cGAS-stimulated cells serve as the membrane source for LC3 conjugation by the cytosolic ATG5 conjugation machinery.

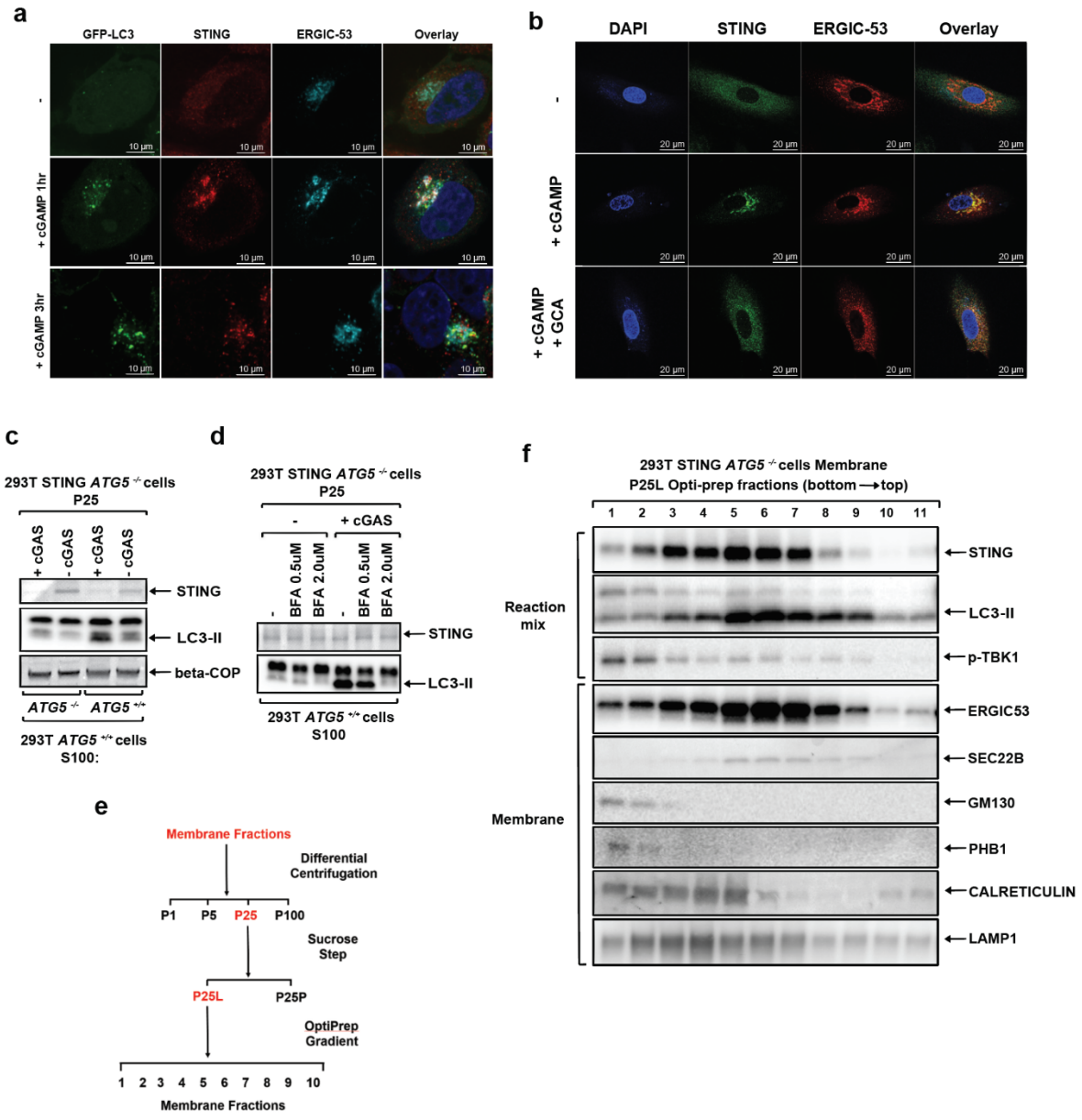

Figure 2.3. STING translocates to ERGIC to trigger autophagosome formation. a, STING co-localizes with ERGIC and autophagosome in response to cGAMP stimulation. HeLa cells stably expressing GFP-LC3 and STING-Flag were stimulated with cGAMP for the indicated time followed by immunofluorescence microscopy. **b,** STING trafficking to ERGIC is blocked by Golgicide. BJ cells were stimulated with cGAMP for 3 hr in the presence or absence of Golgicide A. Cells were stained with DAPI or the indicated antibodies and examined by confocal microscopy. **c,** LC3 lipidation in vitro requires membranes from cGAS-stimulated cells and cytosolic extracts containing ATG5. *Atg5*$^{-/-}$ HEK293T cells stably expressing STING were transfected with or without a cGAS expression plasmid for 18 hr before membrane pellets

(P25) were prepared by differential centrifugation. The membranes were incubated with cytosolic extracts (S100) from HEK293T cells at 30ºC for 60 min, followed by immunoblotting analysis. **d,** Membrane trafficking of STING is important for it to induce LC3 lipidation in vitro. Similar to **(c)** except that Brefeldin A was added to 293T-STING *Atg5*$^{-/-}$ cells at indicated concentrations before cells were transfected with a cGAS expression plasmid followed by isolation of membranes (P25) for the in vitro LC3 lipidation assay. **e,** Procedure of Opti-gradient fractionation. **f,** ERGIC fractions are enriched with LC3 lipidation activity. Similar to **(b)** except that p25 membranes were further fractionated by Opti-Prep gradient ultracentrifugation. The membrane fractions were incubated with cytosol (S100) from HEK293T cells to detect LC3 lipidation as depicted in **(b).** The reaction mixtures and each fraction from the ultracentrifugation were analyzed by immunoblotting with the indicated antibodies.

To determine the types of vesicles that stimulate LC3 conjugation, we further fractionated the membranes from cGAS-stimulated *Atg5*$^{-/-}$ HEK293T-STING cells by differential centrifugation followed by sucrose gradient ultracentrifugation and OptiPrep^{TM} (iodixanol) density gradient ultracentrifugation (Fig. 2.3d). Each membrane fraction was analyzed by immunoblotting and tested for its ability to support LC3 conjugation by cytosol from WT HEK293T cells (Extended Data Fig. 2.5b, 2.5c and Fig. 2.3f). This analysis revealed that membrane fractions enriched in STING and the ERGIC markers ERGIC-53 and Sec22b had the enhanced activity in stimulating LC3 conversion, suggesting that ERGIC serves as a membrane source for LC3 conjugation (Fig. 2.3f). This membrane activity assay can be also applied to reconstitute TBK1/IRF3 recruitment and activation using *TBK1/IKKi*$^{-/-}$ cell membrane containing STING with cytosol of unstimulated WT cells (Extended Data Fig. 2.5d). Both LC3 lipidation and TBK1/IRF3 activation require the membrane integrity of STING-containing membrane as disruption of the membrane using detergent also destroyed the downstream activities (Extended Data Fig. 2.5d). Unlike ERGIC membrane fraction capable of LC3 lipidation, heavier membrane fractions enriched in the trans-Golgi marker

TGN38 and endosome marker EEA1 had more activity in TBK1 phosphorylation (Extended Data Fig. 2.5e).

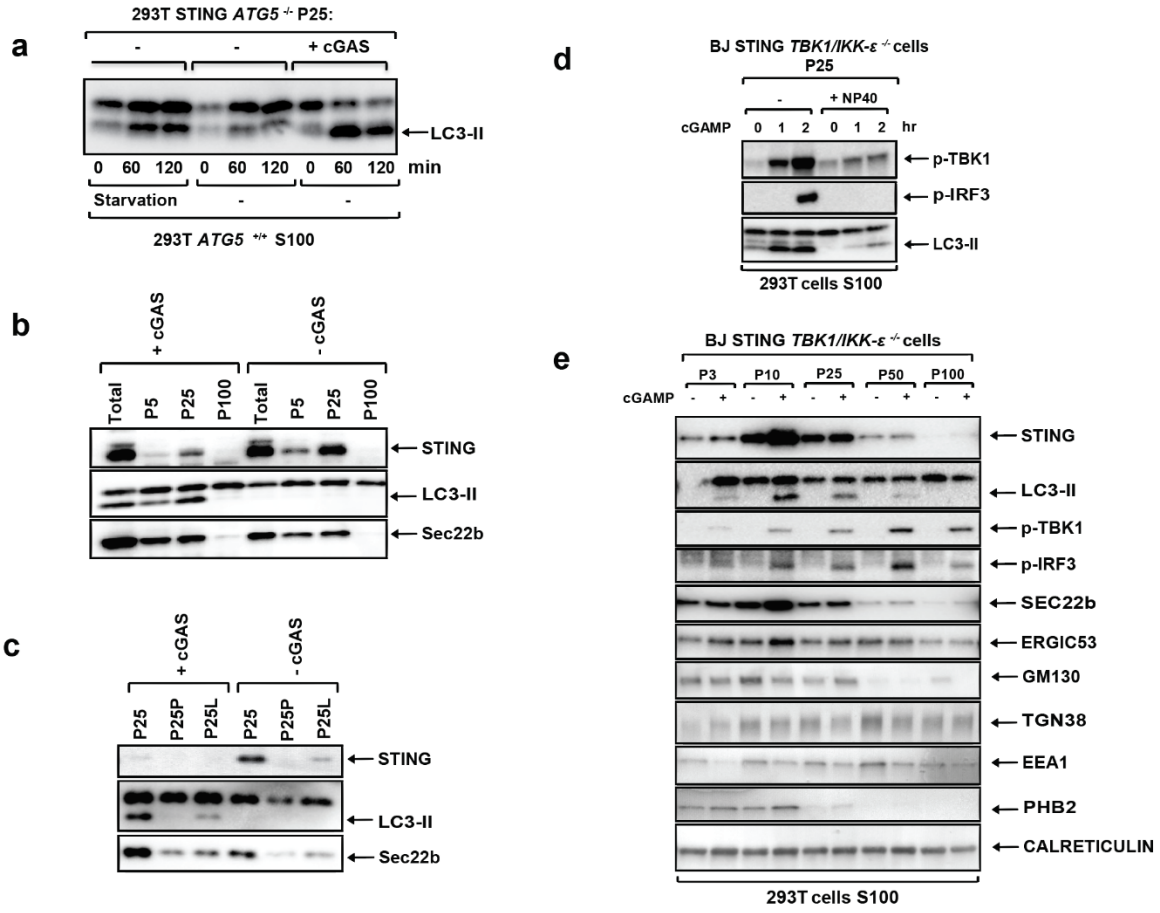

Extended Data Figure 2.5. In vitro assays of STING-induced LC3 lipidation and TBK1/IRF3 activation. a, *ATG5*$^{-/-}$ 293T cells stably expressing Flag-STING were transfected with a cGAS expression plasmid or an empty vector for 24 hr. Membrane pelleted at 25,000 g (P25) from these cells was incubated with cytosolic extracts (S100) from starved or untreated 293T cells in the presence of GTP and ATP regenerating system. After incubation at 30^{o}C for 60 min, the reaction mixtures were analyzed by immunoblotting. **b,** Similar to **(a)** except that different organelle membranes enriched by differentiation centrifugation were prepared and incubated with cytosol (S100) from HEK293T cells to detect LC3 lipidation. **c,** Similar to **(a)** except that P25 membrane was further fractionated by sucrose step gradient ultracentrifugation to generate P25P (pellet) and P25L (light) and incubated with cytosol (S100) from HEK293T cells to detect LC3 lipidation. **d,** Similar to **(a)** except that the organelle membrane (P25) was prepared from BJ cells deficient in TBK1/IKK-ε and phosphorylation of TBK1 and IRF3 was

examined this time. The P25 pellet were pretreated with NP40 to disrupt the membrane integrity to assess the importance of membrane in STING activation. **e,** Similar to **(a)** except that in addition to use P25 membrane for the reaction, P3, P10, P25, P50 and P100 were all collected using differentiation centrifugation to incubate with cytosolic extracts (S100) from HEK293T cells to detect LC3 lipidation as well as TBK1 and IRF3 phosphorylation.

STING-induced LC3 lipidation requires WIPI2, independent of cytosol mTOR inhibition.

To test if canonical autophagy induction is required for cGAMP-induced STING degradation, we used CRISPR technology to knock out key autophagy genes, including ATG5 and ATG9. Interestingly, ATG5 deficiency abolished LC3 lipidation but not STING degradation (Extended Data Fig. 2.6a). Basal levels of LC3 lipidation appeared to be higher in ATG9-deficient cells, but cGAMP-induced STING degradation was normal in these cells (Extended Data Fig. 2.6b). As ER stress induces autophagy (Hoyer-Hansen and Jaattela, 2007), we next tested whether STING, as an ER transmembrane adapter protein, activated autophagy through inducing ER stress or directly functioning as an ER stress sensor. Dithiothreitol (DTT) or Thapsigargin, known to induce the accumulation of misfolded proteins on the ER, led to the proteolytic cleavage of ATF6 and its trafficking from the ER to the Golgi, similar to STING (Ye et al., 2000); however, no LC3 conversion was detected (Extended Data Fig. 2.6d). In contrast, STING induced LC3 conversion without causing ATF6 cleavage and elevation of downstream CHOP protein expression (Extended Data Fig. 2.6d), indicating that STING activation does not induce autophagy through ER stress. STING activation also does not inhibit mTOR as mTOR and 4E-BP1 were dephosphorylated after treatment with Torin1 or EBSS but not after HT-DNA or cGAMP despite that HT-DNA and cGAMP triggered more robust LC3

conversion(Extended Data Fig. 2.6c). We further asked whether STING directly activates ULK1 kinase to induce autophagy. MEF cells deficient in both ULK1 and ULK2 showed normal STING degradation and more LC3 conversion after HT-DNA, cGAMP or DMXAA treatment (Fig. 2.4a). However, ULK1/2 deficiency showed a moderate decrease in LC3 conversion after Torin1 and Rapamycin treatment (Extended Data Fig. 2.6d). It has been reported that not all autophagy initiations were dependent on ULK1/2 (Cheong et al., 2011); moreover, ULK1/2 not only functions importantly in autophagosome nucleation but also maturation (Petherick et al., 2015). We also detected the accumulation of P62 in ULK1/2 deficient cells (Extended Data Fig. 2.6d) and accumulation of premature autophagosome structures in ULK1 Hela cells (Fig. 2.4d). This indicates that ULK1/2 deficiency results in not only the impairment of autophagy induction (LC3 lipidation) but also the blockade of autophagy maturation (LC3-II turn-over). Thus, the overall LC3-II level after conventional autophagy induction remained almost unchanged in ULK1/2-deficient MEF cells (Extended Data Fig. 2.6e) while STING-induced LC3-II levels were much higher (Fig. 2.4a). In conclusion, STING-induced autophagy is uncoupled from cytosolic mTOR inhibition.

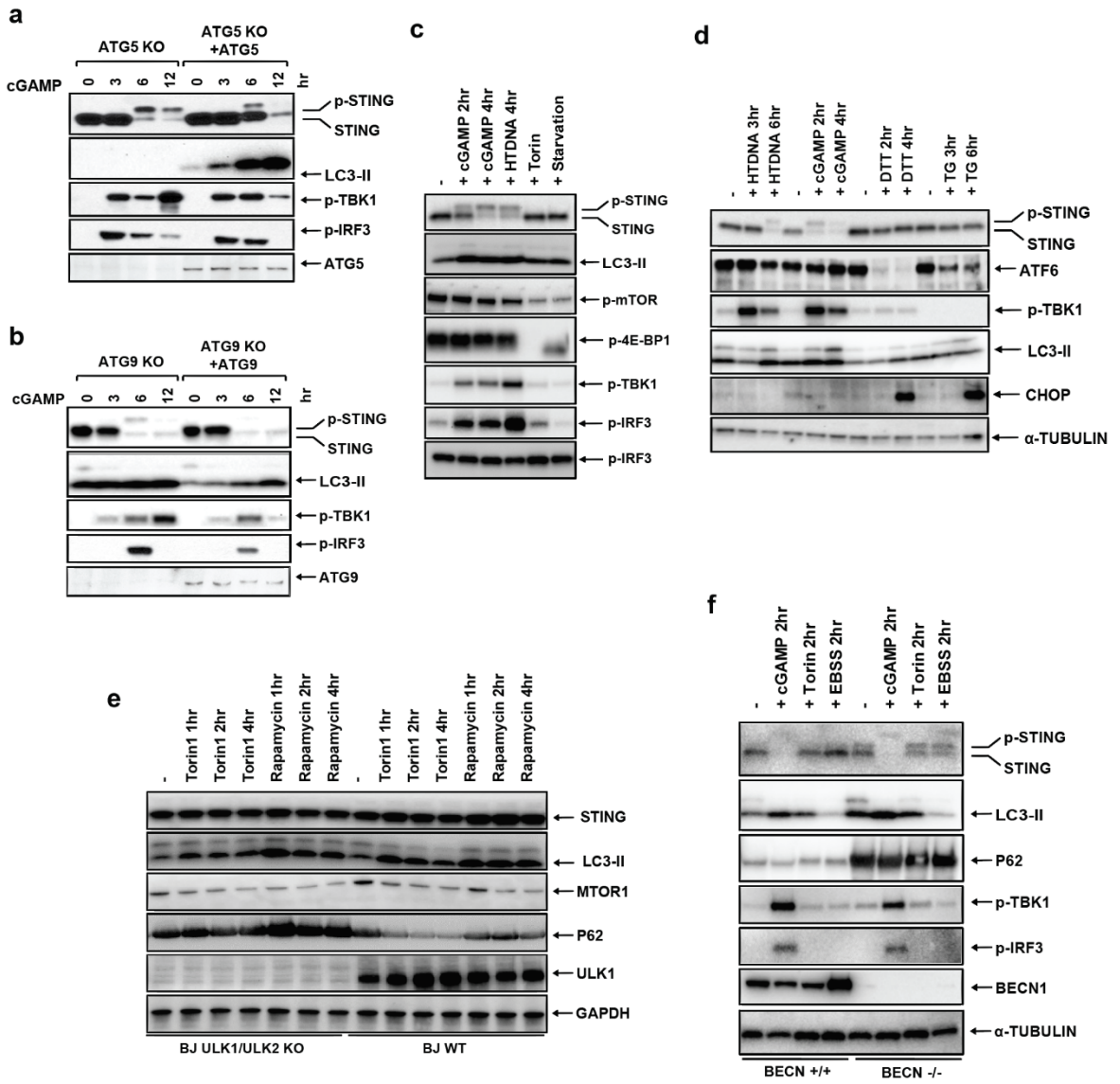

Extended Data Figure 2.6. STING-induced autophagy is uncoupled from cytosol mTOR inhibition. a, ATG5 is required for LC3 lipidation but dispensable for STING degradation induced by cGAMP. *Atg5*$^{-/-}$ or *Atg5*-reconstituted BJ cells were stimulated with cGAMP for indicated time followed by immunoblotting of cell lysates. **b,** ATG9 is dispensable for STING degradation. *Atg9*$^{-/-}$ or *Atg9*-reconstituted BJ cells were stimulated with cGAMP for indicated time followed by immunoblotting of cell lysates. **c,** STING activation does not induce mTOR inhibition. BJ cells were treated with cGAMP, HT-DNA, Torin or Rapamycin for indicated time followed by immunoblotting of cell lysates. **d,** STING activation does not induce ER stress. BJ cells were treated with cGAMP, HT-DNA, DTT or Thapsigargin (TG) for indicated time followed by immunoblotting of cell lysates. **e,** Similar to **Fig. 2.4a,** ULK1 and ULK2 are

not essential for LC3 conversion by conventional autophagy. Wild type and *ULK1/2*$^{-/-}$ MEF cells were stimulated with Torin 1 or Rapamycin at indicated time followed by immunoblotting of cell lysates. **f,** Similar to **Fig. 2.4c,** BECN1 is not essential for LC3 conversion by conventional autophagy. Wild type and *BECN1*$^{-/-}$ BMDM were stimulated with cGAMP, Torin1 or EBSS at indicated time followed by immunoblotting of cell lysates.

Interestingly, in WIPI2-deficient cells, LC3 lipidation and P62 degradation was largely abolished after HT-DNA or cGAMP treatment while TBK1 and IRF3 phosphorylation as well as STING degradation remained unaffected (Fig. 2.4b). This indicates that STING requires WIPI2 for further LC3-II lipidation independent of downstream TBK1/IRF3 activation, consistent with our previous results. Next, we asked if the VPS34/BECN1 complex, generating PI3P for WIPI2 recruitment (Dooley et al., 2014; Kim et al., 2013a; Russell et al., 2013), functions importantly in STING-mediated LC3 lipidation. Surprisingly, macrophages deficient in BECN1 (*Becn1Fl/Fl, LysM-Cre*) showed higher LC3 conversion than autophagy-sufficient (*Becn1Fl/Fl*) cells after cGAMP, HT-DNA, Torin1 or EBSS treatment (Fig. 2.4c and Extended Data Fig. 2.6f). Similarly, knockout of VPS34 did not abolish LC3 conversion but actually resulted in the additional accumulation of LC3-II after cGAMP treatment (Fig. 2.4f). Recent studies reported that PI3P generation can be recovered by other PI3P resources (Devereaux et al., 2013), and in BECN1 or VPS34 deficient cells, LC3 conversion was not abolished but actually occasionally accumulated (Devereaux et al., 2013; He et al., 2015; Jaber et al., 2012). The different results of LC3 conversion in WIPI2-deficient or VPS34/BECN1-deficient cells are possibly due to the extra role of the VPS34/BECN1 complex in autophagosome maturation (Extended Data Fig. 2.6d and 2.6e). In conclusion, STING activation requires WIPI2 to induce

LC3 lipidation and further autophagosome maturation depends on the formation VPS34/BECN1 and ULK1 complexes.

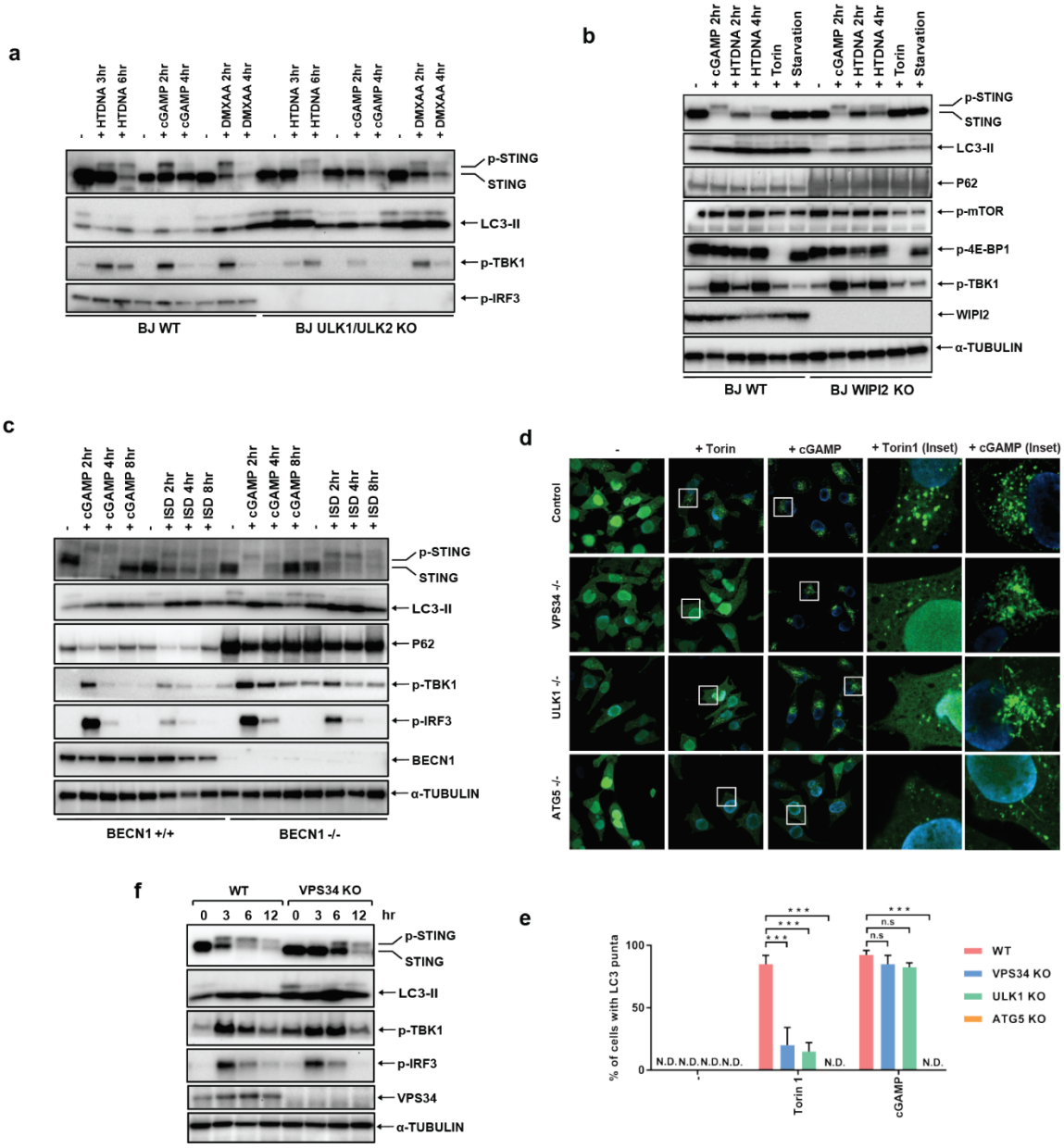

Figure 2.4. STING-induced LC3 lipidation requires WIPI2 and STING degradation is dependent on VPS34. a, STING induced LC3 conversion independent of ULK1 and ULK2. Wild type and *ULK1/2*$^{-/-}$ MEF cells were treated with cGAMP, HT-DNA, or DMXAA for indicated time followed by immunoblotting of cell lysates. **b,** WIPI2 is required for STING-induced LC3 conversion. WIPI2 knock-out BJ cell pool was generated using sgRNA targeting WIPI2. Cells were treated with cGAMP, HT-DNA, Torin and Rapamycin for indicated time followed by immunoblotting of cell lysates. **c,** BECN1 is not essential for LC3 conversion triggered by cGAMP. Wild type and *BECN1*$^{-/-}$ BMDM were stimulated with cGAMP or HTDNA at indicated time followed by immunoblotting of cell lysates. **d,** ULK1 and VPS34 are not required for LC3 lipidation but important for autophagosome maturation induced by cGAMP. *ULK1*$^{-/-}$, *VPS34*$^{-/-}$, or *Atg5*$^{-/-}$ Hela GFP-LC3 cell pools were generated using CRISPR and stimulated with cGAMP or Torin for indicated time. GFP-LC3 puncta formation was showed by fluorescence microscopy. **e,** Quantification of the percentage of cells with GFP-LC3 peri-nuclear foci formation. N.D., not detectable. **f,** VPS34 is required for STING degradation. VPS34 knock-out BJ cell pool was generated using sgRNA targeting VPS34. Cells were treated with cGAMP for indicated time followed by immunoblotting of cell lysates.

Previous results showed that deficiencies of autophagy genes including ATG5, ATG9, WIPI2, BECN1 and ULK1/2 do not block STING degradation, indicating that autophagy is not essential for STING degradation. However, in VPS34 knockout cells, STING degradation was greatly inhibited (Fig. 2.4f). This is consistent with previous studies that VPS34 is not only important for autophagy but also for the multivesicular bodies pathway (MVB) by incorporating into different complexes (Funderburk et al., 2010; Futter et al., 2001; Jaber et al., 2012). Imaging at different time points also revealed that STING partially colocalized with markers of several organelles and vesicles along the trafficking pathway, specifically into two routes: ERGIC (ERGIC53) - autophagosome (GFP-LC3) - lysosome (LAMP1) (Fig. 2.3a) and cis-Golgi (GM130) - trans-Golgi network (TGN38) - endosomes derived from TGN (GGA3) - late endosome (CD63) - lysosome (LAMP1); Extended Data Fig. 2.7a and 2.7b). In the presence of bafilomycin A1, STING colocalized with Rab7a, a GTPase associated with the late endosome (Extended Data Fig. 2.7c and 2.7d). Knockdown of Rab7a by RNAi slowed

down STING degradation and led to accumulation of phosphorylated forms of TBK1 and IRF3 (Extended Data Fig. 2.7e). Rab7a depletion also led to enhanced LC3 conversion even in the absence of stimulation (Extended Data Fig. 2.7e), consistent with an important role of Rab7a in the degradation of LC3-positive autophagosomes (Eskelinen, 2005; Gutierrez et al., 2004; Hyttinen et al., 2013; Jager et al., 2004).

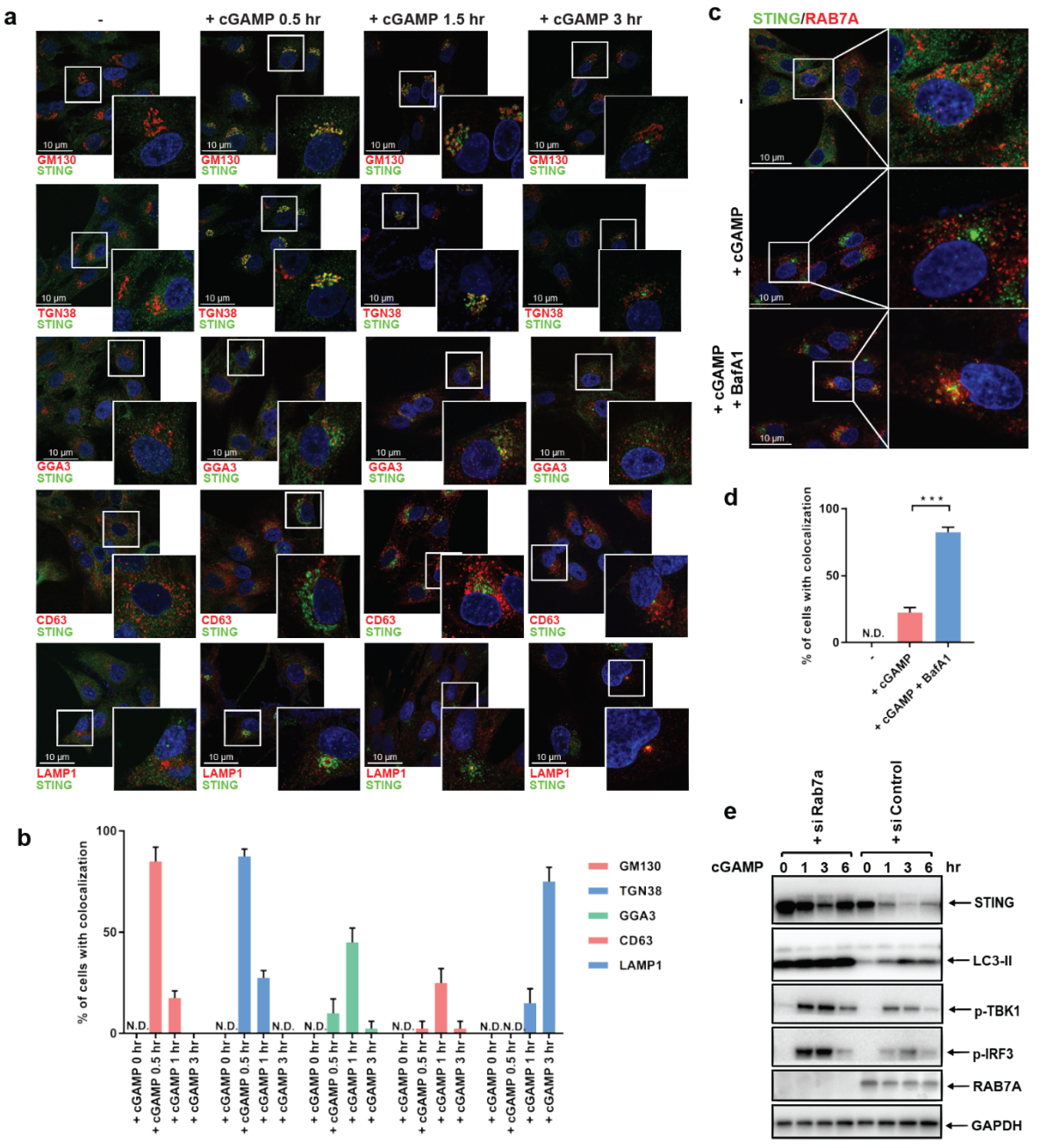

Extended Data Figure 2.7. cGAMP-bound STING traffics through Golgi-endosome or ERGIC-autophagosome to lysosome. a, BJ cells were stimulated with cGAMP for indicated time. Cells were immunostained with a STING antibody together with an antibody against GM130 (cis-Golgi), TGN38 (trans-Golgi), GGA3 (post-Golgi vesicles), CD63 (late endosome) or LAMP1 (lysosome), followed by immunofluorescence microscopy. **b,** Quantification of the percentage of cells in which STING colocalized with different organelle

markers. N.D., not detectable. **c,** BJ cells were stimulated with cGAMP in the presence or absence of Bafilomycin A1 (BafA1). Cells were immunostained with an antibody specific for STING or RAB7A followed by microscopy. **d,** Quantification of the percentage of cells that STING colocalized with RAB7A. N.D., not detectable. **e,** BJ cells were transfected with siRNA targeting RAB7A or a control siRNA for 3 days, followed by stimulation with cGAMP for indicated time. Cell lysates were analyzed by immunoblotting.

ARFs GTPase are required for STING trafficking and signaling

Brefeldin A and Golgicide A inhibit ARF GTPases by competitively binding to ARFGEF family including GBF1 to block COP-I vesicle trafficking (Niu et al., 2005; Saenz et al., 2009). Both inhibitors blocked phosphorylation of TBK1 and IRF3 induced by DNA but not Poly(I:C) (Extended Data Fig. 2.2c) as well as LC3 conversion triggered by cGAMP (Extended Data Fig. 2.2b), suggesting that ARF proteins and ARFGEF proteins are specifically involved in the DNA signaling pathway. To test if cGAMP activates ARF1, we stimulated BJ and HEK293T-STING cells with cGAMP and then immunoprecipitated GGA3, an effector protein that is known to bind specifically to GTP-bound ARF1. At 4 hours after cGAMP stimulation, which corresponded to the peak of phosphorylation of STING, TBK1 and IRF3, GGA3 associated with ARF1, indicating that ARF1 was activated (Fig. 2.5a). In support of an important role of ARF1 in STING signaling, two different pairs of siRNA against ARF1 strongly inhibited induction of IFN-β and CXCL10 by HT-DNA but not Poly(I:C) in BJ cells (Fig. 2.5b and 2.5c). Knockdown of ARF1 but not ARF4 also blocked STING translocation to Golgi in Hela cells, whereas knockdown of ARF3, ARF5 and ARF6 partially inhibited STING trafficking (Fig. 2.5d). It indicates that in most cell lines, ARF1 plays a major role in STING trafficking and downstream activities. As GBF1, one of the major GEF regulators of ARF GTPase, is a

target of Brefeldin A and Golgicide A, we tested its interaction with STING by coimmunoprecipitation. Indeed, GBF1 was associated with STING in cGAS-stimulated HEK293T cells stably expressing WT STING, but not a STING mutant defective in cGAMP binding (Extended Data Fig. 2.8a). cGAMP stimulation also led to co-localization of STING with GBF1, ERGIC-53, the COP-I coat protein β-COP and the cis-Golgi marker GM130; such co-localization was abolished by Golgicide A (Extended Data Fig. 2.8b). These results suggest that cGAMP induces STING interaction with ARF GTPase GEF regulator on ERGIC further triggering ARF GTPase activity for STING membrane trafficking which licenses downstream autophagy activation and interferon response.

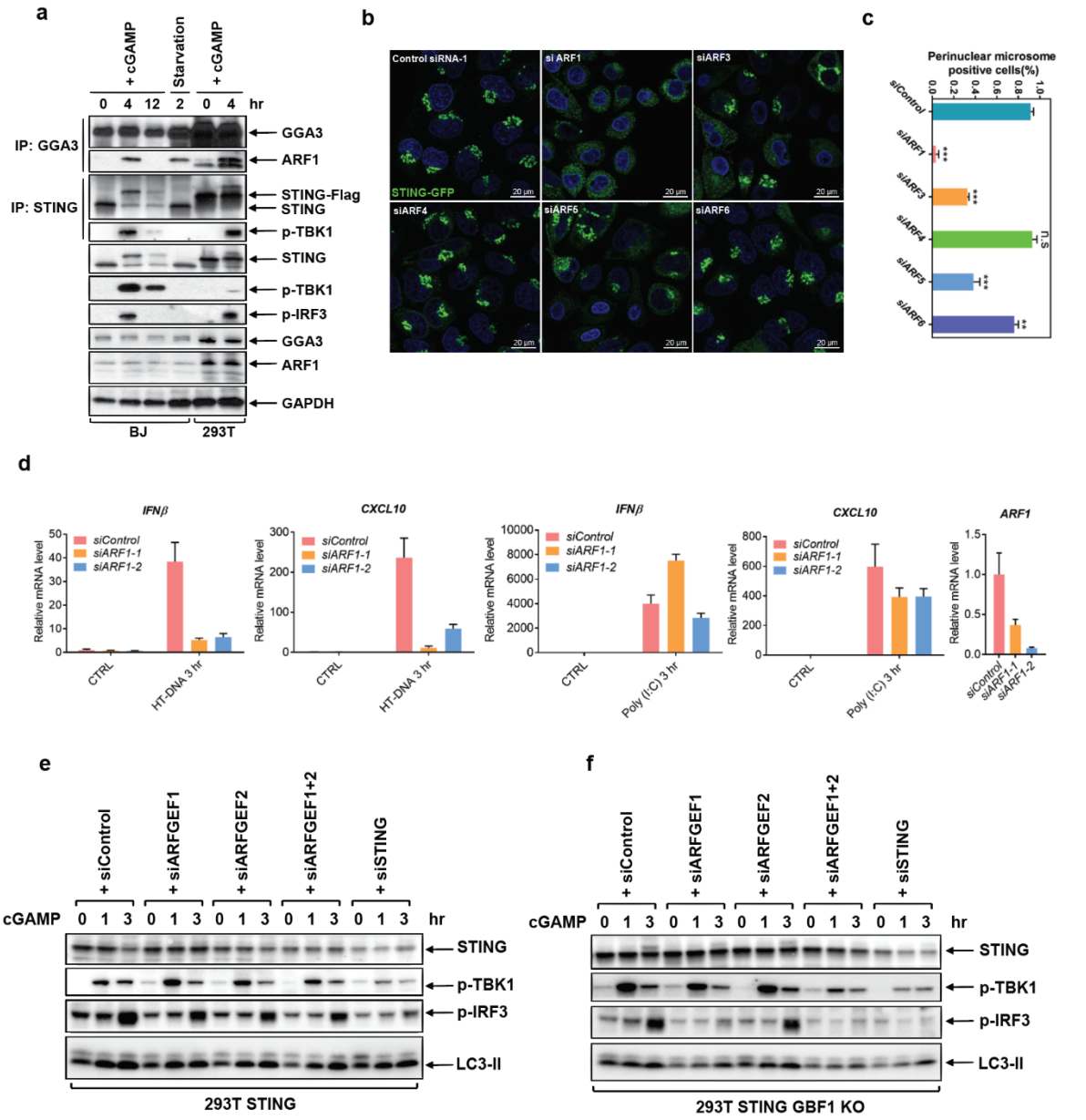

Figure 2.5. STING activates ARFGEF and ARF GTPase families for its membrane trafficking. a, cGAMP stimulates ARF1 GTPase activity. BJ cells were treated with cGAMP or starvation for the indicated time before cell lysates were immunoprecipitated with an antibody against GGA3 or STING, followed by immunoblotting with the indicated antibodies. **b,** Hela STING-GFP cells were transfected with siRNA targeting different ARF family members for 3 days and then stimulated with cGAMP (75 nM) for 1 hr. STING-GFP foci were quantified by confocal microscopy. **c,** Quantification of the percentage of cells with STING peri-nuclear foci formation. N.D., not detectable. **d,** BJ cells were transfected with two

different siRNAs targeting ARF1 followed by transection with HT-DNA or Poly(I:C) for indicated time. Total RNA was isolated to measure the expression of indicated genes by RT-qPCR. **e,** siRNA targeting ARFGEF1 or ARFGEF2 was transfected into 293T STING-Flag cells before stimulation with cGAMP (0.5 μM) for indicated time. Cell lysates were analyzed by immunoblotting. **f,** Similar to **e,** except that GBF1-deficient 293T-STING-Flag cells were used.

However, BJ cell clones depleted of ARF1 or GBF1 by CRISPR were still capable of lipidating LC3 and phosphorylating TBK1 and IRF3 in response to cGAMP stimulation (Extended Data Fig. 2.8c and 2.8d). The cGAMP signaling pathway in ARF1-/- cells was still sensitive to inhibition by Brefeldin A, suggesting that Brefeldin A also targets at least one other protein in these cells to inhibit cGAMP signaling (Extended Data Fig. 2.8c). It is possible that cloning of ARF1-/- cells leads to a compensatory response such as upregulation of other ARF family member (Donaldson and Jackson, 2011; Popoff et al., 2011; Volpicelli-Daley et al., 2005). Similarly, two different clones of 293T STING-Flag cells depleted of GBF1 by CRISPR were largely normal in lipidating LC3 and activating TBK1 and IRF3 in response to cGAS transfection (Extended Data Fig. 2.8c). To test if the other GTP exchange factors (GEF) for ARF, ARFGEF1 and ARFGEF2, could compensate for the loss of GBF1, we used RNAi to knock down the expression of these proteins in HEK293T-STING cells lacking GBF1. Knockdown of both GEF proteins in the GBF1 knockout cells, but not in WT cells, strongly inhibited TBK1 and IRF3 phosphorylation as well as LC3 lipidation in response to cGAMP (Fig. 2.5e and 2.5f). Knock down of ARFGEF1 alone, but not ARFGEF2 alone, in the GBF1 knockout cells also led to significant inhibition of IRF3 phosphorylation and LC3 conversion. These results suggest that GBF1 and ARFGEF1, and to a lesser extent ARFGEF2, play an

important albeit redundant role in STING trafficking, IRF3 activation and autophagy induction.

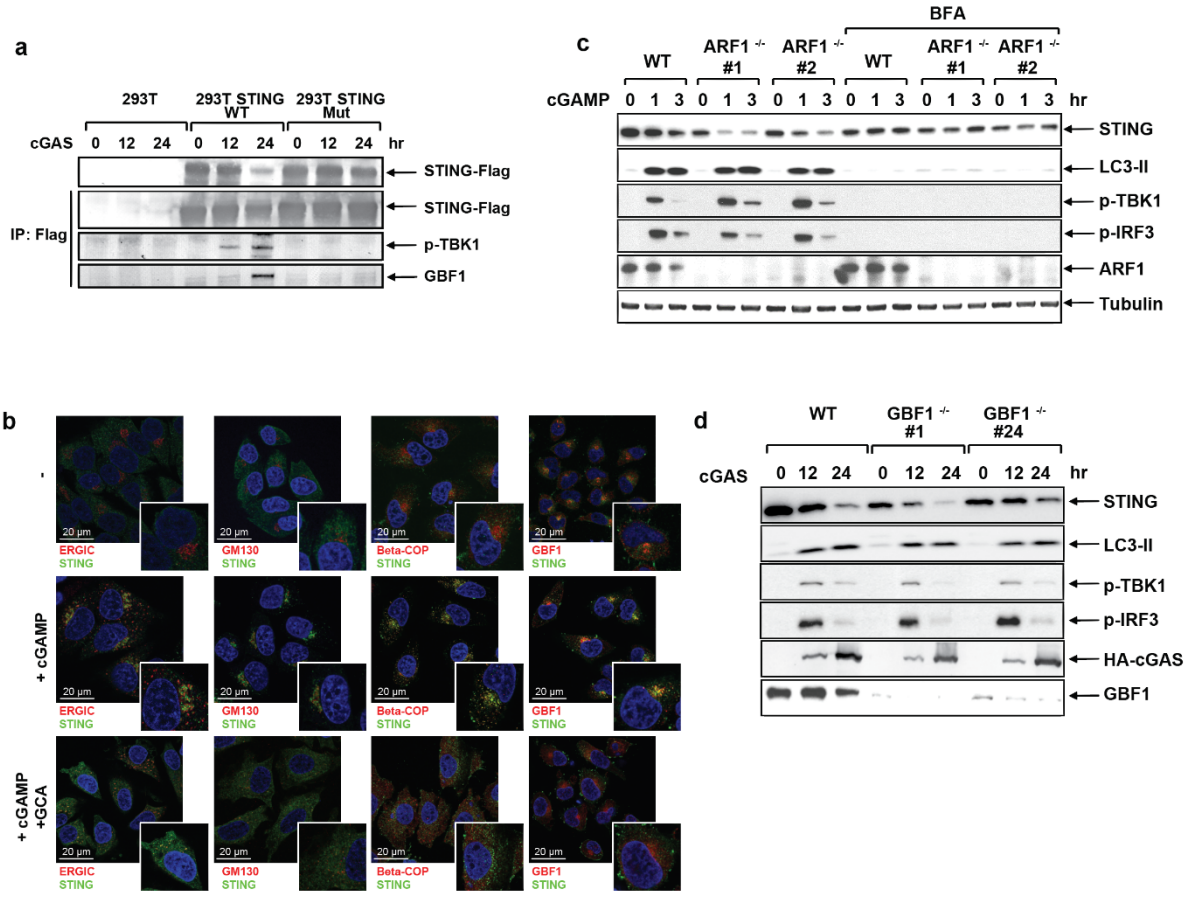

Extended Data Figure 2.8. Deficiency in GBF1 or ARF1 is not sufficient for abolishing STING trafficking and activation. a, cGAMP induces STING interaction with GBF1. 293T cells stably expressing WT or mutant STING were transfected with a cGAS expression plasmid (0.5 μg/ml) for the indicated time. STING in the cell lysates was immunoprecipitated with a Flag antibody, and the precipitates were analyzed by immunoblotting with indicated antibodies. **b,** cGAMP induces STING colocalization with GBF1. HeLa cells stably expressing STING-Flag were stimulated with cGAMP in the presence or absence of Golgicide A (GCA). Cells were immunostained with indicated antibodies followed by fluorescence microscopy. **c,** Two independent clones of ARF1-/- HEK293T STING-flag cells were generated by CRISPR. These and WT cells were stimulated with cGAMP (0.5 μM) for the indicated time in the presence or absence of Brefeldin A (BFA, 2 μM). Cell lysates were analyzed by immunoblotting. **d,** Two GBF1-/- clones were generated in 293T STING-flag cells by

CRISPR. cGAS expression plasmids (0.5 μg/ml) were transfected into these as well as WT cells for the indicated time before cell lysates were analyzed by immunoblotting.

SEC24C is essential for STING membrane trafficking and downstream activation

Trafficking of proteins in the membrane and lumen of the ER initiates through the budding of vesicles that requires the GTPase SAR1A and the COP-II complex that includes SEC24 (Brandizzi and Barlowe, 2013; Saitoh et al., 2009). To test the role of SEC24C and SAR1A in the cGAS-STING signaling pathway, we used siRNA to knock down the expression of SAR1A or SEC24C in HeLa cells stably expressing STING-GFP. Two different pairs of siRNA targeting SAR1A or SEC24C largely blocked STING puncta formation induced by cGAMP (Fig. 2.6a and 2.6b). The depletion of each protein also inhibited induction of IFNβ and the chemokine CXCL10 by DNA or cGAMP, but not Poly(I:C) (Fig. 2.6c and 2.6d). Similar to siRNA that targets STING, two pairs of siRNA targeting SEC24C largely abolished the phosphorylation of TBK1 and IRF3 triggered by cGAMP (Fig. 2.6e). We further used CRISPR technology to knock out SEC24C in HEK293T-STING cells. A single-guide RNA (sgRNA) against SEC24C was efficient in nearly depleting endogenous SEC24C in these cells without single cell cloning (Fig. 2.6f). Depletion of SEC24C inhibited LC3 conversion and phosphorylation of TBK1 and IRF3 (the residual activity may be due to the presence of some WT cells in the pool). When the knockout cells were repleted with Sec24C, the cGAMP signaling pathway was fully restored (Fig. 2.6f). The mutagenesis screen of STING identified the region spanning residues 330-334 as being important for STING trafficking and downstream signals, including TBK1/IRF3 phosphorylation and LC3 lipidation (Extended

Data Fig. 2.3a and 2.3b). The sequence surrounding the ‘LR’ motif (L333 and R334) is evolutionarily conserved among species in which STING is capable of binding cGAMP (Fig. 2.2e). Co-immunoprecipitation experiments showed that cGAMP induced the interaction between STING and SEC24C at early time points and that this interaction was disrupted by the double mutations of L333 and R334 in STING (Fig. 2.6g). These results indicate that formation of the COP-II vesicle is important for the signaling events after cGAMP binds to STING.

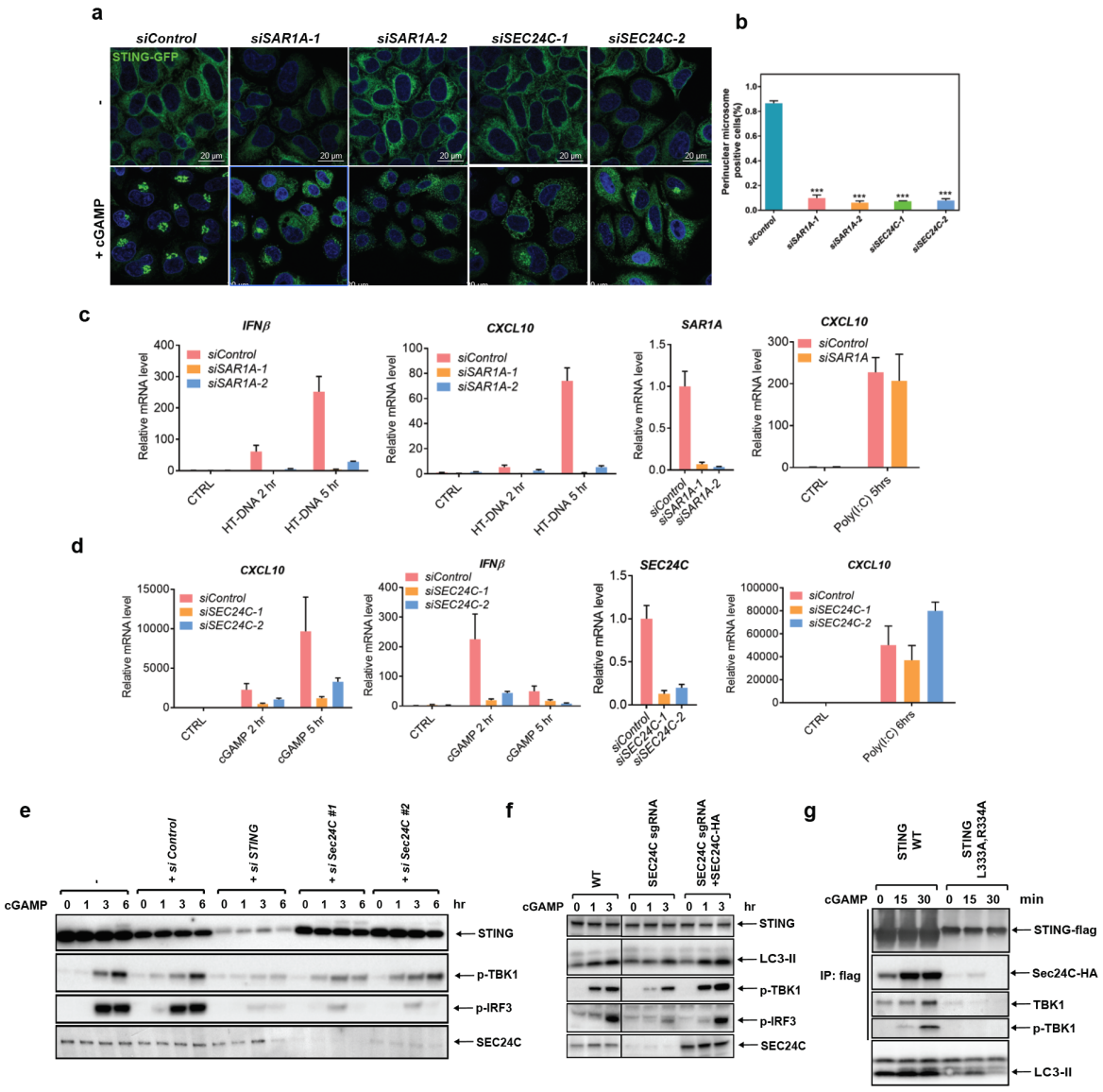

Figure 2.6. SEC24C is important for STING trafficking and downstream activities. a, Hela STING-GFP cells were transfected with siRNAs targeting SAR1A, SEC24C or luciferase (control) for 3 days before stimulation with cGAMP (75 nM) for 1 hr. STING-GFP foci were detected and quantified by confocal microscopy. **b,** Quantification of the cell percentage with colocalized LC3 and STING puncta. All results in this and other figures are representative of at least two independent experiments. N.D., not detectable. **c,** BJ cells were transfected with siRNAs targeting SAR1A for 3 days before transfection with HT-DNA or Poly(I:C) for the indicated time. Total RNA was isolated to measure the expression of indicated genes by RT-qPCR. **d,** Similar to **(c)** except that Hela cells were transfected with siRNAs targeting SEC24C, and cells were stimulated with cGAMP or Poly(I:C). **e&f,** SEC24C is required for LC3

lipidation and IRF3 phosphorylation. **e,** SEC24C were depleted using two pairs of siRNA separated. The cells were stimulated with cGAMP followed by immunoblotting **f,** HEK293T cells stably expressing STING were infected with lentiviruses harboring SEC24C sgRNA to deplete endogenous SEC24C. To restore SEC24C expression, an aliquot of the cells was infected with lentiviruses expressing a sgRNA-resistant SEC24C cDNA. The cells were stimulated with cGAMP followed by immunoblotting. **g,** cGAMP induces STING binding to SEC24C. HEK293T cells stably expressing SEC24C-HA and WT STING-FLAG or the indicated mutant STING were stimulated with cGAMP before cell lysates were prepared for immunoprecipitation using the Flag antibody. Precipitated proteins were analyzed by immunoblotting with the indicated antibodies.

cGAMP-induced autophagy promotes the clearance of cytosolic DNA and viruses

Our findings that the autophagy- and interferon-inducing activities of STING can be uncoupled and that the autophagy-inducing activity of STING predates its interferon-inducing activity during evolution raise the question of the role of autophagy induction by the cGAS-STING pathway. We first examined whether autophagy induction by cytosolic DNA provides a mechanism for the clearance of DNA from the cytosol. HeLa cells stably expressing GFP-LC3 alone or together with STING were permeabilized with the bacterial toxin perfringolysin O (PFO) before delivery of Cy3-labelled ISD. The DNA activates endogenous cGAS to produce cGAMP, which leads to LC3 puncta formation in STING-expressing but not STING-deficient cells (Fig. 2.7a). Co-localization of the LC3 puncta with Cy3-ISD was evident in cells expressing WT STING, but not a STING mutant defective in cGAMP binding (Fig. 2.7a and Extended Data Fig. 2.9a, 2.9b). The intensity of Cy3-ISD in cells expressing the mutant STING was greater than that in cells expressing WT STING (Extended Data Fig. 2.9a), suggesting that DNA accumulated in the cells that failed to activate autophagy. Treatment of cells with Brefeldin A abolished the colocalization of LC3 puncta with Cy3-ISD which also accumulate

cytosolic Cy3-ISD (Extended Data Fig. 2.9b). These results suggest that cytosolic DNA was delivered to the LC3-containing autophagosomes triggered by STING trafficking. Live cell imaging further revealed the process by which Cy3-ISD in the cytosol led to LC3 puncta formation and was then wrapped up by LC3 puncta followed by DNA degradation (Supplementary Video 5). cGAMP delivery further accelerated LC3 puncta formation and DNA degradation (Supplementary Video 6). These results indicate that cGAMP-induced autophagy facilitates the clearance of cytosolic DNA.

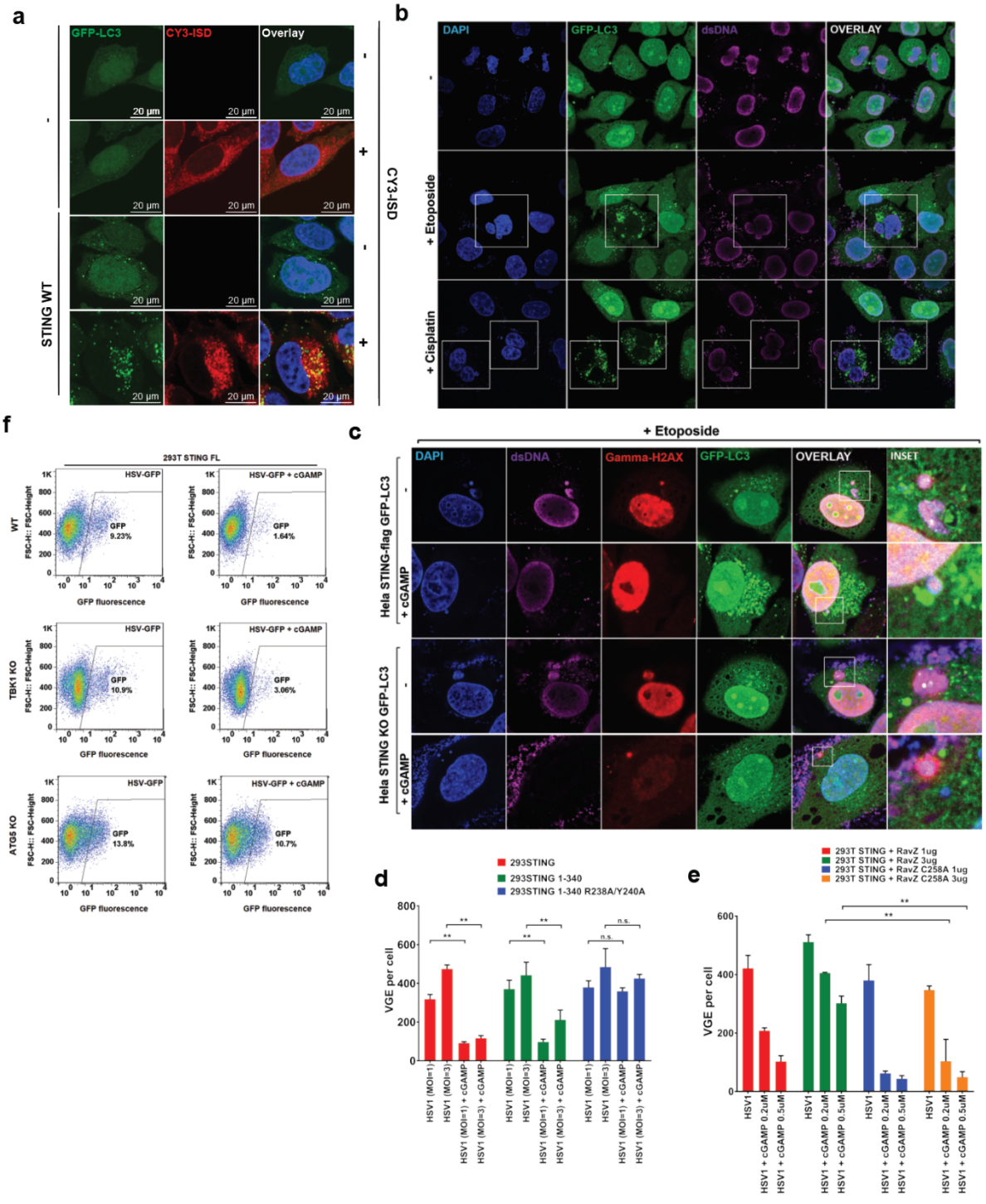

Figure 2.7. cGAMP-induced autophagy mediates the clearance of cytosolic DNA from micronuclei and viruses. a, Cytosolic DNA colocalizes with LC3 vesicles in STING expressing cells. CY3-ISD DNA was delivered into HeLa-GFP-LC3 cells or those stably

expressing STING in the presence of PFO, followed by fluorescence microscopy. Higher magnification of single cell images was shown, representing > 90 % of the cells under examination. **b,** Micronuclei formation induces autophagy. Hela cells stably expressing GFP-LC3 and STING-flag were treated with Etoposide or Cisplatin for 24 hours. Immunofluorescence of anti - double strand DNA and GFP-LC3 were examined for micronuclei and autophagosomes. **c,** STING was knocked out using CRISPR technique and lentiviral vector expressing STING-flag or empty control were used for rescue in Hela cells expressing GFP-LC3. The cells were treated with Etoposide combined with or without cGAMP. The micronuclei were detected using antibodies against gamma H2AX or double strand DNA and autophagosomes were examined using GFP-LC3. **d,** Autophagy induction through STING 1-340 is sufficient to suppress HSV1 replication. HEK293T cells stably expressing WT or mutant STING were stimulated with cGAMP and then infected with HSV1ΔICP34.5 for 12 hr at MOI of 1 or 3. Viral DNA in the infected cells was quantified by qPCR using primers targeting the HSV1 genome. VGE: virus genome equivalent. **e,** LC3 deconjugation by RavZ abrogates cGAMP's anti-viral effects. HEK293T-STING stable cells transiently expressing WT or C258A RavZ were stimulated with indicated concentrations of cGAMP before infection by HSV1Δ ICP34.5 for 8 hr. Viral DNA in infected cells was measured by qPCR to calculate VGE. Data are presented as mean ± SD. **, $p < 0.001$; n.s., not significant (t test, alpha = 0.01). **f,** ATG5 knockout partially reverses cGAMP stimulated anti-HSV1 repression. ATG5 or TBK1 were knocked out using CRISPR technique in STING-expressing HEK293T cells. The cells were then infected with GFP-HSV-1 with or without cGAMP stimulation. FACS were performed to quantify relative viral GFP intensity in each cell line.

To investigate whether cGAMP enhances the clearance of endogenous DNA, we used arabinofuranosyl cytidine (Ara-C) and aphidicolin, two compounds that cause DNA damage by interfering with DNA synthesis. Both Arc-C and aphidicolin treatments led to the appearance of DNA in the cytosol which was detected by an antibody against dsDNA (Extended Data Fig. 2.9c and 2.9d). Importantly, cGAMP treatment led to the disappearance of cytosolic DNA and this effect of cGAMP was blocked by Golgicide A (Extended Data Fig. 2.9c and 2.9d). These results suggest that nuclear DNA damage causes the release of DNA into the cytosol, which is cleared by cGAS-induced autophagy and subsequent degradation in the lysosome. Recent studies also indicate that micronuclei formed by chromosome mis-

segregation during mitosis can trigger the activation of cGAS-STING pathway by the leakage of nuclear DNA(Bakhoum et al., 2018; Harding et al., 2017; Mackenzie et al., 2017; Yang et al., 2017). We used Etoposide or Cisplatin to induce micronuclei formation in Hela cells and found that they recruited cGAS (Extended Data Fig. 2.9e) and also stimulated GFP-LC3 puncta formation (Fig. 2.7b). Moreover, the GFP-LC3 vesicles triggered by Etoposide or combined with cGAMP, targeted micronuclei in cytoplasm, potentially for its clearance (Fig. 2.7c and Extended Data Fig. 2.9e).

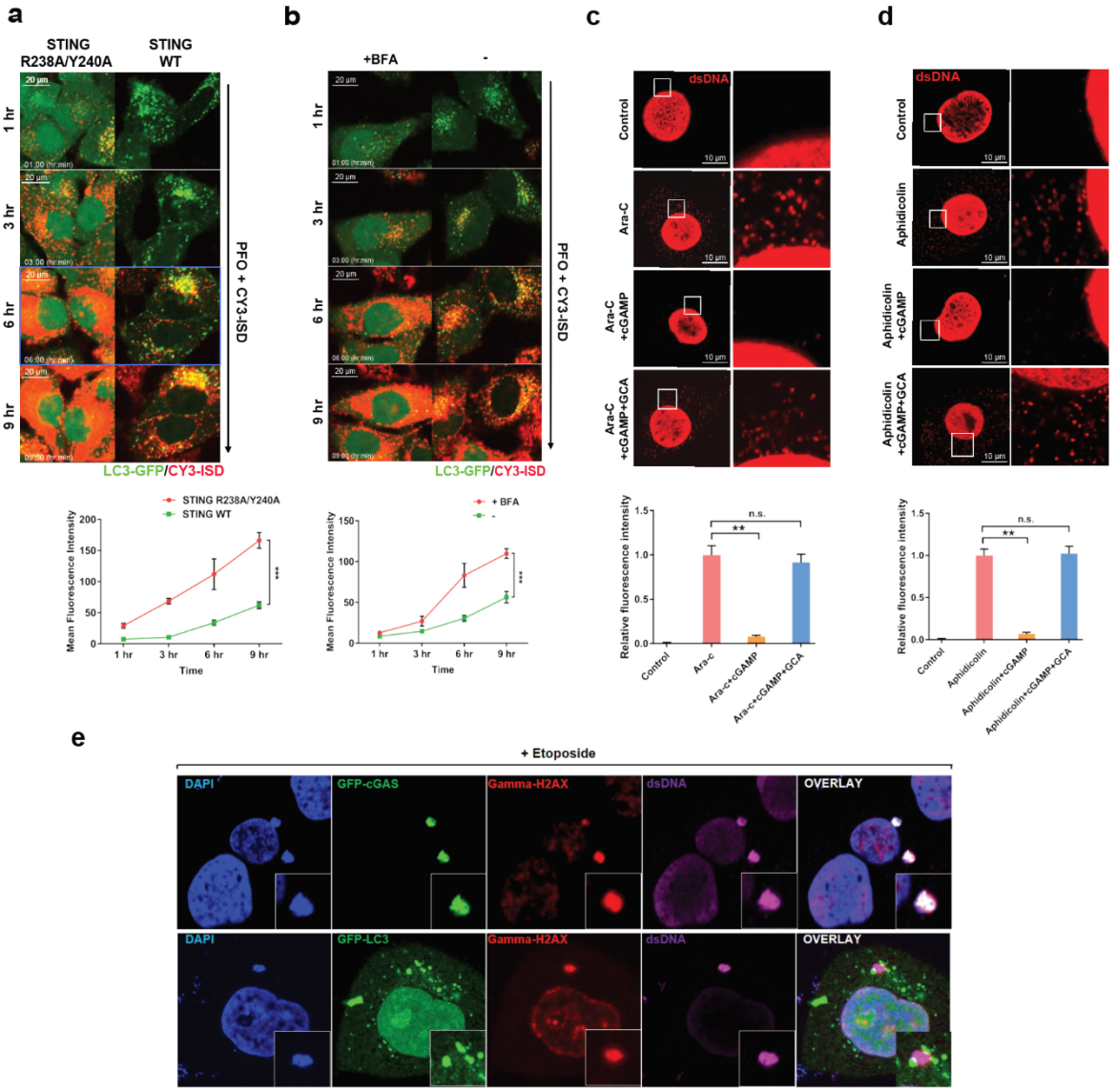

Extended Data Figure 2.9. cGAMP enhances the clearance of cytosolically damaged DNA and micronuclei. a, cGAMP binding by STING enhances the clearance of cytosolic DNA. CY3-ISD was delivered into HeLa-GFP-LC3 cells stably expressing WT or mutant (R238A/Y240A) STING. Live cell imaging was carried out with still frames shown at the indicated time. Fluorescence intensity was quantified using Image J from three different areas each of which contains three cells. **b,** DNA-induced autophagy facilitates clearance of cytosolic DNA. HeLa cells stably expressing GFP-LC3 and STING-Flag were treated with Brefeldin A1 (BFA, 2 μM) for 60 min. CY3-ISD was delivered into cells that were permeabilized by PFO. GFP-LC3 and Cy3-ISD fluorescence were monitored by live cell imaging. Still frames at the indicated time are shown, and fluorescence intensity was calculated

from three different areas each of which contains three cells. cGAMP enhances degradation of cytosolic DNA generated by DNA damage drug. **c&d,** cGAMP facilitates clearance of cytosolic DNA generated by Ara-C or aphidicolin. **c,** MEF cells were treated with Ara-C for 12 hr and then stimulated with cGAMP in the presence or absence of Golgicide A (GCA) for another 12 hr. Cytosolic DNA was immunostained with a dsDNA-specific antibody. Intensity of cytosolic DNA staining was quantified using Image J by deducting nucleus staining. Calculations were based on five cells from three different areas. **d,** MEF cells were treated with aphidicolin (10 μg/ml) for 12 hr and then stimulated with cGAMP in the presence or absence of Golgicide A (10 μM). After another 12 hr, cells were immunostained with an antibody specific for dsDNA. Intensity calculations of cytosolic DNA staining were done using Image J by deducting nucleus staining. Quantifications were based on five cells from three different areas. **e,** Micronuclei are targeted by cGAS and autophagosome. Hela cells expressing GFP-LC3 and STING-flag were treated with Etoposide as described above to generate micronuclei. The immunofluorescence staining was carried out using antibodies for double strand DNA, gamma-H2AX and cGAS.

Our previous works suggest that 1-340 STING did not activate TBK1 and IRF3 but was still capable of inducing autophagy activity. To understand the pattern of cellular activity downstream of STING signaling after cGAMP stimulation, we further performed RNA sequencing in HEK293T cells expressing different STING mutants such as full length wild type STING, full length S366A STING, wild type 1-340 STING and 1-340 STING R238A. Many interferon-stimulated genes (ISGs) and TNF-related genes were upregulated in HEK293T cells expressing full length wild type STING after transfection with plasmids expressing cGAS (Extended Data Fig. 2.10a). In the cells expressing S366A STING, upregulation of ISGs were abolished while the expression of TNF related genes was elevated, consistent with our previous study that S366A is only important for IRF3 phosphorylation through TBK1 activation but not necessary for IKKβ activation (Extended Data Fig. 2.10a and 2.10b). The upregulation of ISGs and TNF-related genes was abolished in 1-340 STING-expressing cells and almost all the previously noted gene expression was unchanged in the 1-

340 STING R238A cells (Extended Data Fig. 2.10a and 2.10b). It suggests that this truncated form of STING can be used as a specific system to study other functions of STING that are uncoupled from interferon and other inflammatory responses. Next, we tested whether cGAMP-induced autophagy is important for host defense against virus infection. HEK293T cells expressing full-length STING were treated with or without cGAMP, followed by infection with HSV1. Quantitative PCR (qPCR) measurement of the viral genome equivalents (VGE) revealed that cGAMP treatment significantly decreased virus titer (Fig. 2.7d). Importantly, cells expressing STING (1-340), but not a STING mutant defective in cGAMP binding (R238A/Y240A), also had reduced HSV1 titer in response to cGAMP treatment (Fig. 2.7d), indicating that the autophagy-inducing function of truncated STING (1-340) is potentially important for cytosolic clearance of the virus. Similarly, HIV1-GFP and HSV1-GFP viral titers were significantly lower in cGAMP-stimulated HEK293T cells expressing full-length STING or STING (1-340), but not the STING (1-340, R238A/Y240A) mutant (Extended Data Fig. 2.11a and 2.11b). Hela cells expressing STING (1-340) showed a constant slower HSV1 growth curve compared with the STING (1-340, R238A/Y240A) mutant after cGAMP stimulation (Extended Data Fig. 2.11c). To further evaluate the role of autophagy in antiviral defense, we employed the Legionella protein RavZ, an enzyme that irreversibly cleaves LC3 from phosphatidylethanolamine on the membrane (Choy et al., 2012). Transfection with 3 μg of WT RavZ expression plasmid in HEK293T-STING cells removed LC3 conjugation (Extended Data Fig. 2.11d) and largely obliterated the inhibitory effect of cGAMP on HSV1 replication (Fig. 2.7e); the residual inhibitory effect of cGAMP may be due to induction of interferons or other antiviral downstream events. In contrast, a catalytically

inactive mutant of RavZ (C258A) did not interfere with the inhibition of HSV1 replication by cGAMP (Fig. 2.7f and Extended Data Fig. 2.11d). Consistently, knocking out of ATG5 but not TBK1 significantly rescued cGAMP-stimulated anti-HSV1 repression as measured by GFP-HSV1 fluorescence intensity and viral genome equivalents (VGE) (Fig. 2.7f and Extended Data Fig. 2.11e). Taken together, these results suggest that cGAMP-induced autophagy plays a crucial role in antiviral defense.

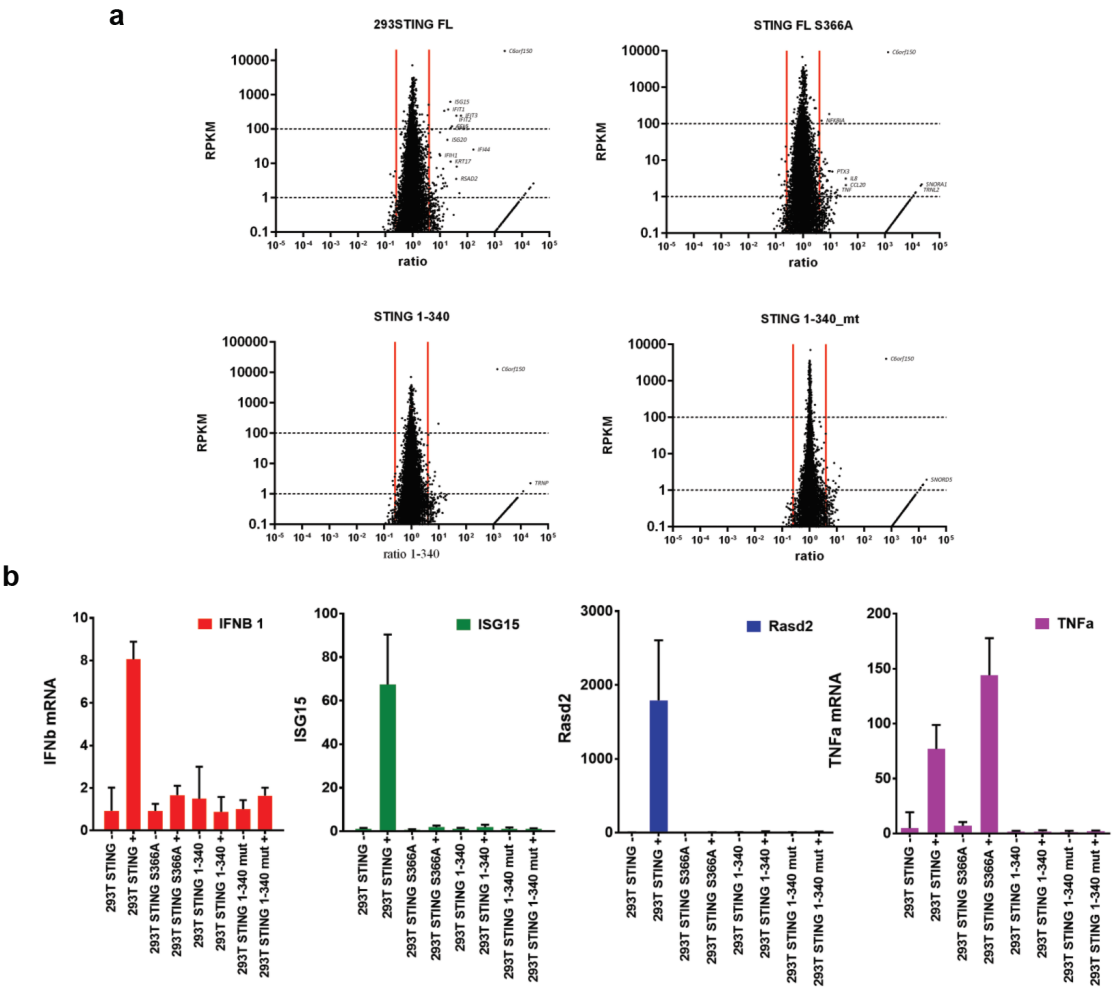

Extended Data Figure 2.10. 1-340 STING is incapable of inducing interferon and inflammatory gene expression. a, HEK293T cells expressing different STING mutants were transfected with plasmids expressing wild type or mutant cGAS. Cells were collected for RNA sequencing as described in METHOD. **b,** Similar to **(a)**, except that cells were collected for RT-qPCR using primers for ISGs, TNFa and GADD34 and GADD45.

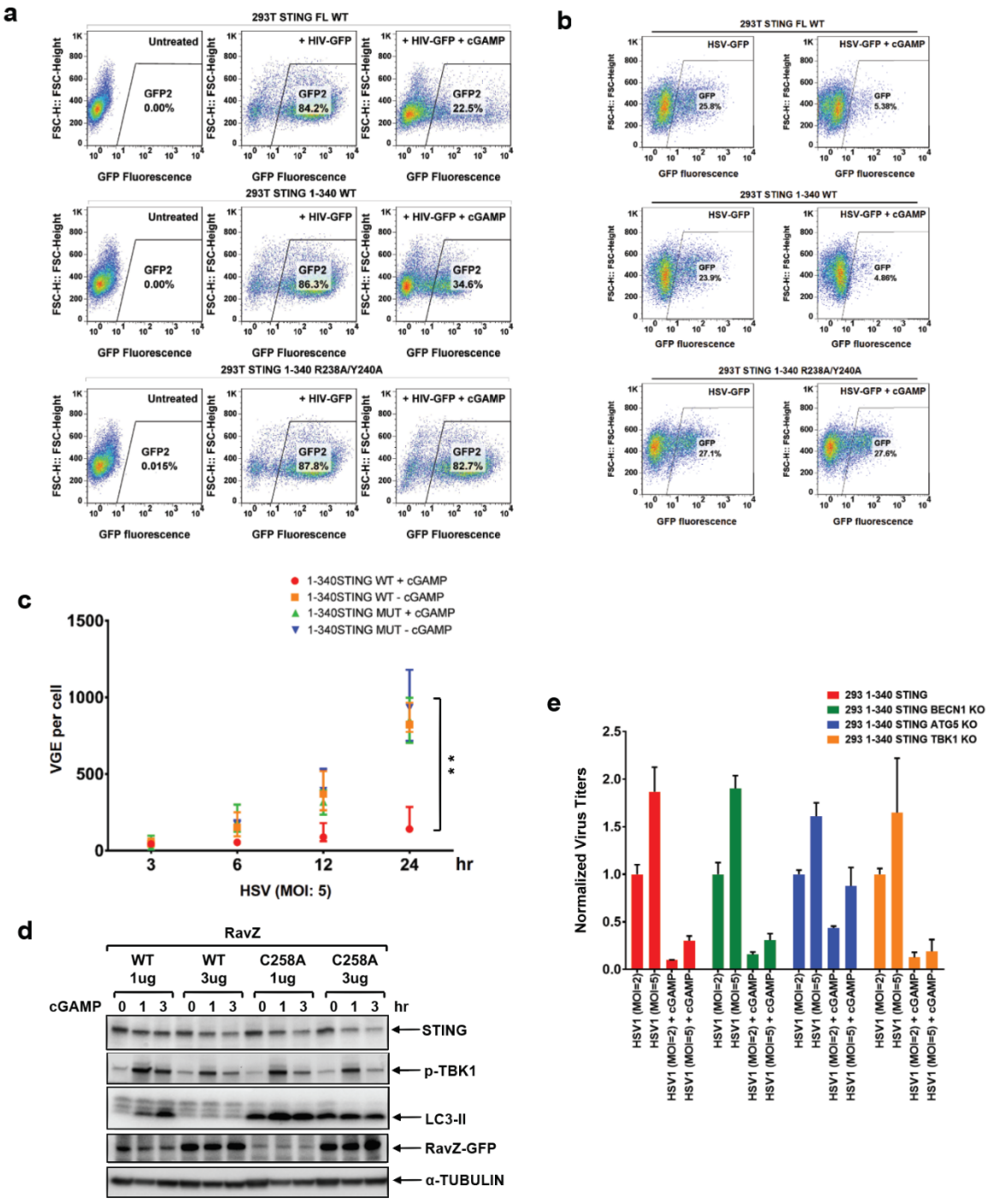

Extended Data Figure 2.11. cGAMP induces anti-viral defense through autophagy. a, cGAMP-induced STING 1-340 activation enhances HIV-1 clearance. 293T cells reconstituted with WT or mutant STING were stimulated with cGAMP and then infected with the

pseudotyped HIV1-GFP virus for 24 hr at MOI = 1. GFP+ cells were analyzed by FACS. The results are representative of two independent experiments. **b,** cGAMP-induced STING 1-340 activation enhances HSV-1 clearance. 293T cells reconstituted with WT or mutant STING were stimulated with cGAMP and then infected with the HSV1-GFP virus for 18 hr. GFP+ cells were analyzed by FACS. The results are representative of two independent experiments. **c,** cGAMP-induced STING 1-340 activation enhances HSV-1 clearance. HEK293T cells stabling expressing 1-340 STING wild type or R238A mutant were stimulated with cGAMP as described before and infected with HSV-1 virus at MOI = 5. At indicated time points, the cells were harvested and virus genome DNA was purified for q-PCR quantification using HSV-1 targeting primer as described before. **d,** RavZ catalyzes LC3 deconjugation. 293T-STING stable cells were transfected with the RavZ expression plasmids (WT or C258A mutant) for 36 hr and then stimulated with cGAMP for indicated time. Cell lysates were analyzed by immunoblotting with the indicated antibodies. **e,** ATG5 knockout partially reverses the cGAMP stimulated anti-HSV1 repression. BECN1, ATG5 or TBK1 were knocked out using CRISPR technique in STING-expressing HEK293T cells. The cells were then infected with HSV1ΔICP34.5 with or without cGAMP stimulation. qPCR using HSV-1 primer were performed to quantify relative virus titers in each cell line.

CHAPTER THREE

CONCLUSION

A unique and important feature of the cGAS-STING pathway of cytosolic DNA sensing is the robust activation of autophagy in addition to induction of interferons and inflammatory cytokines. Both activities depend on the production of cGAMP and its binding to STING as well as STING membrane trafficking. Interestingly, cGAMP-induced LC3 lipidation is independent of TBK1 and the C-terminal signaling domain of STING, which is required for type-I interferon induction (Liu et al., 2015a; Tanaka and Chen, 2012). Conversely, activation of TBK1 and IRF3 is intact in ATG5 deficient cells that are defective in LC3 lipidation and autophagosome formation. Thus, the autophagy- and interferon-inducing activities of STING can be uncoupled. We propose that after cGAMP binding to STING, STING binds to ARFGEF proteins to initiate ARF GTPases activities which then translocates to ERGIC through COP-I and COP-II vesicles. ERGIC serves as the membrane source for WIPI2 recruitment and LC3 lipidation, leading to formation of autophagosomes that target cytosolic DNA and DNA viruses for degradation by the lysosome. A fraction of STING traffics from ERGIC through the Golgi network and post-Golgi vesicles including late endosomes, whereby STING activates TBK1 and IRF3, leading to type-I interferon induction. STING on the autophagosomes or endosomes continue to traffic to the lysosome where STING is degraded in a VPS34 and RAB7 dependent manner (Fig. 2.8).

Unlike the canonical autophagy pathway involving amino acid deprivation, LC3 lipidation induced by cGAMP occurred normally in the absence of mTOR inhibition from the cytosol.

As STING is an ER membrane protein that traffics to ERGIC, which provides the membrane source for LC3 lipidation, it may bypass signal from the cytosol including ULK1 complex activation that is normally required to for autophagosome initiation through mTOR inhibition or AMPK activation. Using an in vitro reconstitution assay, we found that membranes from cGAMP-stimulated ATG5-/- cells can be conjugated with LC3 by cytosolic extracts from ATG5+/+ cells. Imaging and biochemical experiments suggest that ERGIC likely serves as a membrane source of LC3 lipidation. Similarly, ERGIC has been proposed to function as the membrane source for LC3 lipidation in the canonical autophagy pathway induced by starvation (Ge et al., 2013; Ge et al., 2014). However, biochemical reconstitution experiments revealed a marked difference between autophagy induced by cGAMP and that induced by starvation. In the case of cGAMP-induced autophagy, the activity of the membrane fraction is regulated and the cytosolic activity is constitutive. The opposite is true for starvation-induced autophagy. Consistently, we found that, unlike Torin1 or Rapamycin treatment, cGAMP did not induce mTOR inhibition. It is still not clear why ERGIC from cGAMP-stimulated cells gains the ability to conjugate with LC3 and what is the direct autophagy machinery targeted by activated STING. Interestingly, we found that WIPI2 was essential for cGAMP-induced LC3 lipidation and was possibly recruited to the STING-activated ERGIC membrane. We next tested whether the VPS34/BECN1 complex is essential in this scenario since WIPI2 is a PI3P sensor, and the VPS34 complex functions as a PI3P kinase which recruits the WIPI family for LC3 conjugation. However, genetic knockout of VPS34 or BECN1 did not impair LC3 conversion in either conventional autophagy induction using Torin1 or after cGAMP stimulation. It is possible that other sources of PI3P generated by other kinases exists, which may still weakly

support LC3 lipidation and autophagosome initiation (Devereaux et al., 2013). Surprisingly, but consistent with other recent studies (Devereaux et al., 2013; He et al., 2015; Jaber et al., 2012), we did not see the suppression of but rather the occasional additional accumulation of lipid in these KO cells, which indicates that VPS34/BECN1 function is important in not only autophagy initiation but also maturation of the autophagosome. Indeed, cells deficient in VPS34 cannot generate mature GFP-LC3 vesicles despite recruitment of GFP-LC3 to peri-nuclear regions.

Brefeldin A and Golgicide A strongly inhibit STING trafficking and all of its downstream functions, suggesting that GBF1 and ARF GTPases are important for STING trafficking. Indeed, RNAi of ARF1 or GBF1 markedly inhibits interferon induction. However, cell lines completely depleted of either ARF1 or GBF1 do not exhibit an obvious defect of STING trafficking or signaling. This may be due to compensatory expression of other ARFs or ARFGEFs in stable cells that are permanently depleted of ARF1 or GBF1. Indeed, in GBF1-/- but not wild-type cells, knockdown of ARFGEF1 and ARFGEF2 led to a strong inhibition of IRF3 phosphorylation and LC3 conversion. It is also interesting to note that ARF1 is activated in cells stimulated with cGAMP and that cGAMP induces the association of STING with GBF1, which activates ARF1. In this regard, it is possible that cGAMP-bound STING activates ARF GTPases through ARFGEF to potentialize ERGIC, leading to enhanced LC3 lipidation and autophagosome formation.

After STING activates autophagy and the interferon pathway, STING itself is degraded, providing a mechanism for termination of the signaling cascade. Surprisingly, STING

degradation is not impaired in cells lacking ATG5, ATG9, WIPI2, BECN1 or ULK1, suggesting that autophagy is not essential for STING degradation. However, STING degradation is inhibited by Bafilomycin A or Chloroquine, suggesting that STING is degraded in the lysosome through an alternative membrane traffic route. Since STING traffics from ER to Golgi, it is plausible that STING buds out from Golgi into endosomes, which subsequently form multivesicular bodies that then fuse with lysosome where STING is degraded. In support of this model, time-lapse imaging of STING shows that STING traffics not only to COP-I vesicles (marked by β-COP), ERGIC (ERGIC-53) and autophagosomes (LC3-II) (Fig. 2.3a and Supplementary Video 1, 2, 3) but also to cis-Golgi (marked by GM130), trans-Golgi (TGN38), Golgi-derived endosomes (GGA3), late endosomes (CD63) and lysosomes (LAMP1) (Extended Data Fig. 2.7a and 7b). RAB7A has been reported to play an important role in the maturation of both autophagosomes and endosomes and their subsequent fusion with lysosomes. (Gutierrez et al., 2004; Jager et al., 2004). Consistent with an important role of RAB7A in STING degradation, we found that depletion of RAB7A significantly inhibited STING degradation and enhanced phosphorylation of TBK1 and IRF3. Unlike other autophagy genes including ATG5, ATG9, WIPI2, ULK1 or BECN1, VPS34 is important for STING degradation (Fig. 2.4f) which is consistent with its multiple roles in both autophagosome maturation and multivesicular bodies (MVB) formation (Funderburk et al., 2010). VPS34 functions separately by forming different complexes with either ATG14 in autophagy or UVRAG in the MVB pathway (Itakura and Mizushima, 2009).

Remarkably, the sea anemone, which predates humans by more than 500 million years, possesses a STING homologue (nvSTING) lacking the C-terminal TBK1 activation domain

(Kranzusch et al., 2015) but still capable of stimulating LC3 conversion in response to cGAMP. Thus, autophagy induction is an ancient and highly conserved function of the cGAS-STING pathway that predates the emergence of the type-I interferon pathway in vertebrates. We found that cGAMP-induced autophagy is important for the clearance of cytoplasmic DNA and viruses, including HSV-1 and HIV-1. It is tempting to speculate that this clearance of DNA and microbes in the cytoplasm by autophagy may be the primordial function of the cGAS-STING pathway prior to emergence of the interferon pathway in vertebrates. It remains to be determined how DNA and viruses are targeted to the LC3-containing autophagosome. Intriguingly, recent studies have shown that autophagy is important for cytoplasmic antigen presentation through MHC-II (Crotzer and Blum, 2009; Lee and Iwasaki, 2008; Lee et al., 2007; Schmid and Munz, 2007). Moreover, ERGIC plays a critical role in cross-presentation of antigens through MHC-I (Cebrian et al., 2011; Joffre et al., 2012). Thus, the cGAS-STING pathway not only directly eliminates cytoplasmic invaders through autophagy and by producing antiviral effects such as IFNs, but also activates adaptive immune responses by enhancing antigen presentation and expression of costimulatory molecules. Such a unique mechanism of action of cGAMP, namely induction of vesicle trafficking, autophagy and innate immunity, may explain why the cGAS-STING pathway is particularly important for immune defense against microbial pathogens and malignant cells (Chen et al., 2016b; Deng et al., 2014; Wang et al., 2017; Woo et al., 2014).

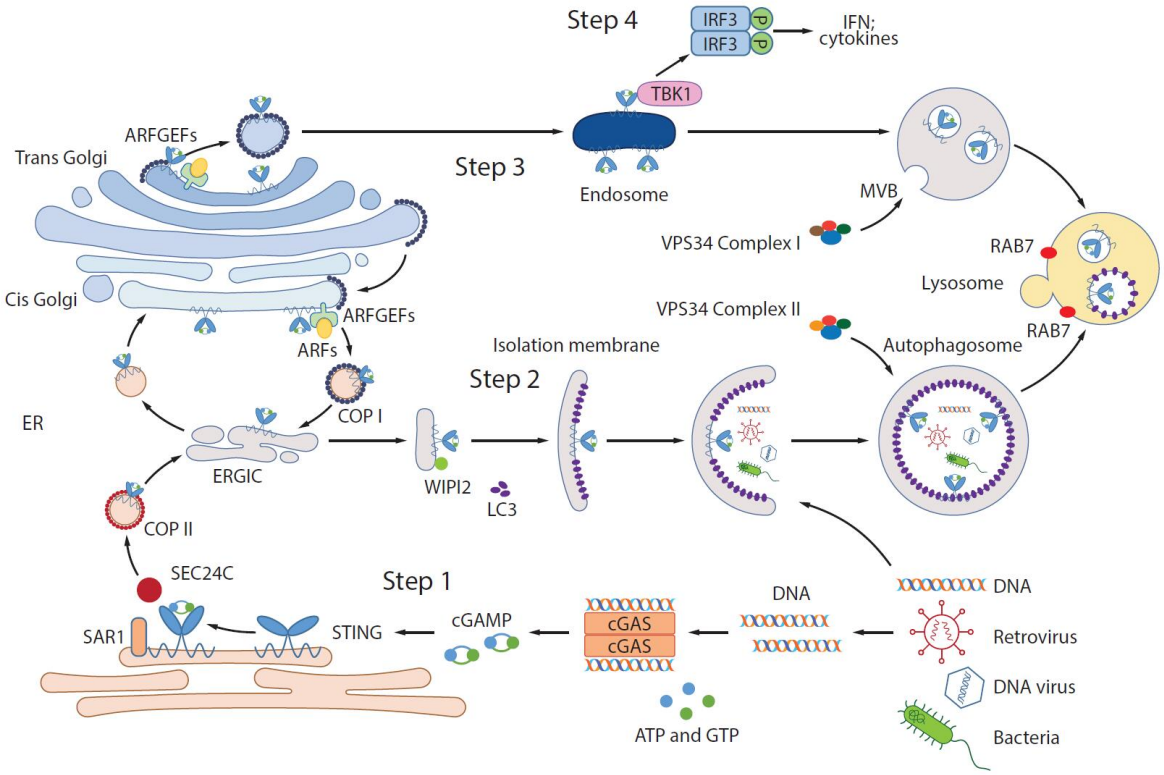

Figure 2.8. Model of STING membrane trafficking and autophagy induction. A model of DNA-induced autophagy through the cGAS-STING pathway. Step 1: DNA from pathogens or damaged cells activates cGAS to synthesize cGAMP. cGAMP binds to STING and triggers STING translocation from ER to ERGIC and Golgi in a process that depends on SAR1, SEC24C and ARFs. Step 2: ERGIC containing cGAMP-bound STING serves as a membrane source for LC3 recruitment and lipidation dependent on WIPI2. LC3 positive membranes target DNA and pathogens to autophagosomes which are subsequently fused with lysosome. Step 3: cGAMP-bound STING can further translocate through trans-Golgi network (TGN) and endosomes to lysosomes for degradation through the multivesicular body (MVB) pathway. Both MVB pathway and autophagosome maturation requires VPS34 kinase but in different complexes. The vesicles all fuse with lysosomes which requires RAB7 GTPase. Step 4: cGAMP-bound STING activates TBK1 and IRF3 to induce type-I interferons.

CHAPTER FOUR

METHODS

Reagents and general methods.

2'3'-cGAMP was synthesized as previously described (Zhang et al., 2013). Poly(I:C), herring testis (HT) DNA, Ara-C and Aphidicolin were from Sigma-Aldrich. ISD and CY3-ISD were prepared from equimolar amounts of sense and antisense DNA oligonucleotide (sense: 5-TACAGATCTACTAGTGATCTATG-3; anti-sense: 5-ACTGATCTGTACATGATCTACA-3). The oligonucleotides, synthesized at Sigma-Aldrich, were heated at 95°C for 5 min and cooled to room temperature. Brefeldin A, Golgicide A, BX-795, TPCA-1, MG132 and Velcade were purchased from Selleckchem; Bafilomycin A1 and Chloroquine were from Invivogen; siRNA oligos were purchased from Sigma and transfected into cells using Lipofectamine RNAiMAX (Thermo Fisher Scientific). The sense strand sequences are shown in Table S1.

The procedures for IRF3 dimerization assay, SDS-PAGE, Western blotting, immunoprecipitation have been described previously (Seth et al., 2005). Different proteins were immunoblotted with their antibodies on the same membrane but if unsuccessful, we used the exact same amount of samples loaded in a different gel for immunoblotting. cGAMP was delivered into cells by permeabilization with digitonin (10 μg/ml) for 15 min in buffer A (50 mM HEPES-KOH, pH 7.2, 100 mM KCl, 3 mM MgCl2, 0.1mM DTT, 85 mM Sucrose, 0.2% BSA, 1mM ATP). The concentration of cGAMP used in stimulating BJ cells was 0.2 μM or 0.5 μM unless indicated otherwise. ISD, HT-DNA and Poly(I:C) were transfected into cells

using lipofectamine 2000 (Thermo Fisher) at a concentration of 2 μg/ml. CY3-ISD (1 μg/ml) was delivered into cells by permeabilization with perfringolysin O (PFO; 0.1 μg/ml). All inhibitors were used to treat cells for 1 hour before DNA transfection or cGAMP stimulation at the following concentrations: Brefeldin A: 2 μM; Bafilomycin A1: 0.2 μM; Chloroquine: 20 μM; MG132: 10 μM; Velcade: 2 μM; Golgicide A: 10 μM.

Antibodies.

The rabbit polyclonal antibodies against human STING were generated and purified as described previously (Tanaka and Chen, 2012). Rabbit antibodies against mouse STING, p-IRF3(Ser396), p-TBK1(Ser172), p-IKKβ(Ser177), ATG5, ATG9, Beclin1, calreticulin and GAPDH were from Cell Signaling. Mouse antibody against STING was purchased from R&D Systems; rabbit antibodies against human IRF3, TGN38 and ARF1 and mouse antibody against CD63 were from Santa Cruz Biotechnology; rabbit antibody against LC3 was from Novus Biologicals; mouse antibodies against P62 and GGA3 were from BD Transduction Laboratories; mouse antibody against ERGIC-53 was from Axxora; mouse antibody against Flag tag, rabbit antibodies against ERGIC53, β-tubulin and anti-Flag (M2)-conjugated agarose were from Sigma; HA antibody and anti-HA–conjugated agarose were from Covance; rabbit antibodies against GBF1, LAMP2, Giantin were from Abcam; rabbit antibody against β-COP was from Thermo Fisher; rabbit antibodies against ARFGEF1 and ARFGEF2 were from Bethyl Laboratories.

Expression constructs, viruses, cells, and transfection.

For transient expression in mammalian cells, human cDNAs encoding N-terminal tagged cGAS and C-terminal tagged STING were cloned into pcDNA3. For stable expression in mammalian cells, human cDNAs encoding C-terminal Flag-tagged STING and its mutants were cloned into pTY-EF1A-IRES lentiviral vector (Liu et al., 2015a), which was modified from PTY-shRNA-EF1a-puroR-2a-Flag provided by Dr Yi Zhang (Harvard Medical School). These lentiviruses were packaged in HEK293T cells and transduced into target cells as described previously (Tanaka and Chen, 2012). STING mutants were constructed using the QuikChange Site-Directed Mutagenesis Kit. Plasmids for mammalian expression of WT and C258A RavZ were kindly provided by Dr. Craig Roy (Yale). Plasmids and HT-DNA were transfected into cells using lipofectamine 2000 (Life Technologies).

All cells were cultured at 37°C in an atmosphere of 5% (v/v) CO2. HEK293T and HeLa cells were cultured in Dulbecco's modified Eagle's medium (DMEM) supplemented with 10% (v/v) cosmic calf serum (Hyclone), penicillin (100 U/ml), and streptomycin (100 μg/ml). MEF, L929, and BJ-hTERT cells were cultured in DMEM supplemented with 10% (v/v) fetal bovine serum (FBS, Atlanta) and antibiotics. THP1 cells were cultured in RPMI 1640 supplemented with 10% FBS, 2 mM β-mercaptoethanol, and antibiotics. Hela cells stably expressing GFP-LC3 were provided by Dr. Beth Levine (UT Southwestern). To induce autophagy by starvation, cells were washed with PBS three times, and cultured in Earles Balanced Salt Solution (EBSS).

Sendai virus (Cantell strain, Charles River Laboratories) was used at a final concentration of 50 hemagglutinating units/ml. HSV1 WT strain was propagated and titered by plaque assays

on Vero Cells and used at the indicated multiplicity of infection (MOI) in BJ cells. The HSV ΔICP34.5 strain was used at the indicated MOI in BJ and HEK293T cells. Plasmids for HIV-GFP and VSV-G had been described previously (Gao et al., 2013a). Basically, HIV-GFP lentiviral plasmid was co-transfected with the VSV-g plasmid into HEK293T cells for packaging the virus. Supernatants containing the viruses were harvested, filtered and concentrated by PEG8000 precipitation. The titers of HIV-GFP virus were measured using HEK293T cells by flow cytometry analysis of GFP+ cells 24 hours after infection in the presence of 10 g/mL polybrene.

Generation of knockout cells by CRISPR/Cas9.

Single-guide RNA (sgRNA) was designed to target human cGAS, STING, TBK1, ARF1, GBF1, ATG5, ATG9, ULK1, BECN1 and SEC24C genomic loci (Table S2). The sgRNA sequence driven by a U6 promoter was cloned into a lentiCRISPR vector that also expresses Cas9 as previously described (Shalem et al., 2014). The lentiviral plasmid DNA was then packaged into a lentivirus for infection in HEK293T cells or BJ cells. Infected cells were selected in puromycin (2 μg/ml) for 2 weeks before single colonies were selected and tested by immunoblotting, TA cloning and DNA sequencing.

Generation of primary mouse embryonic fibroblasts (MEFs) and bone marrow derived macrophages (BMDM).

cGas-/- mice were generated as described previously (Li et al., 2013b). Sting gt/gt mice were from the Jackson laboratory (Sauer et al., 2011). These strains were maintained on C57BL/6J

background. MEFs were generated from E13.5 embryos of WT and mutant mice under the normal culture conditions (Yang et al., 2017). BMDMs were generated as described previously (Li et al., 2013b). All mice were bred and maintained under specific pathogen-free conditions in the animal care facility of University of Texas Southwestern Medical Center at Dallas according to experimental protocols approved by the Institutional Animal Care and Use Committee.

Immunostaining, confocal microscopy, and live cell imaging.

For immunostaining, cells were fixed with 4% paraformaldehyde, permeabilized with Triton X100 (0.2%), and stained with a primary antibody followed by a fluorescent secondary antibody. Nuclei were labeled by staining with DAPI in the mounting medium (Vectashield). Images of cells were collected with a Zeiss LSM710 META laser scanning confocal microscope and processed using Zeiss LSM image browser. In some experiments, images were collected with a Nikon A1R confocal microscope and processed using ImageJ. For live cell imaging, cells were grown on a four-chambered cover glass (Lab-Tek II, 155382) at a density of 40,000 cells per chamber (~50% confluency) in 5% CO2 and 20% O2 at 37 °C, and videos were recorded using a Nikon A1R confocal laser microscope system and further processed and analyzed using ImageJ.

Flow cytometry.

After HIV-GFP infection, cells were washed in FACS buffer (PBS, 1% BSA), fixed with 2% paraformaldehyde, and analyzed on BD FACSCALIBUR (BD Biosciences). Data analysis was performed using FlowJo software.

Electron microscopy.

BJ cells were grown on glass bottom plates before stimulation with cGAMP or switched to starvation medium for the indicated time. Samples were fixed, sectioned, stained and coated by UTSW Electron Microscopy core facility. The images were visualized using FEI Tecnai™ transmission electron microscopes (TEMs).

RT-qPCR and HSV1 genome qPCR.

Reverse transcription quantitative PCR (RT-qPCR) reactions were carried out by using the iScript cDNA synthesis kit and iQ SYBR Green Supermix (Bio-Rad). qPCR was performed on an Applied Biosystems Vii7 using the primers shown in Table S1. HSV1-infected cells were washed and lysed in a buffer containing 1% SDS, 50mM Tris-CL (pH 7.5), and 10mM EDTA, and the cell extract was incubated with proteinase K (2 mg/mL) at 37 °C for 30 min. DNA was extracted via phenol/chloroform extraction and ethanol precipitation. Viral DNA was quantified by qPCR using three different pair of primers corresponding to distinct regions of HSV1 genome (Table S3).

In vitro LC3 lipidation assay.

In vitro LC3 assay was modified from published methods (Ge et al., 2013). Cytoplasmic extract (S100) was prepared from WT or ATG5-/- HEK293T cells growing in normal or EBSS

starvation media for 2 hours. After washing with PBS, cells were lysed by passing through a 25 G needle in a 3x cell pellet volume of hypotonic buffer (20 mM HEPES-KOH, pH 7.2, 10 mM KCl, 3 mM MgCl2) plus cocktail protease inhibitors and phosphatase inhibitors (Roche). The cell lysate was centrifuged at 100,000×g for 2 hours to collect the S100 supernatant. For P25 membrane preparation, ATG5-/- HEK293T cells were either untreated or transfected with a cGAS expression plasmid for 12 hours. Then, cells were washed with PBS and homogenized by douncing 20 times in a buffer (20 mM HEPES-KOH, 400 mM sucrose, 0.5 mM EDTA). The homogenate was centrifuged at 1000 x g for 5 minutes to remove cell debris and nuclei. The supernatant (S1) was further centrifuged at 5,000 x g for 10 minutes to precipitate mitochondria and other heavy organelles (P5). The supernatant (S5) was further centrifuged at 25,000 x g for 30 minutes to pellet membranes (P25). For each reaction, S100 (2 mg/ml final concentration), ATP regeneration system (40 mM creatine phosphate, 0.2 mg/ml creatine phosphokinase, and 1 mM ATP), GTP (0.15 mM), P25 or different membrane fractions (0.2 mg/ml) were incubated in a final volume of 30 µl. The mixture was incubated at 30°C for indicated time followed by SDS-PAGE and immunoblotting.

Membrane fractionation.

(A) Differential centrifugation of membranes. Cells (five 15-cm dishes) were cultured to confluence, harvested and homogenized by passing through a 25 G needle ten times in a 5x cell pellet volume of hypotonic buffer. Homogenates were subjected to sequential centrifugation at 1,000×g (10 minutes), 5,000×g (10 minutes), 25,000×g (20 minutes) and 100,000×g (30 minutes) to collect the P1, P5, P25, P100 membranes, respectively. Membrane

fractions containing equal amounts of proteins were used for LC3 lipidation assay as described above.

(B) Sucrose gradient ultracentrifugation. P25 membrane, which contained the highest LC3 lipidation activity, was used to purify ERGIC and Golgi containing fractions using Golgi isolation kit (Sigma). The P25 membranes were suspended in 0.75 ml 1.25 M sucrose buffer and overlaid with 0.5 ml 1.1 M and 0.5 ml 0.25 M sucrose buffer and centrifuged at 120,000×g for 3 hours. Two fractions, one at the interface between 0.25 M and 1.1 M sucrose (P25 L fraction) and the pellet on the bottom (P25 P fraction), were used to test LC3 lipidation activity.

(C) OptiPrep gradient ultracentrifugation. The P25 L fraction was suspended in 1 ml 19% OptiPrep for a step gradient containing from bottom to top: 0.33 ml 22.5%, 0.66 ml 19% (sample), 0.6 ml 16%, 0.6 ml 12%, 0.66 ml 8%, 0.33 ml 5% and 0.14 ml 0% OptiPrep each. Each density of OptiPrep was prepared by diluting 50% OptiPrep (20 mM Tricine-KOH, pH 7.4, 42 mM sucrose and 1 mM EDTA) with a buffer containing 20 mM Tricine-KOH, pH 7.4, 250 mM sucrose and 1 mM EDTA. The OptiPrep gradient was formed by centrifuging using SW60 Swinging bucket Ti Rotor at 150,000×g for 3 hour and ten fractions were collected from the top to bottom. Fractions were diluted with hypotonic buffer and membranes were collected by centrifugation at 100,000×g for 1 hour. The activity of each fraction was tested as described before (Ge et al., 2013).

cGAMP detection by mass spectrometry.

293T cells were transfected with expression plasmids encoding cGAS, DncV or nvcGAS. Small molecules were extracted from cells as described previously (Gao et al., 2015). Briefly, cells were lysed in 80% methanol and 2% acetic acid solution, and added to it were internal standard and an equal volume of 2% acetic acid. Insoluble fractions were pelleted by centrifugation, and were extracted two more times in 2% acetic acid. After combining all three extracts, cyclic dinucleotides were enriched by solid phase extraction on a Hypersep NH2 column (Thermo), washed with 2% acetic acid and with 80% methanol, and eluted in 20% ammonium hydroxide in methanol. After drying by vacuum centrifugation, samples were reconstituted in water and analyzed by a Dionex U3000 HPLC coupled with TSQ Quantiva Triple Quandruple mass spectrometer. Data was collected by product ion scan that targets m/z of 675, and analyzed with XCalibur (Thermo).

RNA-sequencing process and data analysis

The total RNA from cells after stimulation was extracted with RNeasy Mini Kit from Qiagen (Cat No.: 74104). Samples were then run on the Agilent 2100 Bioanalyzer to determine level of degradation thus ensuring only high quality RNA was used (RIN Score 8 or higher). The samples were sent to UT Southwestern Next Generation Sequencing Core for subsequent preparation and sequencing. The Qubit fluorometer was used to determine the concentration prior to cDNA library preparation. 4 μg of total DNase treated RNA was then prepared with the TruSeq Stranded Total RNA LT Sample Prep Kit from Illumina. Poly-A RNA was purified and fragmented before strand-specific cDNA synthesis. cDNA was then a-tailed and indexed adapters were ligated. After adapter ligation, samples were PCR amplified and purified with

Ampure XP beads, then validated again on the Agilent 2100 Bioanalyzer. Samples were quantified by Qubit before being normalized and pooled, then run on the Illumina HiSeq 2500 using SBS v3 reagents. The sequencing data was processed using RNA-Seq CLC-Bio analysis for mRNA expression values, represented by Reads Per Kilobase per Million mapped reads values (RPKM).

Data availability.

The authors declare that all relevant data supporting the findings of this study are available within the paper and its supplementary information files. Additional information including raw data is available from the corresponding author upon reasonable request.

Table 1: Primers for qPCR.

Genes	**Forward Primers**	**Reverse Primers**
IFN-β	CATTACCTGAAGGCCAAGGA	CAATTGTCCAGTCCCAGAGG
CXCL10	GTGGCATTCAAGGAGTACCTC	TGATGGCCTTCGATTCTGGATT
TNFa	TGCTTGTTCCTCAGCCTCTT	GGTTTGCTACAACATGGGCT
ISG15	CGCAGATCACCCAGAAGATCG	TTCGTCGCATTTGTCCACCA

RSAD2	CAGCGTCAACTATCACTTCACT	AACTCTACTTTGCAGAACCTCAC
SAR1A	TTGATCTTGGTGGGCACGAG	GGATTCCACGAGGCGAGAAT
ARF1	CGTGGAAACCGTGGAGTACA	CGCTCTCTGTCATTGCTGTC
SEC24C	TGATGGTTGTGTCTGATGTGG	TGTCTCTGTTTCCCTTGTGTC
GAPDH	ACAGTCAGCCGCATCTTCTT	ACGACCAAATCCGTTGACTC
HSV1(1)	CATCACCGACCCGGAGAGGGAC	GGGCCAGGCGCTTGTTGGTGTA
HSV1(2)	TACAACCTGACCATCGCTTG	GCCCCCAGAGACTTGTTGTA
HSV1(3)	CATCACCGACCCGGAGAGGGAC	GGGCCAGGCGCTTGTTGGTGTA
GAPDH	ATGACATCAAGAAGGTGGTG	CATACCAGGAAATGAGCTTG

Table 2: sgRNA sequences for CRISPR knock out.

Genes	**sgRNA sequence 1**	**sgRNA sequence 2**
STING	GGATGTTCAGTGCCTGCGAG	AATATGACCATGCCAGCCCA
cGAS	CGATGGATCCCACCGAGTCT	AGGCTTCCGCACGGAATGCC
TBK1	CATAAGCTTCCTTCGTCCAG	GAAGAACCTTCTAATGCCTA

ATG5	TGATATAGCGTGAAACAAGT	TTCCATGAGTTTCCGATTGA
ATG9	AGGATATTCGAGAGAAGAAG	AGGTTTTCAATATGGTGCCA
BECN1	CCTGGACCGTGTCACCATCC	TCCTGGTTTCGCCTGGGCTG
ULK1	GCACTCACCGTGCAGGTAGT	GACCTGGCCGACTACCTGCA
SEC24C	GTGTCACGAACAGCCTTCAC	GTGCCCGTAAGCTATCAATG
VPS34	GAAACCGTTGTTCCTCCTAC	GGAACAACGGTTTCGCTCTT
TRAPCC9	GAGTCCTCTACATCCGCTAC	ACCCACCCGAGAACAACGAG
WIPI2	TTTTGCAGGTCCCTAGCTGT	TCGTCAGCCTTAAAGCACCA
GBF1	CCATCGGGCATTTCGTTTGA	CCATCAAACGAAATGCCCGA

Table 3: siRNA sequences for knock-down experiments.

Genes	**siRNA sequence 1**	**siRNA sequence 2**
Control	AAUUCUCCGAACGUGUCACGU	
STING	GCCCGGAUUCGAACUUACAAU	GUCCAGGACUUGACAUCUUAA
SAR1A	CGUGAGAUAUUUGGGCUUUAU	GAAUCCAAAGUUGAGCUUAAU
SEC24C	ACUUAUGUUAUCGAGUCAAUG	UUGAUGUAAAGCGACUAAUAU
ARF1	CCAUUCCCACCAUAGGCUU	CACCAUAGGCUUCAACGUGGA
ARF3	CAAGAGCCUGAUUGGGAAGAA	
ARF4	CCAUCAGUGAAAUGACAGAUA	
ARF5	UGCAUGUUCUCUCUGUUGUUG	
ARF6	AGCUGCACCGCAUUAUCAAUG	
ATG7	CUUGACAUUUGCAGAUCUAAA	CACCAGUUCAGAGCUAAAUAA
WIPI2	GCUGUCAAUCAACAACGACAA	CCCUAGCUGUUGGUAGUAAGU

CHAPTER FIVE

APPENDIX

Supplementary Video 1. Live cell imaging of cGAMP-induced GFP-LC3 puncta formation

Hela cells stably expressing STING-Flag and GFP-LC3 were stimulated with cGAMP (1 μM; cells were transiently permeabilized with PFO at 0.1 μg/ml). As a control, cells were also growing in EBSS starvation medium in the presence of Bafilomycin A1 (BafA1, 0.2 μM). Recording started at 20 minutes after adding cGAMP or changing to the starvation medium, and lasted 160 minutes with 2 minute intervals.

Supplementary Video 2. Live cell imaging of cGAMP-stimulated STING translocation to autophagosome

HeLa cells stably expressing STING-GFP and RFP-LC3 were stimulated with cGAMP (1 μM) in the presence or absence of Brefeldin A (BFA, 5 μM) or Bafilomycin A1 (BafA1, 0.2 μM). Recording started at 1 hour after adding cGAMP, and lasted 5 hours and 30 minutes with 2 minute intervals.

Supplementary Video 3. Live cell imaging of DNA-stimulated STING translocation to autophagosome

HeLa cells stably expressing STING-GFP and RFP-LC3 were transfected with HT-DNA (2 μg/ml) in the presence or absence of Brefeldin A (BFA, 5 μM) or bafilomycin A1 (BafA1, 0.2

μM). Recording started at 1 hour after DNA transfection and lasted about 11 hours with 4 minute intervals.

Supplementary Video 4. 3D imaging of STING translocation to ERGIC and LC3 positive autophagosome

HeLa cells stably expressing STING-Flag and GFP-LC3 were stimulated with cGAMP (1 μM) for 2 hours, then cells were immunostained with antibodies against Flag and ERGIC53, respectively. 3D fluorescence micrograph shows that, after cGAMP stimulation, STING (red) co-localizes with ERGIC (cyan) and GFP-LC3 (green) in the peri-nuclear region.

Supplementary Video 5. Live cell imaging of cytosolic DNA clearance by DNA-induced autophagy

Cy3-ISD (0.5 μg/ml or 2 μg/ml) was delivered into HeLa cells stably expressing STING-Flag and GFP-LC3 that were transiently permeabilized with PFO (0.1 μg/ml) for 3 hours. After medium was replaced with fresh DMEM (10% FBS), cells were recorded by live cell imaging for another 3 hours. Video was tracked to detect CY3-ISD translocation to GFP-LC3 puncta. Recording started at 20 minutes after adding CY3-ISD and lasted about 6 hours in total with 4 minute intervals.

Supplementary Video 6. Live cell imaging of cytosolic DNA clearance by cGAMP-induced autophagy

Cy3-ISD was delivered together with different amounts of cGAMP (as indicated in movie) into HeLa cells stably expressing STING-Flag and GFP-LC3 that were transiently permeabilized with PFO (0.1 μg/ml) for 1.5 hours. Medium was replaced with fresh DMEM (10% FBS) and cells were recorded by live cell imaging for another 5 hours. Video was tracked to detect CY3-ISD translocation to GFP-LC3 puncta. Recording started at 20 minutes after adding CY3-ISD and lasted about 7 hours with 4 minute intervals.

CHAPTER SIX

BIBLIOGRAPHY

Ablasser, A., Goldeck, M., Cavlar, T., Deimling, T., Witte, G., Rohl, I., Hopfner, K.P., Ludwig, J., and Hornung, V. (2013a). cGAS produces a 2'-5'-linked cyclic dinucleotide second messenger that activates STING. Nature *498*, 380-384.

Ablasser, A., and Gulen, M.F. (2016). The role of cGAS in innate immunity and beyond. J Mol Med (Berl) *94*, 1085-1093.

Ablasser, A., Schmid-Burgk, J.L., Hemmerling, I., Horvath, G.L., Schmidt, T., Latz, E., and Hornung, V. (2013b). Cell intrinsic immunity spreads to bystander cells via the intercellular transfer of cGAMP. Nature *503*, 530-534.

Ahn, J., Konno, H., and Barber, G.N. (2015). Diverse roles of STING-dependent signaling on the development of cancer. Oncogene *34*, 5302-5308.

Andrade, W.A., Agarwal, S., Mo, S., Shaffer, S.A., Dillard, J.P., Schmidt, T., Hornung, V., Fitzgerald, K.A., Kurt-Jones, E.A., and Golenbock, D.T. (2016). Type I Interferon Induction by Neisseria gonorrhoeae: Dual Requirement of Cyclic GMP-AMP Synthase and Toll-like Receptor 4. Cell Rep *15*, 2438-2448.

Bakhoum, S.F., Ngo, B., Laughney, A.M., Cavallo, J.A., Murphy, C.J., Ly, P., Shah, P., Sriram, R.K., Watkins, T.B.K., Taunk, N.K.*, et al.* (2018). Chromosomal instability drives metastasis through a cytosolic DNA response. Nature *553*, 467-472.

Brandizzi, F., and Barlowe, C. (2013). Organization of the ER-Golgi interface for membrane traffic control. Nat Rev Mol Cell Biol *14*, 382-392.

Bridgeman, A., Maelfait, J., Davenne, T., Partridge, T., Peng, Y., Mayer, A., Dong, T., Kaever, V., Borrow, P., and Rehwinkel, J. (2015). Viruses transfer the antiviral second messenger cGAMP between cells. Science *349*, 1228-1232.

Cavlar, T., Deimling, T., Ablasser, A., Hopfner, K.P., and Hornung, V. (2013). Species-specific detection of the antiviral small-molecule compound CMA by STING. EMBO J *32*, 1440-1450.

Cebrian, I., Visentin, G., Blanchard, N., Jouve, M., Bobard, A., Moita, C., Enninga, J., Moita, L.F., Amigorena, S., and Savina, A. (2011). Sec22b regulates phagosomal maturation and antigen crosspresentation by dendritic cells. Cell *147*, 1355-1368.

Cerboni, S., Jeremiah, N., Gentili, M., Gehrmann, U., Conrad, C., Stolzenberg, M.C., Picard, C., Neven, B., Fischer, A., Amigorena, S.*, et al.* (2017). Intrinsic antiproliferative activity of the innate sensor STING in T lymphocytes. J Exp Med *214*, 1769-1785.

Chen, Q., Boire, A., Jin, X., Valiente, M., Er, E.E., Lopez-Soto, A., Jacob, L., Patwa, R., Shah, H., Xu, K.*, et al.* (2016a). Carcinoma-astrocyte gap junctions promote brain metastasis by cGAMP transfer. Nature *533*, 493-498.

Chen, Q., Sun, L., and Chen, Z.J. (2016b). Regulation and function of the cGAS-STING pathway of cytosolic DNA sensing. Nat Immunol *17*, 1142-1149.

Cheong, H., Lindsten, T., Wu, J., Lu, C., and Thompson, C.B. (2011). Ammonia-induced autophagy is independent of ULK1/ULK2 kinases. Proc Natl Acad Sci U S A *108*, 11121-11126.

Choy, A., Dancourt, J., Mugo, B., O'Connor, T.J., Isberg, R.R., Melia, T.J., and Roy, C.R. (2012). The Legionella effector RavZ inhibits host autophagy through irreversible Atg8 deconjugation. Science *338*, 1072-1076.

Christensen, M.H., Jensen, S.B., Miettinen, J.J., Luecke, S., Prabakaran, T., Reinert, L.S., Mettenleiter, T., Chen, Z.J., Knipe, D.M., Sandri-Goldin, R.M.*, et al.* (2016). HSV-1 ICP27 targets the TBK1-activated STING signalsome to inhibit virus-induced type I IFN expression. EMBO J *35*, 1385-1399.

Civril, F., Deimling, T., de Oliveira Mann, C.C., Ablasser, A., Moldt, M., Witte, G., Hornung, V., and Hopfner, K.P. (2013). Structural mechanism of cytosolic DNA sensing by cGAS. Nature *498*, 332-337.

Collins, A.C., Cai, H., Li, T., Franco, L.H., Li, X.D., Nair, V.R., Scharn, C.R., Stamm, C.E., Levine, B., Chen, Z.J.*, et al.* (2015). Cyclic GMP-AMP Synthase Is an Innate Immune DNA Sensor for Mycobacterium tuberculosis. Cell Host Microbe *17*, 820-828.

Conlon, J., Burdette, D.L., Sharma, S., Bhat, N., Thompson, M., Jiang, Z., Rathinam, V.A., Monks, B., Jin, T., Xiao, T.S.*, et al.* (2013). Mouse, but not human STING, binds and signals in response to the vascular disrupting agent 5,6-dimethylxanthenone-4-acetic acid. J Immunol *190*, 5216-5225.

Corrales, L., Glickman, L.H., McWhirter, S.M., Kanne, D.B., Sivick, K.E., Katibah, G.E., Woo, S.R., Lemmens, E., Banda, T., Leong, J.J.*, et al.* (2015). Direct Activation of STING

in the Tumor Microenvironment Leads to Potent and Systemic Tumor Regression and Immunity. Cell Rep *11*, 1018-1030.

Crotzer, V.L., and Blum, J.S. (2009). Autophagy and its role in MHC-mediated antigen presentation. J Immunol *182*, 3335-3341.

Crow, Y.J. (2015). Type I interferonopathies: mendelian type I interferon up-regulation. Curr Opin Immunol *32*, 7-12.

Demaria, O., De Gassart, A., Coso, S., Gestermann, N., Di Domizio, J., Flatz, L., Gaide, O., Michielin, O., Hwu, P., Petrova, T.V.*, et al.* (2015). STING activation of tumor endothelial cells initiates spontaneous and therapeutic antitumor immunity. Proc Natl Acad Sci U S A *112*, 15408-15413.

Deng, L., Liang, H., Xu, M., Yang, X., Burnette, B., Arina, A., Li, X.D., Mauceri, H., Beckett, M., Darga, T.*, et al.* (2014). STING-Dependent Cytosolic DNA Sensing Promotes Radiation-Induced Type I Interferon-Dependent Antitumor Immunity in Immunogenic Tumors. Immunity *41*, 843-852.

Deretic, V., Saitoh, T., and Akira, S. (2013). Autophagy in infection, inflammation and immunity. Nat Rev Immunol *13*, 722-737.

Devereaux, K., Dall'Armi, C., Alcazar-Roman, A., Ogasawara, Y., Zhou, X., Wang, F., Yamamoto, A., De Camilli, P., and Di Paolo, G. (2013). Regulation of mammalian autophagy by class II and III PI 3-kinases through PI3P synthesis. PLoS One *8*, e76405.

Diner, E.J., Burdette, D.L., Wilson, S.C., Monroe, K.M., Kellenberger, C.A., Hyodo, M., Hayakawa, Y., Hammond, M.C., and Vance, R.E. (2013). The innate immune DNA sensor cGAS produces a noncanonical cyclic dinucleotide that activates human STING. Cell Rep *3*, 1355-1361.

Dobbs, N., Burnaevskiy, N., Chen, D., Gonugunta, V.K., Alto, N.M., and Yan, N. (2015). STING Activation by Translocation from the ER Is Associated with Infection and Autoinflammatory Disease. Cell Host Microbe *18*, 157-168.

Donaldson, J.G., Finazzi, D., and Klausner, R.D. (1992). Brefeldin A inhibits Golgi membrane-catalysed exchange of guanine nucleotide onto ARF protein. Nature *360*, 350-352.

Donaldson, J.G., and Jackson, C.L. (2011). ARF family G proteins and their regulators: roles in membrane transport, development and disease. Nat Rev Mol Cell Biol *12*, 362-375.

Dooley, H.C., Razi, M., Polson, H.E., Girardin, S.E., Wilson, M.I., and Tooze, S.A. (2014). WIPI2 links LC3 conjugation with PI3P, autophagosome formation, and pathogen clearance by recruiting Atg12-5-16L1. Mol Cell *55*, 238-252.

Eskelinen, E.L. (2005). Maturation of autophagic vacuoles in Mammalian cells. Autophagy *1*, 1-10.

Fitzgerald, K.A., McWhirter, S.M., Faia, K.L., Rowe, D.C., Latz, E., Golenbock, D.T., Coyle, A.J., Liao, S.M., and Maniatis, T. (2003). IKKepsilon and TBK1 are essential components of the IRF3 signaling pathway. Nat Immunol *4*, 491-496.

Funderburk, S.F., Wang, Q.J., and Yue, Z. (2010). The Beclin 1-VPS34 complex--at the crossroads of autophagy and beyond. Trends Cell Biol *20*, 355-362.

Futter, C.E., Collinson, L.M., Backer, J.M., and Hopkins, C.R. (2001). Human VPS34 is required for internal vesicle formation within multivesicular endosomes. J Cell Biol *155*, 1251-1264.

Gaidt, M.M., Ebert, T.S., Chauhan, D., Ramshorn, K., Pinci, F., Zuber, S., O'Duill, F., Schmid-Burgk, J.L., Hoss, F., Buhmann, R.*, et al.* (2017). The DNA Inflammasome in Human Myeloid Cells Is Initiated by a STING-Cell Death Program Upstream of NLRP3. Cell *171*, 1110-1124 e1118.

Gall, A., Treuting, P., Elkon, K.B., Loo, Y.M., Gale, M., Jr., Barber, G.N., and Stetson, D.B. (2012). Autoimmunity initiates in nonhematopoietic cells and progresses via lymphocytes in an interferon-dependent autoimmune disease. Immunity *36*, 120-131.

Gao, D., Li, T., Li, X.D., Chen, X., Li, Q.Z., Wight-Carter, M., and Chen, Z.J. (2015). Activation of cyclic GMP-AMP synthase by self-DNA causes autoimmune diseases. Proc Natl Acad Sci U S A *112*, E5699-5705.

Gao, D., Wu, J., Wu, Y.T., Du, F., Aroh, C., Yan, N., Sun, L., and Chen, Z.J. (2013a). Cyclic GMP-AMP synthase is an innate immune sensor of HIV and other retroviruses. Science *341*, 903-906.

Gao, P., Ascano, M., Wu, Y., Barchet, W., Gaffney, B.L., Zillinger, T., Serganov, A.A., Liu, Y., Jones, R.A., Hartmann, G.*, et al.* (2013b). Cyclic [G(2',5')pA(3',5')p] is the metazoan second messenger produced by DNA-activated cyclic GMP-AMP synthase. Cell *153*, 1094-1107.

Gao, P., Ascano, M., Zillinger, T., Wang, W., Dai, P., Serganov, A.A., Gaffney, B.L., Shuman, S., Jones, R.A., Deng, L.*, et al.* (2013c). Structure-function analysis of STING activation by c[G(2',5')pA(3',5')p] and targeting by antiviral DMXAA. Cell *154*, 748-762.

Ge, L., Melville, D., Zhang, M., and Schekman, R. (2013). The ER-Golgi intermediate compartment is a key membrane source for the LC3 lipidation step of autophagosome biogenesis. Elife *2*, e00947.

Ge, L., Zhang, M., and Schekman, R. (2014). Phosphatidylinositol 3-kinase and COPII generate LC3 lipidation vesicles from the ER-Golgi intermediate compartment. Elife *3*, e04135.

Gentili, M., Kowal, J., Tkach, M., Satoh, T., Lahaye, X., Conrad, C., Boyron, M., Lombard, B., Durand, S., Kroemer, G.*, et al.* (2015). Transmission of innate immune signaling by packaging of cGAMP in viral particles. Science *349*, 1232-1236.

Gough, D.J., Messina, N.L., Clarke, C.J., Johnstone, R.W., and Levy, D.E. (2012). Constitutive type I interferon modulates homeostatic balance through tonic signaling. Immunity *36*, 166-174.

Gray, E.E., Treuting, P.M., Woodward, J.J., and Stetson, D.B. (2015). Cutting Edge: cGAS Is Required for Lethal Autoimmune Disease in the Trex1-Deficient Mouse Model of Aicardi-Goutieres Syndrome. J Immunol *195*, 1939-1943.

Gulen, M.F., Koch, U., Haag, S.M., Schuler, F., Apetoh, L., Villunger, A., Radtke, F., and Ablasser, A. (2017). Signalling strength determines proapoptotic functions of STING. Nat Commun *8*, 427.

Gutierrez, M.G., Munafo, D.B., Beron, W., and Colombo, M.I. (2004). Rab7 is required for the normal progression of the autophagic pathway in mammalian cells. J Cell Sci *117*, 2687-2697.

Hansen, K., Prabakaran, T., Laustsen, A., Jorgensen, S.E., Rahbaek, S.H., Jensen, S.B., Nielsen, R., Leber, J.H., Decker, T., Horan, K.A.*, et al.* (2014). Listeria monocytogenes induces IFNbeta expression through an IFI16-, cGAS- and STING-dependent pathway. EMBO J *33*, 1654-1666.

Harding, S.M., Benci, J.L., Irianto, J., Discher, D.E., Minn, A.J., and Greenberg, R.A. (2017). Mitotic progression following DNA damage enables pattern recognition within micronuclei. Nature *548*, 466-470.

He, R., Peng, J., Yuan, P., Xu, F., and Wei, W. (2015). Divergent roles of BECN1 in LC3 lipidation and autophagosomal function. Autophagy *11*, 740-747.

Heidegger, S., Haas, T., and Poeck, H. (2017). Cutting Edge in IFN Regulation: Inflammatory Caspases Cleave cGAS. Immunity *46*, 333-335.

Helms, J.B., and Rothman, J.E. (1992). Inhibition by brefeldin A of a Golgi membrane enzyme that catalyses exchange of guanine nucleotide bound to ARF. Nature *360*, 352-354.

Herzner, A.M., Hagmann, C.A., Goldeck, M., Wolter, S., Kubler, K., Wittmann, S., Gramberg, T., Andreeva, L., Hopfner, K.P., Mertens, C.*, et al.* (2015). Sequence-specific activation of the DNA sensor cGAS by Y-form DNA structures as found in primary HIV-1 cDNA. Nat Immunol *16*, 1025-1033.

Hillwig, M.S., Contento, A.L., Meyer, A., Ebany, D., Bassham, D.C., and Macintosh, G.C. (2011). RNS2, a conserved member of the RNase T2 family, is necessary for ribosomal RNA decay in plants. Proc Natl Acad Sci U S A *108*, 1093-1098.

Holm, C.K., Jensen, S.B., Jakobsen, M.R., Cheshenko, N., Horan, K.A., Moeller, H.B., Gonzalez-Dosal, R., Rasmussen, S.B., Christensen, M.H., Yarovinsky, T.O.*, et al.* (2012). Virus-cell fusion as a trigger of innate immunity dependent on the adaptor STING. Nat Immunol *13*, 737-743.

Hoyer-Hansen, M., and Jaattela, M. (2007). Connecting endoplasmic reticulum stress to autophagy by unfolded protein response and calcium. Cell Death Differ *14*, 1576-1582.

Huang, L., Li, L., Lemos, H., Chandler, P.R., Pacholczyk, G., Baban, B., Barber, G.N., Hayakawa, Y., McGaha, T.L., Ravishankar, B.*, et al.* (2013). Cutting edge: DNA sensing via the STING adaptor in myeloid dendritic cells induces potent tolerogenic responses. J Immunol *191*, 3509-3513.

Hyttinen, J.M., Niittykoski, M., Salminen, A., and Kaarniranta, K. (2013). Maturation of autophagosomes and endosomes: a key role for Rab7. Biochim Biophys Acta *1833*, 503-510.

Ishikawa, H., and Barber, G.N. (2008). STING is an endoplasmic reticulum adaptor that facilitates innate immune signalling. Nature *455*, 674-678.

Ishikawa, H., Ma, Z., and Barber, G.N. (2009). STING regulates intracellular DNA-mediated, type I interferon-dependent innate immunity. Nature *461*, 788-792.

Itakura, E., and Mizushima, N. (2009). Atg14 and UVRAG: mutually exclusive subunits of mammalian Beclin 1-PI3K complexes. Autophagy *5*, 534-536.

Jaber, N., Dou, Z., Chen, J.S., Catanzaro, J., Jiang, Y.P., Ballou, L.M., Selinger, E., Ouyang, X., Lin, R.Z., Zhang, J.*, et al.* (2012). Class III PI3K Vps34 plays an essential role in autophagy and in heart and liver function. Proc Natl Acad Sci U S A *109*, 2003-2008.

Jager, S., Bucci, C., Tanida, I., Ueno, T., Kominami, E., Saftig, P., and Eskelinen, E.L. (2004). Role for Rab7 in maturation of late autophagic vacuoles. J Cell Sci *117*, 4837-4848.

Joffre, O.P., Segura, E., Savina, A., and Amigorena, S. (2012). Cross-presentation by dendritic cells. Nat Rev Immunol *12*, 557-569.

Kang, R., Zeh, H.J., Lotze, M.T., and Tang, D. (2011). The Beclin 1 network regulates autophagy and apoptosis. Cell Death Differ *18*, 571-580.

Kawane, K., Fukuyama, H., Kondoh, G., Takeda, J., Ohsawa, Y., Uchiyama, Y., and Nagata, S. (2001). Requirement of DNase II for definitive erythropoiesis in the mouse fetal liver. Science *292*, 1546-1549.

Kim, J., Kim, Y.C., Fang, C., Russell, R.C., Kim, J.H., Fan, W., Liu, R., Zhong, Q., and Guan, K.L. (2013a). Differential regulation of distinct Vps34 complexes by AMPK in nutrient stress and autophagy. Cell *152*, 290-303.

Kim, S., Li, L., Maliga, Z., Yin, Q., Wu, H., and Mitchison, T.J. (2013b). Anticancer flavonoids are mouse-selective STING agonists. ACS Chem Biol *8*, 1396-1401.

Konno, H., Konno, K., and Barber, G.N. (2013). Cyclic dinucleotides trigger ULK1 (ATG1) phosphorylation of STING to prevent sustained innate immune signaling. Cell *155*, 688-698.

Konno, H., Yamauchi, S., Berglund, A., Putney, R.M., Mule, J.J., and Barber, G.N. (2018). Suppression of STING signaling through epigenetic silencing and missense mutation impedes DNA damage mediated cytokine production. Oncogene *37*, 2037-2051.

Kranzusch, P.J., Lee, A.S., Berger, J.M., and Doudna, J.A. (2013). Structure of human cGAS reveals a conserved family of second-messenger enzymes in innate immunity. Cell Rep *3*, 1362-1368.

Kranzusch, P.J., Wilson, S.C., Lee, A.S., Berger, J.M., Doudna, J.A., and Vance, R.E. (2015). Ancient Origin of cGAS-STING Reveals Mechanism of Universal 2',3' cGAMP Signaling. Mol Cell *59*, 891-903.

Lahaye, X., Satoh, T., Gentili, M., Cerboni, S., Conrad, C., Hurbain, I., El Marjou, A., Lacabaratz, C., Lelievre, J.D., and Manel, N. (2013). The capsids of HIV-1 and HIV-2 determine immune detection of the viral cDNA by the innate sensor cGAS in dendritic cells. Immunity *39*, 1132-1142.

Larkin, B., Ilyukha, V., Sorokin, M., Buzdin, A., Vannier, E., and Poltorak, A. (2017). Cutting Edge: Activation of STING in T Cells Induces Type I IFN Responses and Cell Death. J Immunol *199*, 397-402.

Lau, L., Gray, E.E., Brunette, R.L., and Stetson, D.B. (2015). DNA tumor virus oncogenes antagonize the cGAS-STING DNA-sensing pathway. Science *350*, 568-571.

Lee, H.K., and Iwasaki, A. (2008). Autophagy and antiviral immunity. Curr Opin Immunol *20*, 23-29.

Lee, H.K., Lund, J.M., Ramanathan, B., Mizushima, N., and Iwasaki, A. (2007). Autophagy-dependent viral recognition by plasmacytoid dendritic cells. Science *315*, 1398-1401.

Leib, D.A., Alexander, D.E., Cox, D., Yin, J., and Ferguson, T.A. (2009). Interaction of ICP34.5 with Beclin 1 modulates herpes simplex virus type 1 pathogenesis through control of CD4+ T-cell responses. J Virol *83*, 12164-12171.

Lemos, H., Mohamed, E., Huang, L., Ou, R., Pacholczyk, G., Arbab, A.S., Munn, D., and Mellor, A.L. (2016). STING Promotes the Growth of Tumors Characterized by Low Antigenicity via IDO Activation. Cancer Res *76*, 2076-2081.

Levine, B., Mizushima, N., and Virgin, H.W. (2011). Autophagy in immunity and inflammation. Nature *469*, 323-335.

Li, L., Yin, Q., Kuss, P., Maliga, Z., Millan, J.L., Wu, H., and Mitchison, T.J. (2014). Hydrolysis of 2'3'-cGAMP by ENPP1 and design of nonhydrolyzable analogs. Nat Chem Biol *10*, 1043-1048.

Li, X., Shu, C., Yi, G., Chaton, C.T., Shelton, C.L., Diao, J., Zuo, X., Kao, C.C., Herr, A.B., and Li, P. (2013a). Cyclic GMP-AMP synthase is activated by double-stranded DNA-induced oligomerization. Immunity *39*, 1019-1031.

Li, X.D., Wu, J., Gao, D., Wang, H., Sun, L., and Chen, Z.J. (2013b). Pivotal roles of cGAS-cGAMP signaling in antiviral defense and immune adjuvant effects. Science *341*, 1390-1394.

Li, Y., Zhang, C., Chen, X., Yu, J., Wang, Y., Yang, Y., Du, M., Jin, H., Ma, Y., He, B., *et al.* (2011). ICP34.5 protein of herpes simplex virus facilitates the initiation of protein translation by bridging eukaryotic initiation factor 2alpha (eIF2alpha) and protein phosphatase 1. J Biol Chem *286*, 24785-24792.

Liang, D., Xiao-Feng, H., Guan-Jun, D., Er-Ling, H., Sheng, C., Ting-Ting, W., Qin-Gang, H., Yan-Hong, N., and Ya-Yi, H. (2015). Activated STING enhances Tregs infiltration in

the HPV-related carcinogenesis of tongue squamous cells via the c-jun/CCL22 signal. Biochim Biophys Acta *1852*, 2494-2503.

Liang, Q., Seo, G.J., Choi, Y.J., Kwak, M.J., Ge, J., Rodgers, M.A., Shi, M., Leslie, B.J., Hopfner, K.P., Ha, T.*, et al.* (2014). Crosstalk between the cGAS DNA sensor and Beclin-1 autophagy protein shapes innate antimicrobial immune responses. Cell Host Microbe *15*, 228-238.

Lindahl, T., Barnes, D.E., Yang, Y.G., and Robins, P. (2009). Biochemical properties of mammalian TREX1 and its association with DNA replication and inherited inflammatory disease. Biochem Soc Trans *37*, 535-538.

Lio, C.W., McDonald, B., Takahashi, M., Dhanwani, R., Sharma, N., Huang, J., Pham, E., Benedict, C.A., and Sharma, S. (2016). cGAS-STING Signaling Regulates Initial Innate Control of Cytomegalovirus Infection. J Virol *90*, 7789-7797.

Liu, B.L., Robinson, M., Han, Z.Q., Branston, R.H., English, C., Reay, P., McGrath, Y., Thomas, S.K., Thornton, M., Bullock, P.*, et al.* (2003). ICP34.5 deleted herpes simplex virus with enhanced oncolytic, immune stimulating, and anti-tumour properties. Gene Ther *10*, 292-303.

Liu, S., Cai, X., Wu, J., Cong, Q., Chen, X., Li, T., Du, F., Ren, J., Wu, Y.T., Grishin, N.V.*, et al.* (2015a). Phosphorylation of innate immune adaptor proteins MAVS, STING, and TRIF induces IRF3 activation. Science *347*, aaa2630.

Liu, X., Pu, Y., Cron, K., Deng, L., Kline, J., Frazier, W.A., Xu, H., Peng, H., Fu, Y.X., and Xu, M.M. (2015b). CD47 blockade triggers T cell-mediated destruction of immunogenic tumors. Nat Med *21*, 1209-1215.

Liu, Y., Jesus, A.A., Marrero, B., Yang, D., Ramsey, S.E., Montealegre Sanchez, G.A., Tenbrock, K., Wittkowski, H., Jones, O.Y., Kuehn, H.S.*, et al.* (2014). Activated STING in a vascular and pulmonary syndrome. N Engl J Med *371*, 507-518.

Ma, F., Li, B., Liu, S.Y., Iyer, S.S., Yu, Y., Wu, A., and Cheng, G. (2015a). Positive feedback regulation of type I IFN production by the IFN-inducible DNA sensor cGAS. J Immunol *194*, 1545-1554.

Ma, Z., Jacobs, S.R., West, J.A., Stopford, C., Zhang, Z., Davis, Z., Barber, G.N., Glaunsinger, B.A., Dittmer, D.P., and Damania, B. (2015b). Modulation of the cGAS-STING DNA sensing pathway by gammaherpesviruses. Proc Natl Acad Sci U S A *112*, E4306-4315.

Mackenzie, K.J., Carroll, P., Lettice, L., Tarnauskaite, Z., Reddy, K., Dix, F., Revuelta, A., Abbondati, E., Rigby, R.E., Rabe, B.*, et al.* (2016). Ribonuclease H2 mutations induce a cGAS/STING-dependent innate immune response. EMBO J *35*, 831-844.

Mackenzie, K.J., Carroll, P., Martin, C.A., Murina, O., Fluteau, A., Simpson, D.J., Olova, N., Sutcliffe, H., Rainger, J.K., Leitch, A.*, et al.* (2017). cGAS surveillance of micronuclei links genome instability to innate immunity. Nature *548*, 461-465.

Melki, I., Rose, Y., Uggenti, C., Van Eyck, L., Fremond, M.L., Kitabayashi, N., Rice, G.I., Jenkinson, E.M., Boulai, A., Jeremiah, N.*, et al.* (2017). Disease-associated mutations identify a novel region in human STING necessary for the control of type I interferon signaling. J Allergy Clin Immunol *140*, 543-552 e545.

Mizushima, N., Yoshimori, T., and Ohsumi, Y. (2011). The role of Atg proteins in autophagosome formation. Annu Rev Cell Dev Biol *27*, 107-132.

Mukai, K., Konno, H., Akiba, T., Uemura, T., Waguri, S., Kobayashi, T., Barber, G.N., Arai, H., and Taguchi, T. (2016). Activation of STING requires palmitoylation at the Golgi. Nat Commun *7*, 11932.

Ng, K.W., Marshall, E.A., Bell, J.C., and Lam, W.L. (2018). cGAS-STING and Cancer: Dichotomous Roles in Tumor Immunity and Development. Trends Immunol *39*, 44-54.

Niu, T.K., Pfeifer, A.C., Lippincott-Schwartz, J., and Jackson, C.L. (2005). Dynamics of GBF1, a Brefeldin A-sensitive Arf1 exchange factor at the Golgi. Mol Biol Cell *16*, 1213-1222.

Orvedahl, A., Alexander, D., Talloczy, Z., Sun, Q., Wei, Y., Zhang, W., Burns, D., Leib, D.A., and Levine, B. (2007). HSV-1 ICP34.5 confers neurovirulence by targeting the Beclin 1 autophagy protein. Cell Host Microbe *1*, 23-35.

Ouyang, S., Song, X., Wang, Y., Ru, H., Shaw, N., Jiang, Y., Niu, F., Zhu, Y., Qiu, W., Parvatiyar, K.*, et al.* (2012). Structural analysis of the STING adaptor protein reveals a hydrophobic dimer interface and mode of cyclic di-GMP binding. Immunity *36*, 1073-1086.

Paijo, J., Doring, M., Spanier, J., Grabski, E., Nooruzzaman, M., Schmidt, T., Witte, G., Messerle, M., Hornung, V., Kaever, V.*, et al.* (2016). cGAS Senses Human Cytomegalovirus and Induces Type I Interferon Responses in Human Monocyte-Derived Cells. PLoS Pathog *12*, e1005546.

Paludan, S.R. (2015). Activation and regulation of DNA-driven immune responses. Microbiol Mol Biol Rev *79*, 225-241.

Petherick, K.J., Conway, O.J., Mpamhanga, C., Osborne, S.A., Kamal, A., Saxty, B., and Ganley, I.G. (2015). Pharmacological inhibition of ULK1 kinase blocks mammalian target of rapamycin (mTOR)-dependent autophagy. J Biol Chem *290*, 11376-11383.

Pokatayev, V., Hasin, N., Chon, H., Cerritelli, S.M., Sakhuja, K., Ward, J.M., Morris, H.D., Yan, N., and Crouch, R.J. (2016). RNase H2 catalytic core Aicardi-Goutieres syndrome-related mutant invokes cGAS-STING innate immune-sensing pathway in mice. J Exp Med *213*, 329-336.

Popoff, V., Langer, J.D., Reckmann, I., Hellwig, A., Kahn, R.A., Brugger, B., and Wieland, F.T. (2011). Several ADP-ribosylation factor (Arf) isoforms support COPI vesicle formation. J Biol Chem *286*, 35634-35642.

Russell, R.C., Tian, Y., Yuan, H., Park, H.W., Chang, Y.Y., Kim, J., Kim, H., Neufeld, T.P., Dillin, A., and Guan, K.L. (2013). ULK1 induces autophagy by phosphorylating Beclin-1 and activating VPS34 lipid kinase. Nat Cell Biol *15*, 741-750.

Saenz, J.B., Sun, W.J., Chang, J.W., Li, J., Bursulaya, B., Gray, N.S., and Haslam, D.B. (2009). Golgicide A reveals essential roles for GBF1 in Golgi assembly and function. Nat Chem Biol *5*, 157-165.

Saitoh, T., Fujita, N., Hayashi, T., Takahara, K., Satoh, T., Lee, H., Matsunaga, K., Kageyama, S., Omori, H., Noda, T.*, et al.* (2009). Atg9a controls dsDNA-driven dynamic translocation of STING and the innate immune response. Proc Natl Acad Sci U S A *106*, 20842-20846.

Sauer, J.D., Sotelo-Troha, K., von Moltke, J., Monroe, K.M., Rae, C.S., Brubaker, S.W., Hyodo, M., Hayakawa, Y., Woodward, J.J., Portnoy, D.A.*, et al.* (2011). The N-ethyl-N-nitrosourea-induced Goldenticket mouse mutant reveals an essential function of Sting in the in vivo interferon response to Listeria monocytogenes and cyclic dinucleotides. Infect Immun *79*, 688-694.

Schmid, D., and Munz, C. (2007). Innate and adaptive immunity through autophagy. Immunity *27*, 11-21.

Schoggins, J.W., MacDuff, D.A., Imanaka, N., Gainey, M.D., Shrestha, B., Eitson, J.L., Mar, K.B., Richardson, R.B., Ratushny, A.V., Litvak, V.*, et al.* (2014). Pan-viral specificity of IFN-induced genes reveals new roles for cGAS in innate immunity. Nature *505*, 691-695.

Schoggins, J.W., Wilson, S.J., Panis, M., Murphy, M.Y., Jones, C.T., Bieniasz, P., and Rice, C.M. (2011). A diverse range of gene products are effectors of the type I interferon antiviral response. Nature *472*, 481-485.

Seo, G.J., Yang, A., Tan, B., Kim, S., Liang, Q., Choi, Y., Yuan, W., Feng, P., Park, H.S., and Jung, J.U. (2015). Akt Kinase-Mediated Checkpoint of cGAS DNA Sensing Pathway. Cell Rep *13*, 440-449.

Seth, R.B., Sun, L., Ea, C.K., and Chen, Z.J. (2005). Identification and characterization of MAVS, a mitochondrial antiviral signaling protein that activates NF-kappaB and IRF 3. Cell *122*, 669-682.

Shalem, O., Sanjana, N.E., Hartenian, E., Shi, X., Scott, D.A., Mikkelson, T., Heckl, D., Ebert, B.L., Root, D.E., Doench, J.G.*, et al.* (2014). Genome-scale CRISPR-Cas9 knockout screening in human cells. Science *343*, 84-87.

Shang, G., Zhu, D., Li, N., Zhang, J., Zhu, C., Lu, D., Liu, C., Yu, Q., Zhao, Y., Xu, S.*, et al.* (2012). Crystal structures of STING protein reveal basis for recognition of cyclic di-GMP. Nat Struct Mol Biol *19*, 725-727.

Sharma, S., tenOever, B.R., Grandvaux, N., Zhou, G.P., Lin, R., and Hiscott, J. (2003). Triggering the interferon antiviral response through an IKK-related pathway. Science *300*, 1148-1151.

Shi, H., Wu, J., Chen, Z.J., and Chen, C. (2015). Molecular basis for the specific recognition of the metazoan cyclic GMP-AMP by the innate immune adaptor protein STING. Proc Natl Acad Sci U S A *112*, 8947-8952.

Shu, C., Yi, G., Watts, T., Kao, C.C., and Li, P. (2012). Structure of STING bound to cyclic di-GMP reveals the mechanism of cyclic dinucleotide recognition by the immune system. Nat Struct Mol Biol *19*, 722-724.

Storek, K.M., Gertsvolf, N.A., Ohlson, M.B., and Monack, D.M. (2015). cGAS and Ifi204 cooperate to produce type I IFNs in response to Francisella infection. J Immunol *194*, 3236-3245.

Sun, L., Wu, J., Du, F., Chen, X., and Chen, Z.J. (2013). Cyclic GMP-AMP synthase is a cytosolic DNA sensor that activates the type I interferon pathway. Science *339*, 786-791.

Tanaka, Y., and Chen, Z.J. (2012). STING specifies IRF3 phosphorylation by TBK1 in the cytosolic DNA signaling pathway. Sci Signal *5*, ra20.

Tang, C.H., Zundell, J.A., Ranatunga, S., Lin, C., Nefedova, Y., Del Valle, J.R., and Hu, C.C. (2016). Agonist-Mediated Activation of STING Induces Apoptosis in Malignant B Cells. Cancer Res *76*, 2137-2152.

Tsuchida, T., Zou, J., Saitoh, T., Kumar, H., Abe, T., Matsuura, Y., Kawai, T., and Akira, S. (2010). The ubiquitin ligase TRIM56 regulates innate immune responses to intracellular double-stranded DNA. Immunity *33*, 765-776.

Tsuchiya, Y., Jounai, N., Takeshita, F., Ishii, K.J., and Mizuguchi, K. (2016). Ligand-induced Ordering of the C-terminal Tail Primes STING for Phosphorylation by TBK1. EBioMedicine *9*, 87-96.

Volpicelli-Daley, L.A., Li, Y., Zhang, C.J., and Kahn, R.A. (2005). Isoform-selective effects of the depletion of ADP-ribosylation factors 1-5 on membrane traffic. Mol Biol Cell *16*, 4495-4508.

Wang, H., Hu, S., Chen, X., Shi, H., Chen, C., Sun, L., and Chen, Z.J. (2017). cGAS is essential for the antitumor effect of immune checkpoint blockade. Proc Natl Acad Sci U S A *114*, 1637-1642.

Wang, Q., Liu, X., Cui, Y., Tang, Y., Chen, W., Li, S., Yu, H., Pan, Y., and Wang, C. (2014). The E3 ubiquitin ligase AMFR and INSIG1 bridge the activation of TBK1 kinase by modifying the adaptor STING. Immunity *41*, 919-933.

Wang, Y., Lian, Q., Yang, B., Yan, S., Zhou, H., He, L., Lin, G., Lian, Z., Jiang, Z., and Sun, B. (2015). TRIM30alpha Is a Negative-Feedback Regulator of the Intracellular DNA and DNA Virus-Triggered Response by Targeting STING. PLoS Pathog *11*, e1005012.

Wassermann, R., Gulen, M.F., Sala, C., Perin, S.G., Lou, Y., Rybniker, J., Schmid-Burgk, J.L., Schmidt, T., Hornung, V., Cole, S.T.*, et al.* (2015). Mycobacterium tuberculosis Differentially Activates cGAS- and Inflammasome-Dependent Intracellular Immune Responses through ESX-1. Cell Host Microbe *17*, 799-810.

Watson, R.O., Bell, S.L., MacDuff, D.A., Kimmey, J.M., Diner, E.J., Olivas, J., Vance, R.E., Stallings, C.L., Virgin, H.W., and Cox, J.S. (2015). The Cytosolic Sensor cGAS Detects Mycobacterium tuberculosis DNA to Induce Type I Interferons and Activate Autophagy. Cell Host Microbe *17*, 811-819.

Watson, R.O., Manzanillo, P.S., and Cox, J.S. (2012). Extracellular M. tuberculosis DNA targets bacteria for autophagy by activating the host DNA-sensing pathway. Cell *150*, 803-815.

Wild, P., Farhan, H., McEwan, D.G., Wagner, S., Rogov, V.V., Brady, N.R., Richter, B., Korac, J., Waidmann, O., Choudhary, C.*, et al.* (2011). Phosphorylation of the autophagy receptor optineurin restricts Salmonella growth. Science *333*, 228-233.

Woo, S.R., Fuertes, M.B., Corrales, L., Spranger, S., Furdyna, M.J., Leung, M.Y., Duggan, R., Wang, Y., Barber, G.N., Fitzgerald, K.A.*, et al.* (2014). STING-dependent cytosolic

DNA sensing mediates innate immune recognition of immunogenic tumors. Immunity *41*, 830-842.

Wu, J., Sun, L., Chen, X., Du, F., Shi, H., Chen, C., and Chen, Z.J. (2013). Cyclic GMP-AMP is an endogenous second messenger in innate immune signaling by cytosolic DNA. Science *339*, 826-830.

Wu, J.J., Li, W., Shao, Y., Avey, D., Fu, B., Gillen, J., Hand, T., Ma, S., Liu, X., Miley, W.*, et al.* (2015). Inhibition of cGAS DNA Sensing by a Herpesvirus Virion Protein. Cell Host Microbe *18*, 333-344.

Xia, P., Ye, B., Wang, S., Zhu, X., Du, Y., Xiong, Z., Tian, Y., and Fan, Z. (2016a). Glutamylation of the DNA sensor cGAS regulates its binding and synthase activity in antiviral immunity. Nat Immunol *17*, 369-378.

Xia, T., Konno, H., Ahn, J., and Barber, G.N. (2016b). Deregulation of STING Signaling in Colorectal Carcinoma Constrains DNA Damage Responses and Correlates With Tumorigenesis. Cell Rep *14*, 282-297.

Yang, H., Wang, H., Ren, J., Chen, Q., and Chen, Z.J. (2017). cGAS is essential for cellular senescence. Proc Natl Acad Sci U S A *114*, E4612-E4620.

Ye, J., Rawson, R.B., Komuro, R., Chen, X., Dave, U.P., Prywes, R., Brown, M.S., and Goldstein, J.L. (2000). ER stress induces cleavage of membrane-bound ATF6 by the same proteases that process SREBPs. Mol Cell *6*, 1355-1364.

Yin, Q., Tian, Y., Kabaleeswaran, V., Jiang, X., Tu, D., Eck, M.J., Chen, Z.J., and Wu, H. (2012). Cyclic di-GMP sensing via the innate immune signaling protein STING. Mol Cell *46*, 735-745.

Zhang, G., Chan, B., Samarina, N., Abere, B., Weidner-Glunde, M., Buch, A., Pich, A., Brinkmann, M.M., and Schulz, T.F. (2016). Cytoplasmic isoforms of Kaposi sarcoma herpesvirus LANA recruit and antagonize the innate immune DNA sensor cGAS. Proc Natl Acad Sci U S A *113*, E1034-1043.

Zhang, J., Hu, M.M., Wang, Y.Y., and Shu, H.B. (2012). TRIM32 protein modulates type I interferon induction and cellular antiviral response by targeting MITA/STING protein for K63-linked ubiquitination. J Biol Chem *287*, 28646-28655.

Zhang, X., Shi, H., Wu, J., Zhang, X., Sun, L., Chen, C., and Chen, Z.J. (2013). Cyclic GMP-AMP containing mixed phosphodiester linkages is an endogenous high-affinity ligand for STING. Mol Cell *51*, 226-235.

Zhang, X., Wu, J., Du, F., Xu, H., Sun, L., Chen, Z., Brautigam, C.A., Zhang, X., and Chen, Z.J. (2014a). The cytosolic DNA sensor cGAS forms an oligomeric complex with DNA and undergoes switch-like conformational changes in the activation loop. Cell Rep *6*, 421-430.

Zhang, Y., Yeruva, L., Marinov, A., Prantner, D., Wyrick, P.B., Lupashin, V., and Nagarajan, U.M. (2014b). The DNA sensor, cyclic GMP-AMP synthase, is essential for induction of IFN-beta during Chlamydia trachomatis infection. J Immunol *193*, 2394-2404.

Zhong, B., Yang, Y., Li, S., Wang, Y.Y., Li, Y., Diao, F., Lei, C., He, X., Zhang, L., Tien, P.*, et al.* (2008). The adaptor protein MITA links virus-sensing receptors to IRF3 transcription factor activation. Immunity *29*, 538-550.

Zhong, B., Zhang, L., Lei, C., Li, Y., Mao, A.P., Yang, Y., Wang, Y.Y., Zhang, X.L., and Shu, H.B. (2009). The ubiquitin ligase RNF5 regulates antiviral responses by mediating degradation of the adaptor protein MITA. Immunity *30*, 397-407.